University of North Dakota
UND Scholarly Commons

Theses and Dissertations | Theses, Dissertations, and Senior Projects

January 2018

Trpc1-Mediated Ca2+ Entry Regulates Metabolism By Modulating Adipose Differentiation, Autophagy, And Adiponectin Secretion

Anne Schaar

Follow this and additional works at: https://commons.und.edu/theses

Recommended Citation
Schaar, Anne, "Trpc1-Mediated Ca2+ Entry Regulates Metabolism By Modulating Adipose Differentiation, Autophagy, And Adiponectin Secretion" (2018). *Theses and Dissertations*. 2334.
https://commons.und.edu/theses/2334

This Dissertation is brought to you for free and open access by the Theses, Dissertations, and Senior Projects at UND Scholarly Commons. It has been accepted for inclusion in Theses and Dissertations by an authorized administrator of UND Scholarly Commons. For more information, please contact zeineb.yousif@library.und.edu.

TRPC1-MEDIATED Ca^{2+} ENTRY REGULATES METABOLISM BY MODULATING ADIPOSE DIFFERENTIATION, AUTOPHAGY, AND ADIPONECTIN SECRETION

by

Anne Elizabeth Schaar
Bachelor in Science, North Dakota State University, 2005

A Dissertation

Submitted to the Graduate Faculty

of the

University of North Dakota

in partial fulfillment of the requirements

for the degree of

Doctor of Philosophy

Grand Forks, North Dakota

August
2018

Copyright 2018 Anne E. Schaar

This dissertation, submitted by Anne E. Schaar in partial fulfillment of the requirements for the Degree of Doctor of Philosophy from the University of North Dakota, has been read by the Faculty Advisory Committee under whom the work has been done and is hereby approved.

Brij Singh, Chairperson

Archana Dhasarathy

Othman Ghribi

Kate Larson

Manu Manu

This dissertation is being submitted by the appointed advisory committee as having met all of the requirements of the School of Graduate Studies at the University of North Dakota and is hereby approved.

Grant McGimpsey
Dean of the School of Graduate Studies

Date

PERMISSION

Title TRPC1-MEDIATED Ca^{2+} ENTRY REGULATES METABOLISM BY MODULATING ADIPOSE DIFFERENTIATION, AUTOPHAGY, AND ADIPONECTIN SECRETION

Department Biochemistry and Molecular Biology

Degree Doctor of Philosophy

In presenting this dissertation in partial fulfillment of the requirements for a graduate degree from the University of North Dakota, I agree that the library of this University shall make it freely available for inspection. I further agree that permission for extensive copying for scholarly purposes may be granted by the professor who supervised my dissertation work or, in his absence, by the Chairperson of the department or the dean of the School of Graduate Studies. It is understood that any copying or publication or other use of this dissertation or part thereof for financial gain shall not be allowed without my written permission. It is also understood that due recognition shall be given to me and to the University of North Dakota in any scholarly use which may be made of any material in my dissertation.

Anne E. Schaar
6-22-2018

TABLE OF CONTENTS

LIST OF FIGURES ix

LIST OF TABLES xii

ACKNOWLEDGEMENTS xiii

ABSTRACT xv

CHAPTER

I. INTRODUCTION 1

Calcium Signaling 1

TRP Family of Ion Channels 6

TRPC Subfamily 9

TRPC1 Involvement in SOCE 12

Metabolism Regulation 13

II. METHODS 16

Animals 16

Stromal vascular fraction (SVF) and primary adipocyte isolation 17

Adipose cell size and number determination 18

SVF differentiation 18

C2C12 cell culture and differentiation 19

EchoMRI measurements of body composition 19

Red Oil Staining 19

Gas chromatography/mass spectrometry (GC/MS) 20
Blood collection and serum isolation 22
Adiponectin and Leptin Concentrations 22
Glucose tolerance test 23
Measurement of plasma insulin 23
Electrophysiology 23
Calcium imaging 24
PCR analysis 25
qPCR analysis 25
Muscle Isolation and Culture 27
Immunoblotting 28
Co-immunoblotting 29
Adiponectin Secretion from Fresh Adipose Tissue 29
Statistical Analysis 29
III. LOSS OF TRPC1 IN ADIPOCYTES IMPAIRS DIFFERENTIATION 31
Introduction 31
Results 38
Subcutaneous and visceral adipocytes display SOCE mechanisms 38
Differentiated visceral adipocytes exhibit increased store-operated Ca^{2+} entry 43
Inhibition of SOCE impairs ability of adipocytes to differentiate 47
Loss of TRPC1 in adipocytes reduces SOCE 48

Lack of TRPC1 mediated Ca^{2+} influx reduces ability to differentiate 55

$TRPC1^{-/-}$ mice have increased fatty-acid desaturation index and adiposity with age 58

Conclusion 62

IV. THE TRPC1 Ca^{2+}-PERMEABLE CHANNEL INHIBITS EXERCISE-INDUCED PROTECTION AGAINST HIGH-FAT DIET-INDUCED OBESITY AND TYPE II DIABETES 68

Introduction 68

Results 74

Body fat mass is decreased in TRPC1 KO mice fed a HF diet and exercised 74

TRPC1 KO mice fed a HF diet and exercised are protected from type II diabetes risk 78

Adipocyte numbers are decreased in TRPC1 KO mice fed a HF diet and exercised 80

Autophagy marker expression is decreased while apoptosis marker expression is increased in TRPC1 KO mice fed a HF diet and exercised 82

Conclusion 87

V. TRPC1 TRANSPORTS Ca^{2+} INVOLVED IN SNARE COMPLEX FORMATION DURING ADIPONECTIN SECRETION 91

Introduction 91

Results 98

Serum adipokines levels are reduced in $TRPC1^{-/-}$ mice 98

Exercise recovers diminished serum adiponectin concentrations in $TRPC1^{-/-}$ mice 100

Adiponectin isoforms are altered in $TRPC1^{-/-}$ mice 103

Diminished adiponectin secretion in Subc AT from TRPC1$^{-/-}$ mice 104

Reduced SNARE protein interactions in TRPC1$^{-/-}$ adipose tissue 106

Conclusion 109

VI. LOSS OF TRPC1 IS MOST LIKELY NOT THE CAUSE OF REDUCED ADIPONECTIN SIGNALING IN SKELETAL MUSCLE 115

Introduction 115

Results 121

Reduced expression of adiponectin targets in TRPC1$^{-/-}$ muscle 121

Differentiated muscle cell line exhibits SOCE characteristics 124

Blockage of SOCE reduces AdipoRon Ca^{2+} influx, but not downstream targets 125

SOCE not diminished in primary muscle due to loss of TRPC1 127

Initial influx of Ca^{2+} due to treatment with AdipoRon is not TRPC1 dependent 129

Loss of TRPC1 in EDL impairs the ability of AdipoRon to initiate downstream targets of adiponectin signaling 130

Conclusion 133

VII. DISCUSSION 137

REFERENCES 141

LIST OF FIGURES

Figure		Page
1.	Cellular Ca^{2+} Regulators	2
2.	TRP Channels	8
3.	TRPC Channels	11
4.	Confirmation of TRPC1 loss in subcutaneous adipose tissue	13
5.	Inter-tissue Communication	15
6.	Schematic of adipocyte differentiation	33
7.	TRPC1 and TRPC5 expression in mouse and human adipose	37
8.	Subc AT SVF exhibits SOCE	39
9.	Blockage of SOCE in differentiated Subc AT by SKF	41
10.	Changes in Ca^{2+} channel expression during differentiation in Subc AT and VAT	42
11.	Increased SOCE currents in differentiated VAT	44
12.	Fura-2 Traces of SVF and differentiated VAT	45
13.	Inhibition of SOCE impairs ability of adipocytes to differentiate	46
14.	Loss of TRPC1 in adipocytes reduces SOCE	50
15.	Angiotensin II treatment of differentiated Subc AT	51
16.	SOCE currents in visceral adipocytes reduced	52
17.	SOCE in visceral adipocytes is diminished by loss of TRPC1	53
18.	Ca^{2+} channel expression of WT and $TRPC1^{-/-}$ Subc AT and VAT	54

19. Loss of TRPC1 in adipocytes reduces ability to differentiate 56

20. Adipogenetic protein expression in TRPC1$^{-/-}$ adipocytes diminished 57

21. TRPC1$^{-\backslash-}$ mice have increased adiposity with age 59

22. Desaturation of liver fatty acids increased in TRPC1-/- mice 61

23. Role of intracellular Ca^{2+} and Ca^{2+} permeable channels in autophagy 73

24. TRPC1 KO mice fed a HF diet and exercised have decreased body fat mass 74

25. Daily food intake and exercise is unaltered 75

26. TRPC1 KO mice fed a HF diet and exercised have reduced insulin resistance 77

27. GLUT4 expression is unaltered in Subc AT and skeletal muscle 79

28. TRPC1 KO mice fed a HF diet and exercised have fewer adipocytes 81

29. Autophagy marker expression is decreased whereas apoptosis marker expression is increased in TRPC1 KO mice fed a HF diet and exercised . 84

30. Expression of markers for adipogenesis, beiging, and hypoxia were unaltered in subcutaneous adipose tissue 85

31. Reduced ERK2 phosphorylation observed in in TRPC1 KO mice fed a HF diet and exercised 86

32. Adiponectin synthesis 93

33. SNARE complex formation 97

34. Serum adipokines are altered in TRPC1-/- mice. 98

35. No difference in leptin and adiponectin concentrations within adipose tissue 99

36. Reduced serum adiponectin concentrations in TRPC1$^{-/-}$ mice recovered when exercised 101

37. Serum adiponectin isoforms altered in TRPC1$^{-/-}$ mice 102

38. Insulin stimulated secretion diminished in TRPC1$^{-/-}$ Subc AT 104

39. Distribution of adiponectin isoforms from secretion samples 105

40. Reduced SNARE protein interactions in TRPC1$^{-/-}$ adipose tissue 108

41. Adiponectin signaling through AdipoR1 and AdipoR2..... 116

42. mRNA expression of lipid metabolism and mitochondrial biogenesis genes in liver and muscle..... 123

43. C2C12 myotubes exhibit SOCE properties 124

44. Blockage of SOCE reduces AdipoRon Ca2+ influx, but not downstream targets in C2C12 myotubes..... 126

45. WT EDL muscle exhibits SOCE mediated Ca^{2+} influx which is not diminished by loss of TRPC1 128

46. AdipoRon initiated Ca^{2+} influx is not TRPC1 dependent 130

47. Loss of TRPC1 in EDL impairs the ability of AdipoRon to activate AMPK..... 132

LIST OF TABLES

Table Page

1. Primer Sequences…….....21

ACKNOWLEDGEMENTS

I first thank Dr. Brij Singh for the opportunity to study in his laboratory, for funding this research, and for mentoring me to become an independent scientist. I greatly appreciate him for encouraging me to research a project I am passionate about and allowing me to experiment with new techniques and ideas.

I am extremely grateful to Dr. Kate Larson and other members at the USDA-ARS Grand Forks Human Nutrition Research Center, including Dr. James Roemmich, Dr. Danielle Krout, and Amy Bundy, for collaborating on much of the data presented in this dissertation. The use of their knowledge and equipment was imperative to success of this project. I thank Dr. Larson for the instruction on working with adipose tissue and teaching me about metabolism research. I need to especially thank Amy Bundy for the time and effort she put in to this collaborative work, but also for teaching me adipose SVF isolation and culture.

I thank my lab mates Dr. Yuyang Sun and Dr. Pramod Sukumaran for teaching me about Ca^{2+} signaling and teaching me the techniques necessary for my project. I especially need to thank Dr. Sun for performing all the electrophysiology in this dissertation.

I am grateful to Dr. Archana Dhasarathy, Dr. Kate Larson, Dr. Othman Ghribi, and Dr. Manu for being part of my graduate committee and giving guidance on my research over the years. I thank Dr. Dhasarathy for the extra time and

guidance she has provided me regarding this dissertation but also other collaborative projects. My special thanks to Dr. Mikhail Golovko for performing the GC/MS within this dissertation. Thank you to ND EPSCoR for the Doctoral Dissertation Assistantship that provided me funding to perform experiments necessary for this dissertation.

I would like to thank the laboratories of Dr. Ghribi, Dr. Grove, Dr. Vaughn, Dr. Foster, and Dr. Henry for permitting me to use their equipment and reagents during the last 8 months of my graduate career. I need to especially thank Dr. Foster for allowing me to become a temporary member of his laboratory and use his cell culture hood, incubators and equipment along with his problem-solving skills. I wish to thank all the faculty and staff in the Biomedical Science department for their continued support and encouragement. So many of them have positively influence both my research and my life.

Finally, I thank my friends and family for supporting me during my graduate career. I am grateful to my graduate school friends who helped me through struggles with advice or laughter. I'm appreciative for the opportunity to be a BGSA officer and serve with other amazing students who became my close friends. I thank my friends and family for encouraging me even though they had no clue what I was talking about. I especially thank my mother who has supported me every day of my life and my daughter, Amelia, who makes everything I do in life worth it.

ABSTRACT

A multitude of organs play a critical role in managing metabolism including the liver, pancreas, gut, brain, muscle, and adipose tissue. Abnormal function in any one of these can offset the metabolic balance and negatively affect whole body function thereby contributing to the development of metabolic complications and obesity. Although no single metabolic abnormality is responsible for obesity, understanding how normal cellular processes are regulated provides us with knowledge to reverse them during times of dysfunction. The main focus of this dissertation is on the regulation of adipose tissue due to its dual role of storing excess lipids and endocrine organ capabilities. Adipocytes, along with a majority of other cell types, are highly dependent on calcium (Ca^{2+}), thus the role of Ca^{2+} and the involvement of the Ca^{2+} channel Transient Receptor Potential Canonical 1 (TRPC1) were studied. The evidence provided in this dissertation shows that Ca^{2+} entry in adipocytes, especially upon store-depletion, plays an important role in adipocyte differentiation, autophagy, and adipokine secretion and subsequently metabolic regulation. The endogenous Ca^{2+} entry channel in both subcutaneous and visceral adipocytes was found to be dependent on TRPC1-STIM1 complexes and altering or blocking TRPC1 resulted in dysfunctional adipocytes.

Adipocyte differentiation, the process of pre-adipocytes converting to adipocytes, is a tightly regulated process with Ca^{2+} dependency. Blockage of

TRPC1-mediated Ca^{2+} entry with SKF-96365 inhibited differentiation which was indicated by decreased lipid accumulation and expression of PPARγ, FAPB4, and perilipin in both subcutaneous adipose tissue (Subc AT) and visceral adipose tissue (VAT). Loss of TRPC1 in either adipose tissue type resulted in a reduced ability to differentiate which occurred prior to PPARγ expression indicating TRPC1-mediated Ca^{2+} entry is necessary for the initial stages of differentiation.

Diets high in fat induce unhealthy expansion of adipose tissue, while exercise reduces adipocyte size and lipid content. Mice deficient of TRPC1 function and challenged with both a high-fat diet and exercise had lower fat mass and fasting glucose concentrations along with decreased adipocyte numbers. Further investigation indicated a decrease in autophagy with a concurrent increase in apoptosis. Together, this data shows that TRPC1 inhibits the positive effects of exercise under a high-fat diet-induced obesity environment.

Adipose tissue is an important endocrine organ responsible for secreting a number of cytokines, including adiponectin and leptin, which have a functional role in modulating metabolism. Secretion of adiponectin from adipose tissue has been found to be Ca^{2+} dependent, but the identity of the responsible Ca^{2+} channel is unknown. This study provides evidence that TRPC1 deficient mice have reduced serum adiponectin concentration which is believed to be due to an inability of adipose tissue to properly secrete adiponectin. Further, it was shown that loss of TRPC1-mediated Ca^{2+} influx is involved in SNARE complex formation necessary for proper exocytosis of adiponectin loaded vesicles.

Serum adiponectin concentrations have been shown to be correlated to adiponectin receptor expression, thus it was investigated whether reduces in serum adiponectin concentrations observed in TRPC1 deficient mice was due to dysfunctional adiponectin signaling in muscle. Within this study, it was observed that skeletal muscle of TRPC1 deficient mice have reduced adiponectin targets including PGC1α, lipid metabolism, and mitochondrial biogenesis mRNA expression. Though data suggests AdipoRon initiated adiponectin signaling in muscle is Ca^{2+} and SOCE dependent, TRPC1 is not a contributing member as loss of TRPC1 did not inhibit Ca^{2+} influx or PGC1α expression indicating decreased adiponectin targets is likely due to reduce serum adiponectin concentrations.

Overall, evidence from the combined studies suggests TRPC1-mediated Ca^{2+} influx is an important regulator of adipocyte processes necessary for maintaining a healthy body.

CHAPTER I

INTRODUCTION

Calcium Signaling

The ability of cells to communicate with their environment and respond temporarily to external events is a critical cellular function. This process, called cell signaling or signal transduction, is initiated by a receptor-ligand interaction which triggers a chain reaction of biochemical and molecular steps which alter cell physiology. Calcium (Ca^{2+}) signaling is a particular subtype of cell signaling that involves altering the cellular balance of internal versus external cellular Ca^{2+} concentrations. The Ca^{2+} ion is an important secondary messenger molecule involved in regulating numerous cell processes including cell proliferation and differentiation, motility, gene transcription, and exocytosis (Berridge et al., 2000). At basal conditions, the free intracellular calcium concentration ($[Ca^{2+}]_i$) is measured at ~100 nM, while the extracellular concentrations are more than 20,000-fold greater (Clapham, 2007). Cell stimulation can be in the form of electrical, hormonal, or mechanical and can increase the $[Ca^{2+}]_i$ to around 1,000 nM. Increases in $[Ca^{2+}]_i$ are the result of either direct Ca^{2+} entry from the extracellular milieu upon membrane depolarization (Woodard and Rosado, 2005)

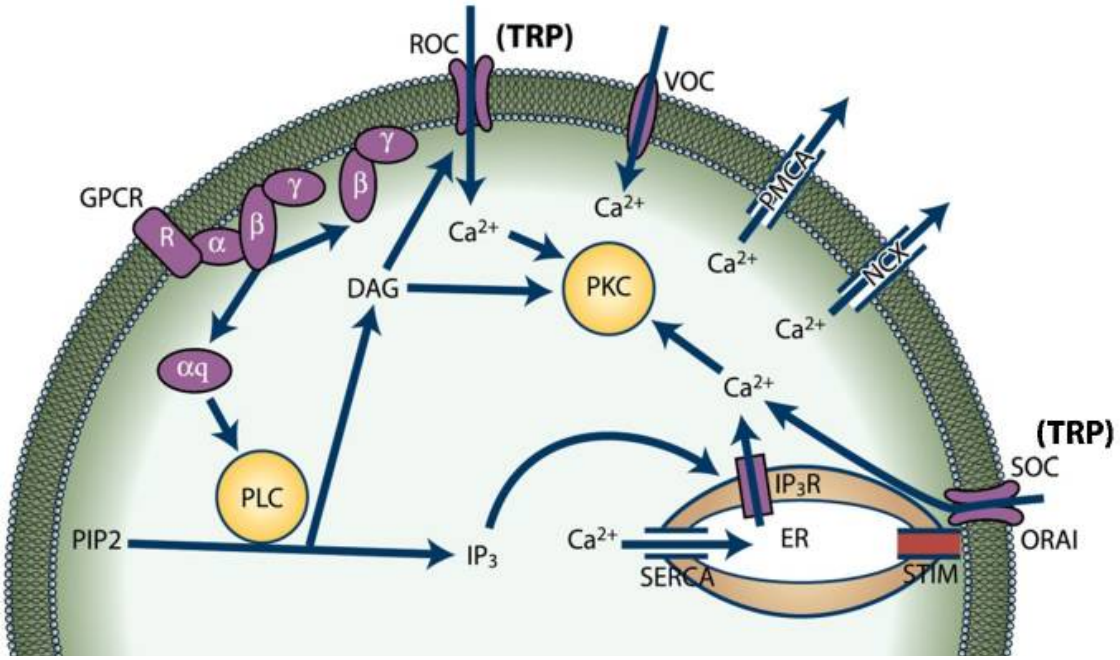

Figure 1 Cellular Ca^{2+} Regulators

Schematic diagram of common Ca^{2+} signaling pathways. Many cells contain multiple pathways, but not necessarily all mechanisms shown here are present in one single cell type. Influx of Ca^{2+} is primarily mediated by voltage-operated channels (VOCs or VGCCs), receptor-mediated Ca^{2+} entry (ROC), transient receptor potential channels (TRP), ligand-gated channels, and store-operated Orai channels (SOC) that are activated by STIM1 protein. Efflux of Ca^{2+} is achieved by PM Ca^{2+} ATPase (PMCA) or Na^{+}/ Ca^{2+} exchanger (NCX). Release of Ca^{2+} from the ER is mediated through IP3 (IP3R) receptors. The reuptake of Ca^{2+} into the ER is mediated by ER Ca^{2+}ATPase (SERCA). Other components shown include: GPCR (G proteins); PIP2 (phosphatidylinositol 4,5-bisphosphate); PLC (phospholipase C); PKC (protein kinase C); DAG (diacylglycerol); IP3 (inositol 1,4,5-trisphosphate); (IP3R inositol 1,4,5-trisphosphate receptor). Reprinted from "Functional role of TRP channels in modulating ER stress and Autophagy" by P. Sukumaran, 2016, *Cell Calcium*, 60, 123-132. Copyright 2016 by Elsevier. Reprinted with permission.

or by the process of store-operated Ca^{2+}entry (SOCE), which includes the release of Ca^{2+} stores from the endoplasmic reticulum (ER) that initiates an influx of Ca^{2+} from the extracellular milieu (Parekh and Putney, 2005; Putney, 1986; Putney et al., 2017).

The direct method of Ca^{2+} entry involves the opening of selective Ca^{2+} channels in the plasma membrane (PM) thus triggering a rapid inflow of Ca^{2+} ions. The most widely understood Ca^{2+} channels in this process are voltage-operated channels (VOCs or VGCCs), which are found in excitable cells and are activated by changes in electrical membrane potential near the channel (Figure 1). VOCs are generally ion-specific and channels have been identified for sodium (Na^{+}), potassium (K^{+}), Ca^{2+}, and Chloride (Cl^{-}). The ability of VOCs to promptly influx Ca^{2+} is needed for cellular processes such as muscle contraction or exocytosis at synaptic endings (Berridge et al., 2003). Along with VOCs, there are many other Ca^{2+} channels that are initiated by different external signals including receptor-operated channels (ROCs), such as the NMDA (N-methyl-D-aspartate) receptors (NMDARs) that respond to glutamate. At the end of the signaling event, Ca^{2+} is removed out of the cytoplasm to return the cell to basal $[Ca^{2+}]_i$ through PM-associated pumps and exchangers. The plasma membrane Ca^{2+} ATPase (PMCA) is important for this process and has low capacity but high affinity for Ca^{2+} transport with a stoichiometry of one Ca^{2+} ion to one ATP (Lopreiato et al., 2014). The Na^{+}/Ca^{2+} (NCX) also performs this job, however, has a low Ca^{2+} affinity but high

capacity for Ca^{2+} transport giving it the ability to transport Ca^{2+} quickly out of the cell but only at higher concentrations (Brini and Carafoli, 2011).

Within the cell, Ca^{2+} is stored inside the ER, mitochondria, lysosomes, Golgi and nucleus (La Rovere et al., 2016). The ER is the main Ca^{2+} storage organelle boasting relatively high Ca^{2+} concentrations that can be quickly released into the cytoplasm. SOCE was identified in 1986 and is a ubiquitous PM Ca^{2+} entry mechanism. The process begins with a ligand, such as a hormone, neurotransmitter, growth factor, glycoprotein, or cytokine, binds to a G protein-coupled receptor (GPCR), thereby activating the receptor (Putney, 1986) (Figure 1). Ligand docking dissociates GDP from the G protein complex, resulting in the detachment of G-alpha subunit and G-beta/G-gamma complex. The GTP bound G-alpha subunit then docks to Phospholipase C (PLC) causing a conformational change of PLC and hydrolyzing phosphatidylinositol biphosphate (PIP2) into the secondary messengers diacylglycerol (DAG) and inositol 1,4,5-trisphosphate (IP3) (Berridge, 1993). The role of the freed IP3 is to bind with IP3 receptors bound to the PM of the ER thus initiating an efflux of ER Ca^{2+} stores necessary for the signaling event (Berridge et al., 2003). When the Ca^{2+} level in the ER lumen drops following IP3 receptor binding, stromal interaction molecule (STIM), a family of single-pass ER membrane bound proteins, senses the depleted Ca^{2+} and translocates to the cell's PM where it activates selective plasma membrane Ca^{2+} channels called SOCs (store-operated Ca^{2+} channels) to transport Ca^{2+} across the PM from the extracellular milieu (Prakriya and Lewis, 2015). Due

to the limited quantity of Ca^{2+} stored of the ER, ER Ca^{2+} release can only produce transient signals; however, sustained store depletion can induce Ca^{2+} entry through SOCs that is prolonged for minutes to hours. SOCs are not voltage dependent, thus they can conduct Ca^{2+} at negative membrane potentials and are complementary to VOCs. The first SOCs were identified in mast cells after whole cell patch clamp recordings identified a Ca^{2+}-selective current which was characterized by an inward rectification and a reversal potential > +40 mv (Hoth and Penner, 1992; Parekh et al., 1997). These channels were termed Ca^{2+} release-activated Ca^{2+} (CRAC) channels and include ORAI1, ORAI2, and ORAI3. The transient receptor potential canonical family (TRPC) of Ca^{2+} channels has also been identified as SOCs and will be discussed more readily in the following sections. The induction of Ca^{2+} influx by SOCs results in an increase in $[Ca^{2+}]_i$ which is used for the signaling event and to refill the ER via the Ca^{2+}-ATPase pump, sarcoendoplasmic reticulum Ca^{2+} ATPase (SERCA) and the golgi via the secretory pathway Ca^{2+} ATPase (SPCA) (Guerini et al., 2005; Strehler and Treiman, 2004). Termination of SOCE occurs following the refilling of the ER by SERCA and SOCs return to their original positions (Cao et al., 2015; Jousset et al., 2007; Manjarrés et al., 2011).To respond dynamically to the fluctuations of Ca^{2+} signaling needs, cells must be able to accurately control the amount and location of Ca^{2+} influxed through Ca^{2+} transporters and channels. In the next section, we will discuss a particular group of Ca^{2+} channels important for this process.

TRP Family of Ion Channels

The transient receptor potential channel genes were first discovered in the fruit fly *Drosophila melanogaster* during research centered on understanding the *Drosophila melanogaster* phototransduction cascade in the retina (Cosens and Manning, 1969). It was found that light-induced conformational changes of the protein rhodopsin stimulated the attached GTP-binding protein thereby activating phospholipase-C and an influx of cations. Within this study, a spontaneously formed mutant with a blind phenotype was analyzed and the correlating gene mutation caused a transient cation influx response to light instead of the expected sustained response. Due to these results, the mutated gene and the corresponding protein were given the name *trp* for Transient Receptor Potential (Cosens and Manning, 1969). Further research identified that the decline of photoreceptor potential in the *trp* mutant was due to exhaustion of Ca^{2+} mobility of TRP and resulted in a tenfold decrease in Ca^{2+} influx (Vaca et al., 1994; Xu et al., 1997). Since the structure of the mutated *trp* protein resulting in changes in Ca^{2+} permeability was similar to other known cation channels, it was hypothesized to be a new Ca^{2+} channel involved in the inositol phosphate signaling system (Hardie and Minke, 1992; Montell, 1999; Montell and Rubin, 1989). Subsequent investigation revealed numerous TRP channels which were grouped into a family.

TRP channels are tetrameric complexes consisting of four pore-forming units (Figure 2). Each unit contains six hydrophobic stretches and a pore loop motif intercalated between the fifth and sixth transmembrane segments (Dietrich et al.,

2014; Nilius, 2007; Pani et al., 2008; Venkatachalam and Montell, 2007). The 1275 amino acid protein has 3 domains with a neutral 333 amino acid N-terminal domain, followed by a 228-amino acid domain with 6 transmembrane segments and a hydrophilic 614 amino acid C-terminal domain. The Transient Receptor Potential superfamily is broken into seven subfamilies which are separated into two groups based on sequence and topological differences. Group 1 consists of five subfamilies and includes TRPC (Canonical) (TRPC1–TRPC7), TRPCV (Vanilloid) (TRPV1–TRPV6), TRPM (Melastatin) (TRPM1–TRPM8), and TRPA (Ankyrin) and TRPN (NOMPC-like). Group 2 includes TRPP (polycystin) (TRPP1-TRPP2) and TRPML (mucolipin) (TRPML1-TRPML3). Of all the mammalian TRP channels, the members of the TRPC sub family are the most closely related to the *Drosophila* TRP (Birnbaumer, 2009; Montell, 2005; Putney, 1986, 1990).

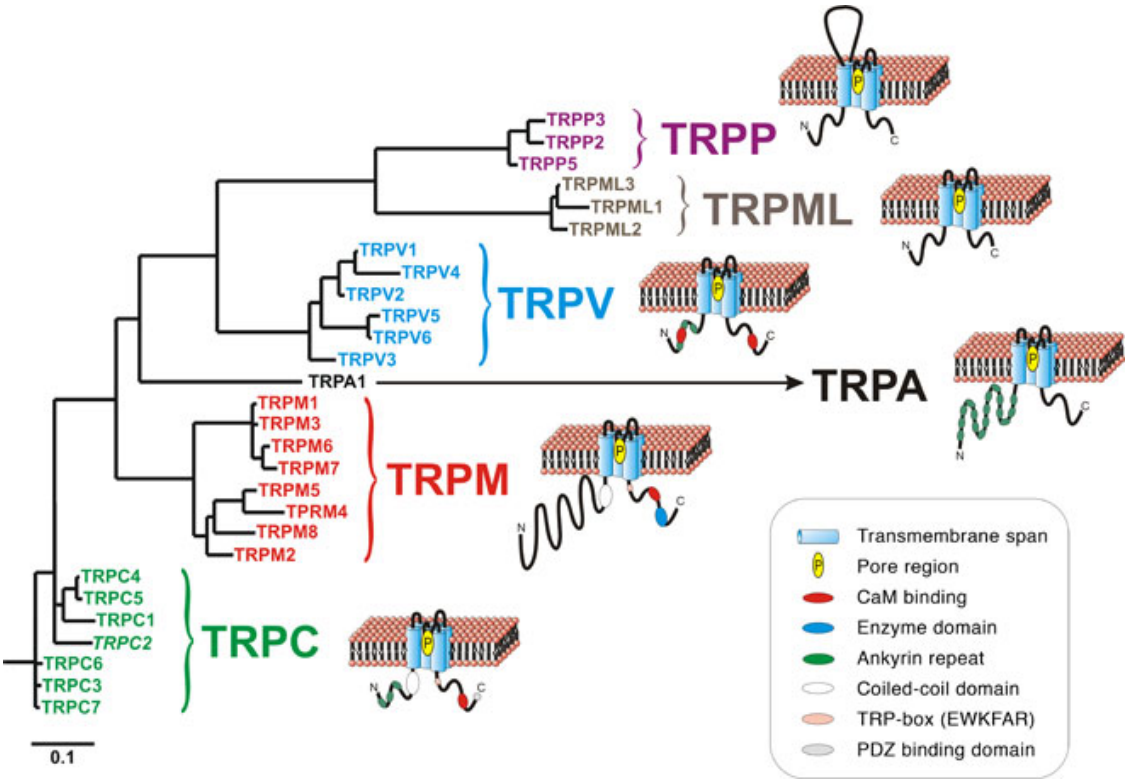

Figure 2 TRP Channels

Phylogenetic tree and topology of TRP channels grouped by structural similarities. Subfamilies include TRPC (Canonical) (TRPC1– TRPC7), TRPCV (Vanilloid) (TRPV1–TRPV6), TRPM (Melastatin) (TRPM1–TRPM8), and TRPA (Ankyrin) and TRPN (NOMPC-like), TRPP (polycystin) (TRPP1-TRPP2) and TRPML. Reprinted from “TRP Channels in Disease” by B. Nilius, 2005, Science Signaling, 2005, 295. Copyright 2005 by The American Association for the Advancement of Science. Reprinted with permission.

TRPC Subfamily

Expression of TRPC channels is ubiquitous in nature and have been found in a wide variety of tissues including the brain, hypothalamus, adipose tissue, smooth and cardiac muscles, endothelium, kidney, adrenal gland, lung, and pituitary glands (Pedersen et al., 2005; Qiu et al., 2010; Sukumar et al., 2012; Zanou et al., 2010). The first mammalian TRPC channel to be identified and cloned was TRPC1 which lead to the identification of the other members (Wes et al., 1995). The human TRPC subfamily contains seven members which are separated into two individual groups (Figure 3) based on their biochemical and functional similarities: TRPC1/4/5 and TRPC3/6/7 (Ong and Ambudkar, 2017). TRPC channels are non-selectively permeable to Ca^{2+}, but the selectivity ratio of PCa/PNa varies significantly between groups (Ong and Ambudkar, 2017; Venkatachalam and Montell, 2007). Sequence homology in TRPC channels is found within the block of roughly 25 residues on the C-terminal tail termed the TRP domains which includes TRP boxes 1 and 2. TRP box 1 is a conserved amino acid sequence of EWKFAR and TRP box 2 is a six-amino acid proline-rich domain. The C-terminal tail also includes binding domains for PIP_2 and calmodulin (CaM) named CIRB. The N-terminal tail of TRPCs contains 3-4 ankyrin repeats and a coiled-coil domain of alpha-helices (Ong and Ambudkar, 2011). The domains for Homer1, IP_3R and caveolin-1 (Cav-1) binding have also been uncovered, but the exact function of each of these remains elusive.

All TRPC channels are activated by PIP2 hydrolysis and ER Ca^{2+}, though not all are involved in SOCE mechanisms (Ong and Ambudkar, 2015). Importantly, none of the TRPCs exhibit currents similar to CRAC channels. TRPC channels display currents with a relatively linear current-voltage relationship with a reversal potential from zero to slightly positive, however this can vary based on cell type and complex formation (Cheng et al., 2013). Figure 3 shows representative current-voltage relationships for groups of TRPCs. The TRPC channels 3/6/7 are unique to the TRPC family as they may be directly activated by DAG or its metabolite polyunsaturated fatty acid (PUFAs) (Poburko et al., 2007; Venkatachalam and Montell, 2007). One study showed exposure of overexpressed TRPC3 channels to exogenous DAG/PUFAs resulted in Ca^{2+} transients indicating TRPC3 channel activation, however, in the presence of DAG activated protein kinase C (PKC), TRPC3 channels were inhibited (Soboloff et al., 2007). In this instance, it was surmised that PKC activation by DAG may be a feedback control for TRPC channels.

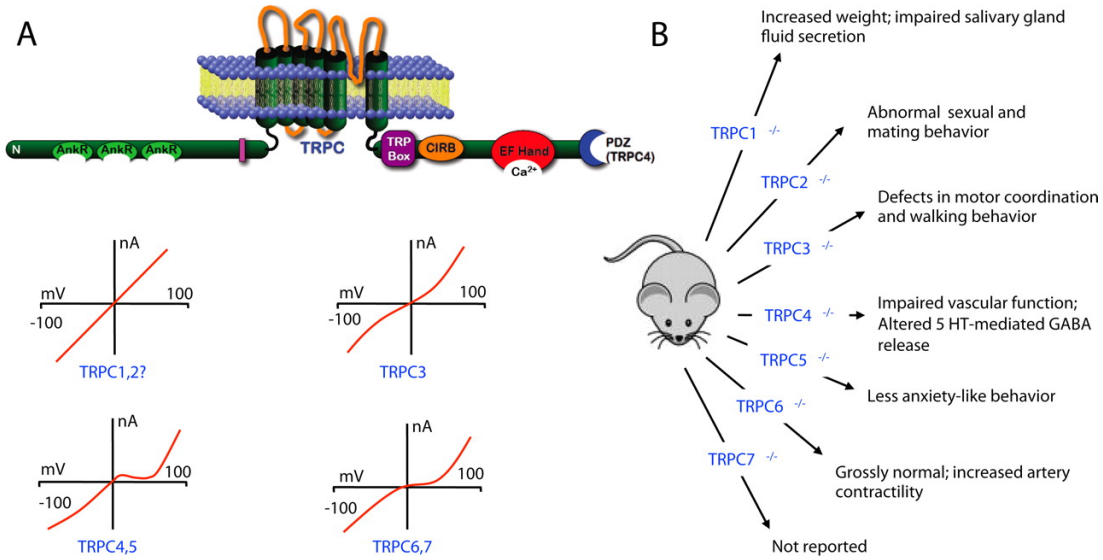

Figure 3 TRPC Channels

(A) Common topography of TRPC channels along with specific current-voltage relationships shown below for each TRPC channel grouping. (B) Phenotype of TRPC channel genetic deletions. The TRPC7 $^{-/-}$ phenotype has not been reported and TRPC2 is a pseudogene in humans. Reprinted from "International Union of Basic and Clinical Pharmacology. LXXVI. Current progress in the mammalian TRP ion channel family" by L-J. Wu, 2010, *Pharmacological Reviews*, 2010;62(3):381:404. Copyright 2010 by American Society for Pharmacology and Experimental Therapeutics. Reprinted with permission.

TRPC1 Involvement in SOCE

Data suggests that TRPCs contribute to SOCE mechanisms, although certain TRPCs have varying findings. The most consistent and soundest studies support a role for TRPC1 in SOCE, however activation of TRPC5, TRPC6, and TRPC7 seem to be also activated via store-independent mechanisms (Cheng et al., 2013). TRPC3 and TRPC4 have also been implicated in SOCE, although to a lesser degree.

The first evidence of involvement of endogenous TRPC1 in SOCE and confirmation of its contribution to Ca^{2+} permeability was found in human submandibular gland (HSG) ductal cells showing that knockdown of TRPC1 decreased SOCE functionality (Liu et al., 2003). The relative Ca^{2+}-selective currents were not consistent to those of CRAC channels, hence, the TRPC1-mediated currents were termed store-operated calcium current channels (I_{SOC}) as they have a reversal potential that is outward rectifying at roughly +15 mV. It had been previously established that STIM1 and ORAI1 were necessary components of SOCE in that knockdown of either protein abolished SOCE currents (Cheng et al., 2008; Jardin et al., 2008; Kim et al., 2009). It was further found that elimination of either ORAI1 or STIM1 completely abolished TRPC1-mediated SOCE. The current understanding of SOCE mechanisms, shown in Figure 1, is that after ER Ca^{2+} store release, STIM1 interacts with both ORAI1 and TRPC1, however a preceding ORAI1-mediated Ca^{2+} influx is required for TRPC1 function (Ambudkar et al., 2017).

Within this study, we utilize the TRPC1$^{-/-}$ mouse which is missing a coding region of exon 8 (Liu et al., 2007). This deletion results in a loss of portions of transmembrane segments 4 and 5 along with a small part of the putative pore domain causing the protein to be expressed but nonfunctional. Confirmation of its competence has been well reported, however we confirmed the absence of TRPC1 in subcutaneous adipose tissue by assessing TRPC1 mRNA (Figure 4).

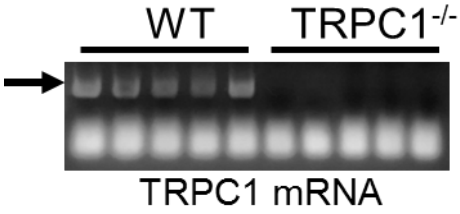

Figure 4 Confirmation of TRPC1 loss in subcutaneous adipose tissue

RT-PCR expression of TRPC1 from subcutaneous adipose tissue of WT and TRPC1$^{-/-}$ mice

Metabolism Regulation

It is well understood that managing energy within the body to create a relatively stable internal environment, or metabolic energy homeostasis, is imperative for survival. Metabolic energy homeostasis is maintained by numerous mechanisms which monitors systemic nutritional status and responds appropriately, both behaviorally and metabolically, to changes in energy availability (Yamada et al., 2008). The amount of energy available is in limited supply requiring tight regulation so that each organ/tissue and consequently its cells function properly. Communication between organs in the form of neuronal and hormone signals is imperative, and dysfunction can lead to an imbalance of

metabolic homeostasis resulting in metabolic disorders. As shown in Figure 5, adipose tissue is a major organ responsible for regulating metabolism. Dysfunction in adipose tissue is thought to contribute toward a proinflammatory, atherogenic, and diabetogenic state along with being linked to the development of chronic inflammation, insulin resistance, metabolic syndrome and other obesity related disorders (Klöting and Blüher, 2014). An understanding of how adipose tissue modulates normal cellular processes is the first step in understanding disease related dysfunction. In the following chapters, I will discuss how the involvement of TRPC1 in adipose tissue is imperative to maintaining proper function needed for metabolic energy homeostasis.

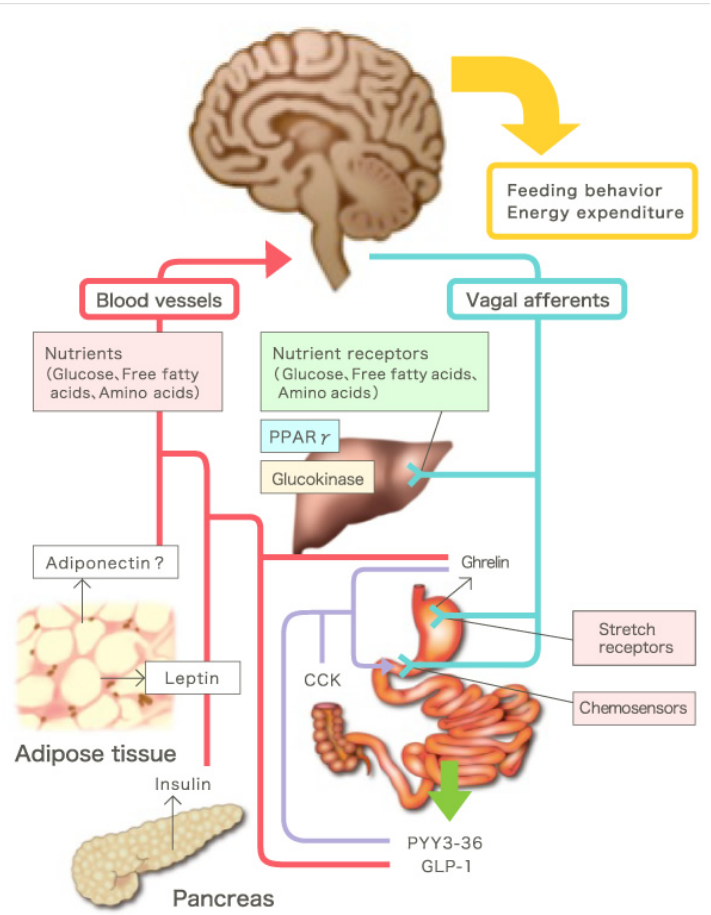

Figure 5 Inter-tissue Communication

Humoral and neuronal pathways allow communication between major organs to regulate metabolic information. Neuronal networks controlled by the brain function as a negative-feedback mechanism to maintain body weight homeostasis, while the liver and other organs possibly representing a positive-feedback mechanism. Reprinted from “Inter-organ metabolic communication involved in energy homeostasis: Potential therapeutic targets for obesity and metabolic syndrome” by T. Yamada, 2008, Pharmacology and Therapeutics, 117(1),11. Copyright 2008 by Elsevier. Reprinted with permission.

CHAPTER II

METHODS

Animals

Chapter III &V

Male B6129SF2/J (WT) or TRPC1 knockout ($TRPC1^{-/-}$) mice (Jackson Laboratories, Bar Harbor, MI) were used for these experiments. All animals were housed in a temperature controlled room under a 12/12 h light/dark cycle with ad libitum access to food and water. All animal experiments were carried out as per the institutional guidelines for the use and care of animals. For high-fat diet and exercise experimentation, four month old males were fed diets containing either 16% (normal-fat, NF) or 45% fat (high-fat, HF) for 12 weeks and subjected to voluntary wheel running exercise. All animal protocols were approved by the institutional IACUC committee.

Chapter IV

Four-month-old male B6129SF2/J (WT) or TRPC1 knockout (KO) mice (Jackson Laboratories, Bar Harbor, MI) were fed diets containing either 16% (normal-fat, NF) or 45% fat (high-fat, HF) for 12 weeks and subjected to voluntary wheel running exercise (exercise, E) or sedentary cage activity (sedentary, S). Experimental groups were labeled according to diet and

exercise conditions yielding eight groups: WT-NF-E, WT-NF-S, WT-HF-E, WT-HF-S, KO-NF-E, KO-NF-S, KO-HF-E, and KO-HF-S. Food intake, body weight, and body composition were measured biweekly on alternating weeks during the experimental feeding period. After 12 weeks, mice were injected with xylazine (Akorn Inc., Decatur, IL) and ketamine (Zoetis Inc., Kalamazoo, MI) and then killed by exsanguination according to the animal use and care protocol approved by the USDA Agricultural Research Service Animal Care and Use Committee.

Stromal vascular fraction (SVF) and primary adipocyte isolation

Subcutaneous and visceral adipose tissue were weighed and digested with 0.5% collagenase type I (Gibco Thermo Fisher Scientific, Waltham, MA) at 37°C for 1 h, adipose tissue cells were filtered using 100 μm nylon cell strainers (Corning Life Sciences, Tewksbury, MA) followed by centrifugation (1000 rpm, 10 min, 4°C) to separate floating primary adipocytes (supernatant) from adipose SVF (cell pellet). The SVF cell pellet was treated with RBC lysis buffer (Sigma Aldrich, St. Louis, MO) then quenched with DMEM (Dulbecco's modified Eagle's medium; high glucose, L-glutamine) and centrifuged (1000 rpm, 10 min, 4°C). Final pellet was resuspended with DMEM + 10% FBS. SVF was plated at 70-80% confluence and grown in DMEM + 10% FBS + Penicillin Streptomycin.

Adipose cell size and number determination

The supernatant from digested adipose tissue (see above) was washed and resuspended in 0.9% NaCl. Adipose cell size and number determination was determined using a Beckman Coulter Multisizer 4 with a 400-μm aperture. The instrument was set to count 6000 particles and the cell suspension was diluted so that coincident counting was <10%. After collection of pulse sizes, the data were expressed as cell numbers per particle diameter.

SVF differentiation

SVF was grown to a minimum of 80% confluence and differentiated for 36 hours in a cocktail of DMEM (10% FBS + Pen/Strep), 25mM glucose, 2 uM dexamethasone (Sigma Aldrich, St. Louis, MO), 300 nM insulin (Sigma Aldrich, St. Louis, MO), and 20 uM PGJ_2 (Caymen Chemical, Ann Arbor, MI). After 36 hours of differentiation, media was removed and cells were grown in DMEM (10% FBS + Pen/Strep) for 7-10 days.

Chapter III

For differentiation experiments utilizing SKF and increased Ca^{2+} concentrations, cells were differentiated with the addition of SKF96365 (Sigma Aldrich, St. Louis, MO) or $CaCl_2$. Final concentrations of Ca^{2+} were 1x-1.8 mM, 2x-3.6mM, 4x-5.4mM.

C2C12 cell culture and differentiation

The mouse skeletal cell line C2C12 was cultured in DMEM (Dulbecco's modified Eagle's medium; high glucose, L-glutamine) + 20% FBS + 1% Pen/Strep and incubated at 37 °C, 5% CO_2. At 80% confluence media was switched to DMEM + 2% horse serum + 1uM Insulin for 3 days and then DMEM + 2% horse serum for the remaining 4-7 days until fully differentiated.

EchoMRI measurements of body composition

Whole body composition, including fat mass and lean mass, was determined biweekly during the 12 week period without sedation using nuclear magnetic resonance technology with the EchoMRI700™ instrument (Echo Medical Systems, Houston, TX).

Red Oil Staining

Culture plates were washed by PBS and cells were fixed in 4% formalin, followed by staining with oil-red-O (Sigma Aldrich, St. Louis, MO) for 10 min, washed, and photographed. The dye was then extracted with 100% isopropanol and the absorbance was determined at 492 nm.

Gas chromatography/mass spectrometry (GC/MS)

Tissue samples were pulverized under liquid nitrogen conditions to a fine homogeneous powder. Lipids were extracted with hexane/2-propanol (3:2, v/v, HIP) as previously described (Saunders and Horrocks, 1984). Briefly, ~10 mg of tissue powder was homogenized in 2 ml of HIP using a 2 mL Tenbroeck tissue grinder (Kontes Glass Co.). HIP contained 0.005% of butylated hydroxytoluene (BHT) to prevent fatty acid oxidation, and a mixture of stable isotope labeled internal standards (Cambridge Isotope Laboratories, Tewksbury, MA) for quantification. For each sample, we used 100 ng of 10:0-$^{2}H_{17}$ for short chain FA quantification, 5 µg of 16:0-$^{13}C_{16}$ for saturated long chain FA, 1 µg of 18:1-$^{13}C_{18}$ for monounsaturated FA, and 1 µg of 20:4n6-$^{2}H_{8}$ for polyunsaturated FA. After centrifugation, HIP supernatant was evaporated under a stream of nitrogen and subjected to saponification to release FA as previously described (Brose et al., 2014). Briefly, lipids were re-dissolved in 260 µL of methanol containing 0.02% BHT (0.158mg/mL) add 40 µL 5M KOH (in water), and saponified at 60°C for 60 min in a water bath. The solution was neutralized with the addition of 20 µL 5 M HCl followed by the addition of 780 µL 0.9% NaCl. The free FA were extracted with 2 mL hexane 3 times. The hexane extracts were combined, dried under nitrogen stream, re-dissolved in 1 mL of hexane, 100 µL (for short chain FA) or 1 µL (for long chain FA) was transferred into micro-inserts (National Scientific,

Rockwoods, TN; catalog No. C4010-S630), evaporated under nitrogen stream, and finally re-dissolved in 100 µL of the initial UPLC gradient for analysis.

UPLC-MS analysis was performed as previously described (Brose et al., 2014; Wang et al., 2014). The UPLC system consisted of a Waters ACQUITY UPLC pump with a well-plate autosampler (Waters, Milford, MA) equipped with an ACUITY UPLC HSS T3 column (1.8 µM, 100 A pore diameter, 2.1×150 mm, Waters) and an ACUITY UPLC HSS T3 Vanguard precolumn (1.8 µM, 100 A pore diameter 2.1 × 5 mm, Waters). One microliter of a sample was injected onto the column. The column temperature was 55°C and the autosampler temperature was 8°C.

Solvent A consisted of acetonitrile : water (40 : 60) with 10 µM ammonium acetate and 0.025% acetic acid. Solvent B was acetonitrile : 2-propanol (10 : 90) containing 10 µM ammonium acetate and 0.02% acetic acid. The flow rate was 0.3 mL/min, and the initial %B was 30%. At 0.1 min %B was increased to 54% over 10 min, to 99% over another 10 min, held at 99% for 8 min, and then returned to initial conditions over 0.5 min. The column was equilibrated for 2.5 min between injections.

FA were quantified using a quadrupole time-of-flight mass spectrometer (Q-TOF, Synapt G2-S, Waters) with electrospray ionization in negative ion mode as described previously (Brose et al., 2014; Wang et al., 2014). The

analyzer was operated with extended dynamic range at 10,000 resolution (fwhm at *m/z* 554) with an acquisition time of 0.1s. MS^E mode was used to collect data. Leucine enkephalin (400 pg/µl, ACN : water, 50 : 50 by volume) was infused at a rate of 10 µl/min for mass correction. MassLynx V4.1 software (Waters) was used for instrument control, acquisition, and sample analysis. FA were quantified against corresponding internal standards using generated standard curves.

Blood collection and serum isolation

Mice were anaesthetized with an injected of xylazine (Akorn Inc., Decatur, IL) and ketamine (Zoetis Inc., Kalamazoo, MI). A 3 cc syringe with a 22-25 gauge x 1" needle was inserted from the posterior aspect and animal was terminally bled. Whole blood was allowed to coagulant for 30 min at room temperature. Blood was then centrifuged at 2,000 x g for 15 minutes at 4°C and serum was removed from clotted blood and frozen at -20°C.

Adiponectin and Leptin Concentrations

Serum, culture media, and protein lysates samples were analyzed for adiponectin and leptin using the adiponectin mouse ELISA kit (Abcam, Cambridge, UK) and Leptin Mouse ELISA kit (Invitrogen, Carlsbad, CA).

Glucose tolerance test

At the end of 12 weeks of feeding, mice were fasted overnight and then injected with 2 g/kg body weight of 20% D-glucose (Sigma Aldrich, St. Louis, MO) intraperitoneally. Approximately 5 µl of tail blood, obtained through tail nick procedure, was used to measure the blood glucose concentrations using the Accu Check Aviva glucometer at baseline and then 15, 30, 60 and 120 min post glucose injection.

Measurement of plasma insulin

Mice were fasted overnight and then plasma was obtained to analyze insulin concentrations (Insulin ELISA kit: EXRMI-13K, EMD Millipore, St. Charles, MO) using the Bio-Rad Luminex system (Hercules, CA) according to manufacturer's protocols.

Electrophysiology

For patch clamp experiments, coverslips with cells were transferred to the recording chamber and perfused with an external Ringer's solution of the following composition (mM): NaCl, 145; CsCl, 5; MgCl2, 1; CaCl2, 1; Hepes, 10; Glucose, 10; pH 7.3 (NaOH). Whole cell currents were recorded using an Axopatch 200B (Axon Instruments, Sunnyvale, CA, USA). The patch pipette had resistances between 3 -5 MΩ after filling with the standard intracellular solution that contained the following (mM): cesium methane

sulfonate, 150; NaCl, 8; Hepes, 10; EGTA, 10; pH 7.2 (CsOH). Basal leak was subtracted from the final currents and average currents are shown. The maximum peak currents were calculated at a holding potential of –80 mV. The voltage-current (I-V) curves were made using a ramp protocol ranging from -100mV to +100mV and 100ms duration were delivered at 2s intervals, whereby current density was evaluated at various membrane potentials and plotted.

Calcium imaging

Cells were incubated with 2uM Fura-2 (Molecular Probes, Eugene, OR, USA) and the fluorescence intensity was monitored with a CCD camera-based imaging system (Compix, Cranbery, PA, USA) mounted on an Olympus (Shinjuku, Tokyo, Japan) XL70 inverted microscope equipped with an Olympus 40× (1.3 NA) objective. A dual wavelength monochromator enabled alternative excitation at 340 and 380 nm, whereas the emission fluorescence was monitored at 510 nm with an Orca Imaging camera (Hamamatsu, Shizuoka Prefecture, Japan). Fluorescence traces shown represent $[Ca^{2+}]i$ values in 340/380 nm ratio that are a representation of results obtained in at least 3-4 individual experiments using 40-70 cells in each experiment.

PCR analysis

Adipose tissue

Total RNA was extracted using the RNeasy Lipid Tissue Mini kit and Qiacube (Qiagen, Valencia, CA) from flash-frozen subcutaneous adipose tissue. cDNA was synthesized using the Quantitect Reverse Transcriptase kit (Qiagen, Valencia, CA) Rox FastStart Universal Probe Master mix assay reagents were purchased from Roche (Indianapolis, IN). Primers were purchased from Integrated DNA Technology (IDT, Coralville, IA). The endogenous control (18S rRNA) was purchased from Applied Biosystems (Foster City, CA). RT-PCR analysis for TRPC1 transcripts was done with primers from the eighth and ninth exons (Up-5' GCAACCTTTGCCCTCAAAGTG and Dn-5' GGAGGAACATT-CCCAGAAATTTCC) after the EcoRI site (Eurofins MWG Operon, Huntsville, AL).

qPCR analysis

Chapter IV

Total RNA was extracted using the RNeasy Lipid Tissue Mini kit and Qiacube (Qiagen, Valencia, CA) from flash-frozen hind leg biceps femoris skeletal muscle or subcutaneous adipose tissue. cDNA was synthesized using the Quantitect Reverse Transcriptase kit (Qiagen, Valencia, CA) and then used to measure expression of glucose transporter type 4 (GLUT4),

hypoxia-inducible factor 1-alpha (HIF1α), fibroblast growth factor 21 (FGF21), peroxisome proliferator-activated receptor gamma (PPARγ), microtubule-associated proteins 1A/1B light chain 3A (MAP1LC3A), and beclin 1 (BECN1) by qPCR (ABI Prism 7500 PCR System, Applied Biosystems, Foster City, CA). Rox FastStart Universal Probe Master mix assay eagents were purchased from Roche (Indianapolis, IN). Primers were purchased from Integrated DNA Technology (IDT, Coralville, IA). The control (18S rRNA) was purchased from Applied Biosystems (Foster City, CA).

Chapter VI

Total RNA was extracted from liver and bicep femoris (BF) skeletal muscle using Quick-RNA Miniprep kit (Zymo Research, Irvine, CA). cDNA was synthesized using the iScript cDNA synthesis kit (Bio-Rad, Hercules, CA) and expression was measured using SsoAdvanced Universal SYBR Green Supermix (Bio-Rad, Hercules, CA). Primers were purchased from Thermo Fisher (Waltham, MA) with the sequences in Table 1. Analysis of expression was calculated by using the endogenous control (18S rRNA) and the ΔΔCT method.

Table 1 Primer Sequences

Symbol	Gene	Accession number	Primer Sequence
ERRα	Estrogen-Related Receptor Alpha	NM_007953.2	fwd-GGAAGTGCTGGTGCTGGGTGT rev-GAATTGGCAAGGGCCAGAGCT
NRF1	Nuclear Respiratory Factor 1	NM_001293164.1	fwd-GGAGCACTTACTGGAGTCC rev-CTGTCCGATATCCTGGTGGT
TFAM	Transcription Factor A	NM_001361693.1	fwd-CCTGAGGAAAAGCAGGCATA rev-ATGTCTCCGGATCGTTTCAC
ACC	Acetyl-Coenzyme A Carboxylase	NM_133360.2	fwd-GTCCCCAGGGATGAACCAATA rev-GCCATGCTCAACCAAAGTAGC
FASN	Fatty Acid Syntase	NM_007988.3	fwd-AGAGATCCCGAGACGCTTCT rev-GCCTGGTAGGCATTCTGTAGT
ACADM	Acyl-Coenzyme A Dehydrogenase, Medium Chain	NM_007382.5	fwd-AGAGCTCTAGACGAAGCCACGA rev-GAGTTCAACCTTCATCGCCATT
PGC1a	PPARG Coactivator 1 Alpha	NM_008904.2	fwd-AAACTTGCTAGCGGTCCTCA rev-TGGCTGGTGCCAGTAAGAG
18s			fwd-GCCGCTAGAGGTGAAATTCTTG rev-CTTTCGCTCTGGTCCGTCTT

Muscle Isolation and Culture

Extensor Digitorum Longus (EDL) muscle was isolated from WT and TRPC1$^{-/-}$ mice and digested using a solution of 0.2% Collagenase type I (Gibco Thermo Fisher Scientific, Waltham, MA) in DMEM (Dulbecco's modified Eagle's medium; high glucose, L-glutamine with 110 mg/ml sodium pyruvate) for 1 hour at 37°C. Tissue was transferred to a horse serum lined dish with DMEM and flushed until individual fibers were released from tissue. Each fiber was moved to a separate dish coated with Matrigel (Corning, Corning, NY) and suspended in DMEM with 20% FBS, 1% Chicken Embryo extract (Accurate Chemical, Westbury, NY) and 1%

Penicillin/Streptomycin. Myofibers were incubated for 4 days at 37 °C, 5% CO_2 without handling to allow myofibers to adhere and activate satellite cells. Following that time frame, media was replaced every other day until cells naturally differentiated ~ 14 days. Confirmation of differentiation was obtained by visually observing new muscle formation and contraction.

Immunoblotting

Crude lysates were prepared from Subc AT and VAT and SVF and differentiated adipocyte cultures. 40 µg of proteins were resolved on NuPAGE Novex 4-12% Bis-Tris gels, transferred to nitrocellulose membranes, and probed with respective antibodies (all from Cell Signaling). Respective peroxidase conjugated secondary antibodies were used to label the proteins, which were then detected by an enhanced chemiluminescence detection kit (SuperSignal West Pico, Pierce, Appleton, WI). Densitometric analysis was performed using image J analysis (National Institutes of Health) and results were corrected for protein loading by normalization to β-actin levels. Non-denaturing PAGE was performed by resolving protein in Novex Tris-Glycine Native Sample Buffer on NuPAGE™ 3-8% Tris-Acetate Protein Gels, transferred to nitrocellulose membranes, and probed with respective antibodies. Membranes were stained with Ponceau S (Sigma Aldrich, St. Louis, MO) and bands were quantified using image J analysis to determine total protein load.

Co-immunoblotting

Subc AT and VAT was manually homogenized in the presence of HBSS containing Ca^{2+} and Mg^{2+} and then treated as described for 30 min at 37°C. Samples were incubated overnight with anti-VAMP2 antibody after which agarose anti-mouse IgG beads were added. Isolated beads were then washed, boiled, and separated by SDS-PAGE. SNARE proteins were detected using the indicated antibodies.

Adiponectin Secretion from Fresh Adipose Tissue

Isolated subcutaneous and visceral adipose tissue was suspended in Hank's balanced salt solution (HBSS) (Gibco) supplemented with 1.26 mM $CaCl_2$, 0.5 mM $MgCl_2$, and 2% bovine serum albumin (Fisher Scientific, Hampton, NH). Adipose tissue was cut into 8-15 mg pieces and suspended in supplemented HBSS for 30 min at 37°C to recover. Samples were then placed into a 96 well plate suspended in DMEM containing 2% BSA, stimulated with 100 nM insulin (Sigma Aldrich, St. Louis, MO) for 6 hours.

Statistical Analysis

Mean and standard error values were computed for all continuous variables and frequency distributions were calculated for all categorical variables using GraphPad Prism 7. Statistical comparisons were made using two-tailed Student's t test or ANOVA and the effects of TRPC1 KO, diet, or

exercise were assessed by three-way ANOVA. When an interaction was significant ($p < 0.05$), Tukey contrasts were used to perform pairwise comparisons. All statistical tests were two-tailed with significant reported as follows: *, $p < 0.05$; **, $p < 0.01$; ***, $p < 0.001$; ****, $p < 0.0001$.

CHAPTER III

LOSS OF TRPC1 IN ADIPOCYTES IMPAIRS DIFFERENTIATION

Introduction

Intracellular Ca^{2+} signaling has been suggested to play several important roles in regulating cellular energy metabolism (Filadi et al., 2017); however, the specific Ca^{2+} ion channels involved have not yet been identified. As we've stated before, TRPC1 functions as a Ca^{2+} entry channel that is found in key metabolic tissues, including the hypothalamus (Qiu et al., 2010), adipose tissue (Sukumar et al., 2012), and skeletal muscle (Zanou et al., 2010), making it a likely candidate for the regulation of cellular energy metabolism. As such, functional disturbance of TRP family channels could play a role in regulating adiposity and obesity-related conditions such as insulin resistance (Graham et al., 2009; Hu et al., 2009; Sabourin et al., 2015).

Adipocytes are vital to maintaining lipid homeostasis and energy balance by storing triglycerides and releasing free fatty acids in response to energy need changes (Rosen and Spiegelman, 2006). Though adipose tissue is an important endocrine organ, excessive accumulation of adipose tissue, defined as obesity, is a major risk factor for insulin resistance and other diseases such as Type II diabetes, dyslipidemia, and cardiovascular disorders (Wu et al., 1999). Adipocytes

are the predominant cell type in adipose tissue; however, not all adipose tissue functions identically. Several studies have shown that anatomical distribution of adipose tissue dictates differing characteristics where subcutaneous adipocytes have distinct metabolic properties from visceral adipocytes (Baglioni et al., 2012). Proliferation of the subcutaneous adipose tissue (Subc AT) may be considered beneficial, in part, by increasing “healthy” lipid storage capacity that produces fewer inflammatory cytokines. Whereas, visceral adipose tissue (VAT) is thought to be more inflammatory (Kadiri et al., 2017; O'Rourke et al., 2009) and leads to the development of obesity and related metabolic diseases (Foster et al., 2011; Seale et al., 2011). Although the debate about the metabolic function of Subc AT and VAT is not yet settled (Fabbrini et al., 2010; Thörne et al., 2002), variances in distribution of lipids in Subc AT and VAT could be critical in the development of metabolic diseases.

One such area to investigate regarding variances between Subc AT and VAT tissues could be the process of differentiation of committed preadipocytes into mature adipocytes. Interestingly, it has been shown that differentiation is impaired in Subc preadipocytes of obese subjects and their ability to differentiate is negatively correlated to BMI and cell size (Isakson et al., 2009). Further, in an obese state, the preadipocyte to mature adipocyte ratio is reduced and the ability of Subc AT to differentiate properly may be diminished pushing the accumulation of fat to visceral depots (Tchoukalova et al., 2007). Similar results have shown an age-dependent decline in differentiation and increases in adipose tissue

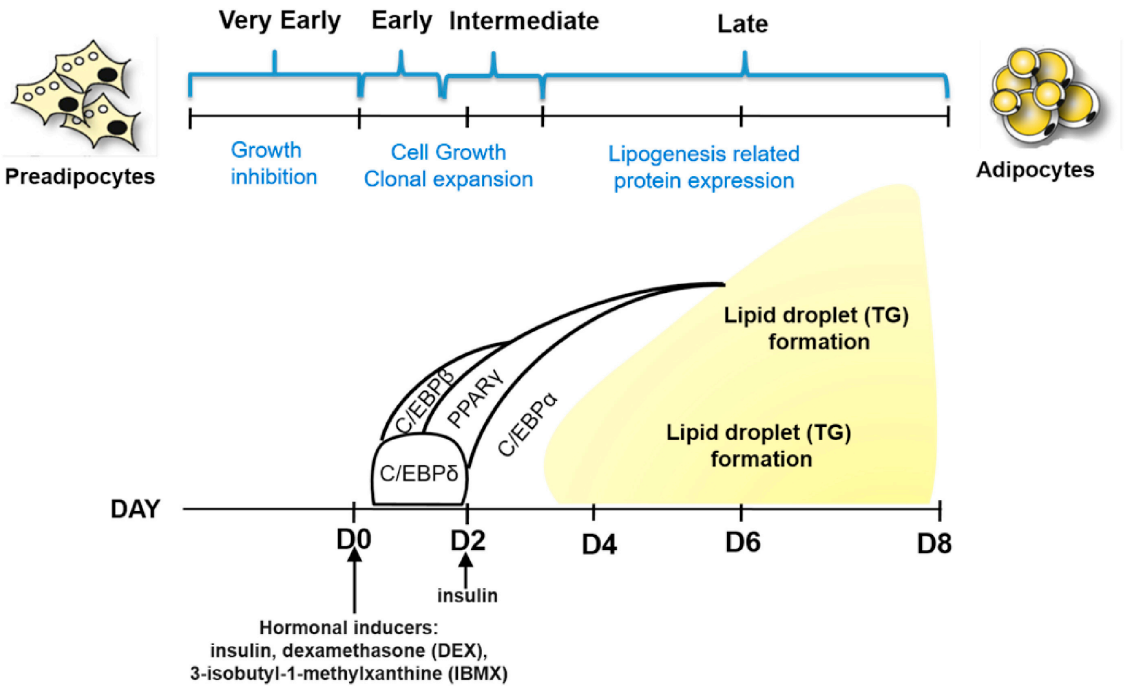

Figure 6 Schematic of adipocyte differentiation

The induction of transcription factors C/EBPβ and C/EBPδ are induced early during adipogenesis with PPARγ induction occurring shortly after. Lipid droplet formation and expression of mature adipocyte proteins such as FAPB4, perilipin, and adiponectin occur during the late stage. Reprinted from “Cellular models for the evaluation of the antiobesity effect of selected phytochemicals from food and herbs” by Y-C. Tung, 2017, Journal of Food and Drug Analysis, 25(1), 100-110. Copyright 2017 by Elsevier. Reprinted with permission.

accumulation in obesity is likely due to hypertrophy instead of hyperplasia (Kim et al., 2014).

Although several nuclear receptors and transcription factors that regulate adipocyte differentiation and adipogenesis have been identified (Farmer, 2006),

factors upstream to the activation of these transcription factors are still unknown. Adipogenesis is an intricate process involving coordinated temporal and spatial control of a transcriptional system which regulates the expression of adipocyte-specific genes (Figure 6). The first step involves the initiation of the CCAAT/enhancer-binding proteins (C/EBPs) family of transcription factors including C/EBPβ and C/EBPδ with C/EBPα and Peroxisome proliferator–activated receptor γ (PPARγ) activation occurring in the intermediate or late stage of adipogenesis (Garin-Shkolnik et al., 2014). Although the C/EBP transcription factors seem to work in conjunction with PPARγ, PPARγ has been determined to have a dominant role and functions as a master regulator of adipogenesis (Haider et al., 2017). PPARγ has been linked to the transcription of genes expressed in mature adipocytes such as fatty acid binding protein (FABP4), required for transport of free fatty acids, and perilipin (PLIN1), which covers the surface of mature lipid droplets in adipocytes and regulates lipolysis. PPARγ also regulates lipoprotein lipase (LPL), adiponectin (ADIPOQ), fatty acid transporter CD36 (CD36), glycerol-3-phosphate dehydrogenase (GPD1), and insulin-responsive glucose transporter 4 (GLUT4), all involved in regulating lipid and glucose metabolism (Rosen et al., 1999; Siersbaek et al., 2010; Tung et al., 2017). Not surprisingly, several studies have demonstrated that PPARγ has a role in metabolic diseases. Mutations to the PPARγ gene have been linked to type II diabetes, obesity, hypertension and insulin resistance (Pap et al., 2016), while adipose-specific knockout of PPARγ in mice fed a high-fat diet display insulin

resistance in adipose tissue and liver, but not in muscle (He et al., 2003). PPARγ agonists, such as rosiglitazone and pioglitazone, which are part of the thiazolidinediones (TZD) family, have been widely used in the treatment of type II diabetes due to their ability to enhance insulin sensitivity and increase adiponectin levels (Mooradian et al., 2002; Saltiel and Olefsky, 1996; Yang et al., 2002).

Calcium has been identified as important for the transcriptional regulation of adipocyte differentiation; however, the molecular identity of the Ca^{2+} channel has yet to be identified. Studies on preadipocytes show that elevating $[Ca^{2+}]i$ early in differentiation inhibits PPARγ induction and triglyceride accumulation (Neal and Clipstone, 2002; Shi et al., 2000). Similarly, elevating extracellular Ca^{2+} concentrations, with no change in $[Ca^{2+}]i$, inhibited adipocyte differentiation in white (Jensen et al., 2004) and brown (Pramme-Steinwachs et al., 2017) adipocytes. In contrast, elevations of $[Ca^{2+}]i$ during late adipogenesis promoted lipogenesis and GPDH activity in white adipocytes (Shi et al., 2000). Though elevating extracellular calcium concentrations had negative effects on white and brown adipocyte differentiation, reducing extracellular concentrations had the opposite effect on brown adipocytes where decreased levels increased brown adipocyte differentiation (Pramme-Steinwachs et al., 2017). Finally, initiating a Ca^{2+} response through the usage of angiotensin II is known to modulate adipocyte proliferation and differentiation, triglyceride accumulation, expression of adipokine-encoding genes and adipokine secretion (Shum et al., 2013). Together these studies demonstrate the importance of modulating Ca^{2+} during differentiation,

however the mechanism and channel necessary is still unknown. Microarray analysis has shown both TRPC1 and TRPC5 expression are amplified when 3T3-L1 adipocytes mature; however, the physiological characterization of the Ca^{2+} entry channel in subcutaneous and visceral adipocytes is still missing (Sukumar et al., 2012). Additional data from this study is shown in Figure 7 confirming the expression of TRPC1 and TRPC5 in mouse epididymal adipose tissue and perivascular adipose from humans with coronary artery disease (CAD). It is notable that this study found TRPC1 expression surmounted TRPC5 expression at both the RNA and protein level. It was also recently shown in El Hachmane et al., 2018 that SOCE proteins STIM1, ORAI1, and TRPC1 are highly expressed in 3T3-L1 adipocyte cell line and play a functional role in SOCE mechanisms further indicating the importance of TRPC1 in adipose function.

The aim of this study was to identify the endogenous Ca^{2+} entry channel in adipocytes cells and establish its physiological function in modulating adipocyte differentiation. We report for the first time the adipose tissue-dependent differences in sensitivity to SOCE, differentiation, and lipid accumulation. We further report that the endogenous Ca^{2+} entry channel in adipocytes is dependent on TRPC1 and loss of TRPC1 function inhibits adipocyte differentiation. These results suggest TRPC1 is crucial for adipocytes differentiation, which plays an important role in regulating metabolic homeostasis.

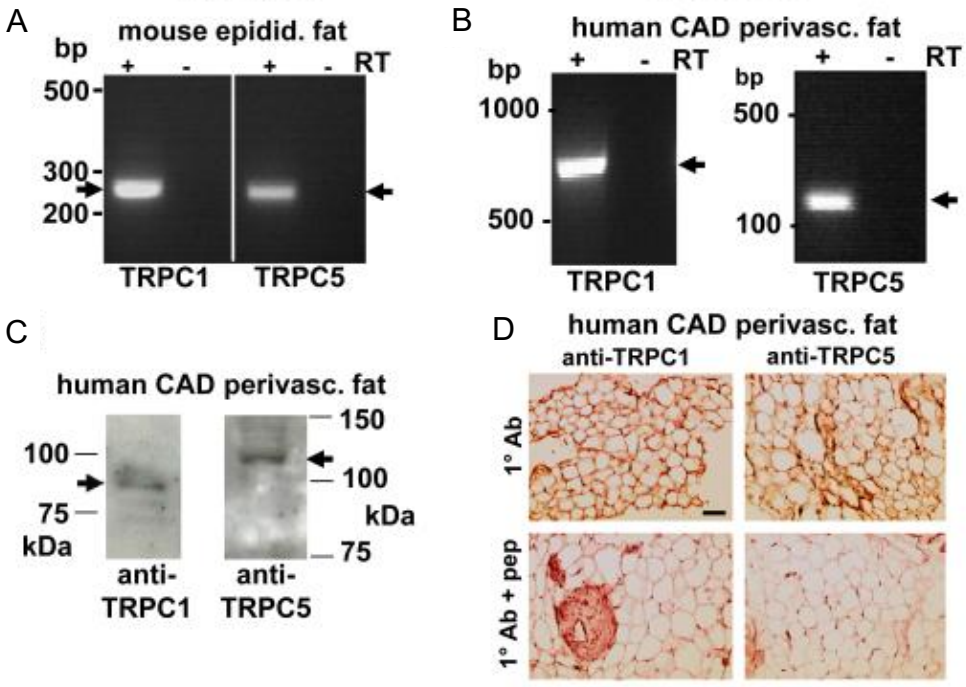

Figure 7 TRPC1 and TRPC5 expression in mouse and human adipose

(A) RNA RT-PCR products from mouse epididymal adipose tissue. Analysis of mRNA from human coronary artery disease (CAD) perivascular adipose by RT-PCR (B) and western blot protein (C). (D) Immunostaining (brown colour in the upper panels indicates channel detection) of TRPC1 and TRPC5. The control was the antibody (Ab) preadsorbed to its antigenic peptide (+pep). Scale bar, 100 μm. Reprinted from "Constitutively Active TRPC Channels of Adipocytes Confer a Mechanism for Sensing Dietary Fatty Acids and Regulating Adiponectin", P. Sukumar, 2012, Circulation Research, 111(2), 191-200. Copyright 2012 by Wolters Kluwer Health, Inc. Reprinted with permission.

Results

Subcutaneous and visceral adipocytes display SOCE mechanisms

To establish the molecular identity of the SOCE channel in adipose cells, we evaluated Ca^{2+} signaling in isolated stromal vascular fraction (SVF) of mouse adipose tissue. Addition of thapsigargin (1mM, Tg), a SERCA pump blocker that causes loss of Ca^{2+} from the internal ER stores, showed a small increase in intracellular Ca^{2+} ($[Ca^{2+}]_i$) levels (first peak) in subcutaneous adipose tissue (Subc AT) SVF cells (Figure 8 A, B). Addition of 1mM external Ca^{2+}, Subc AT SVF cells showed a significant increase in $[Ca^{2+}]_i$ (second peak), indicating the presence of store-mediated Ca^{2+} entry (Figure 8 A, B). Importantly, Subc AT SVF cells treated with SKF96365 (10mM SKF, a blocker of store-mediated Ca^{2+} influx channels) were observed to have a significant reduction in SOCE without any change in internal ER Ca^{2+} release (Figure 8 A, B).

To establish the molecular identity of the Ca^{2+} influx channel in Subc AT SVF cells, electrophysiological recordings of membrane currents were performed. Addition of Tg induced an inward current, which was non-selective in nature and reversed between 0 and -5 mV (Figure 8 C, D). The current properties observed in Subc AT SVF cells were similar with previous recordings observed of TRPC1 channels (Liu et al., 2004; Selvaraj et al., 2012; Shi et al., 2012; Yuan et al., 2007). Moreover, pretreatment with SKF significantly inhibited the Tg-induced

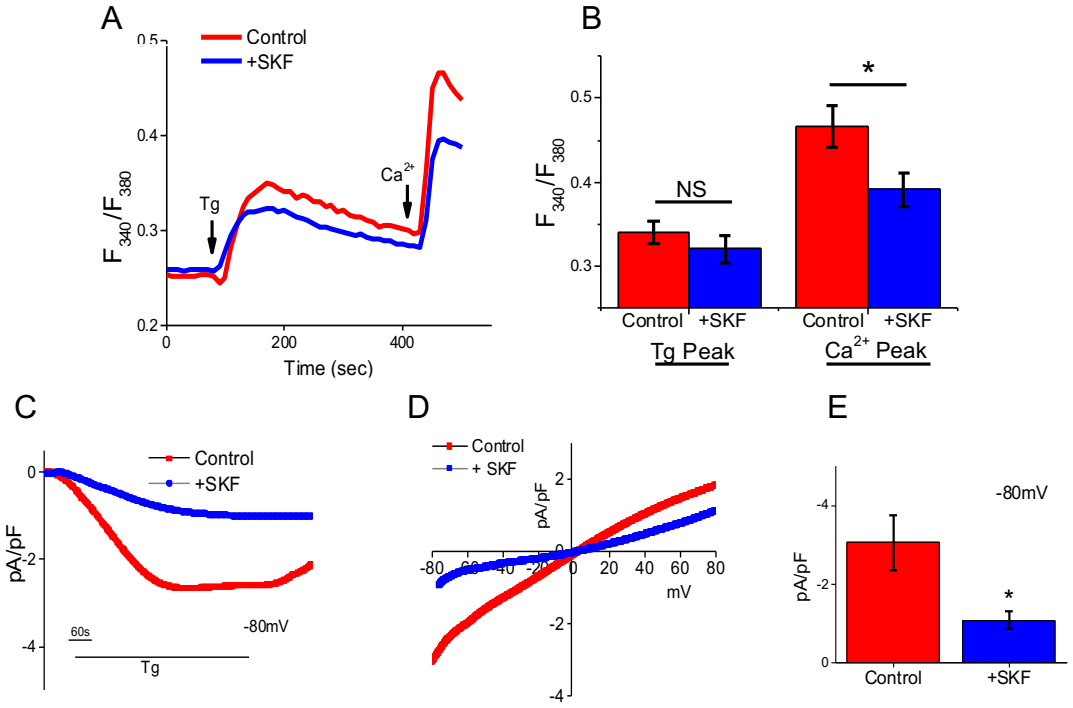

Figure 8 Subc AT SVF exhibits SOCE

Representative Fura-2 traces showing the transient increase in $[Ca^{2+}]_i$ after addition of 1 µM Tg and 1 mM Ca^{2+} to Subc AT SVF cells (A) in control and cells pretreated with 10 µM SKF for 15 min. Bar diagram quantifies Tg-induced ER Ca^{2+} release and Ca^{2+} entry peaks for Subc AT SVF cells (B) under these conditions. Each bar gives the mean ± SEM of 40–60 cells in three separate experiments. Application 1 µM Tg in bath solution induced inward currents at −80mV in control and SKF treated Subc AT SVF cells (C). Respectively IV curves under these conditions are shown for Subc AT SVF in (D). Quantitation (n = 7 recordings) of current intensity at −80 mV is shown for Subc AT SVF in (E). Graphs are mean ± SEM, significance: *, $p < 0.05$.

nonselective current (Figure 8 C-E), suggesting that in Subc AT SVF cells, the SOCE mechanism is dependent on TRPC1 channels.

We next evaluated the physiological properties of the SOCE channels in differentiated adipocytes from Subc AT. Samples taken from both Subc AT deposits were cultured and differentiated into mature adipocytes ex vivo. Similar to the observed response in Subc AT SVF cells, differentiated Subc adipocytes showed no change in the ER Ca^{2+} release (upon addition of Tg, 1mM) (Figure 9 A,B). Addition of 1mM external Ca^{2+} again resulted in an increase in $[Ca^{2+}]_i$, which were significantly reduced when treated with SKF as compared to untreated Control (Figure 9 A,B). Furthermore, a similar TRPC1-like current was observed in differentiated Subc AT adipocytes during whole cell patch clamp recordings and the Tg-induced currents were again inhibited by SKF (Figure 9 C-E). Comparison of Current-Voltage (I-V) Curves of Subc AT SVF and differentiated Subc AT adipocytes indicated a ~25% increase in amplitude of TRPC1-like currents in differentiated Subc AT (Figure 8 E, Figure 9 E).

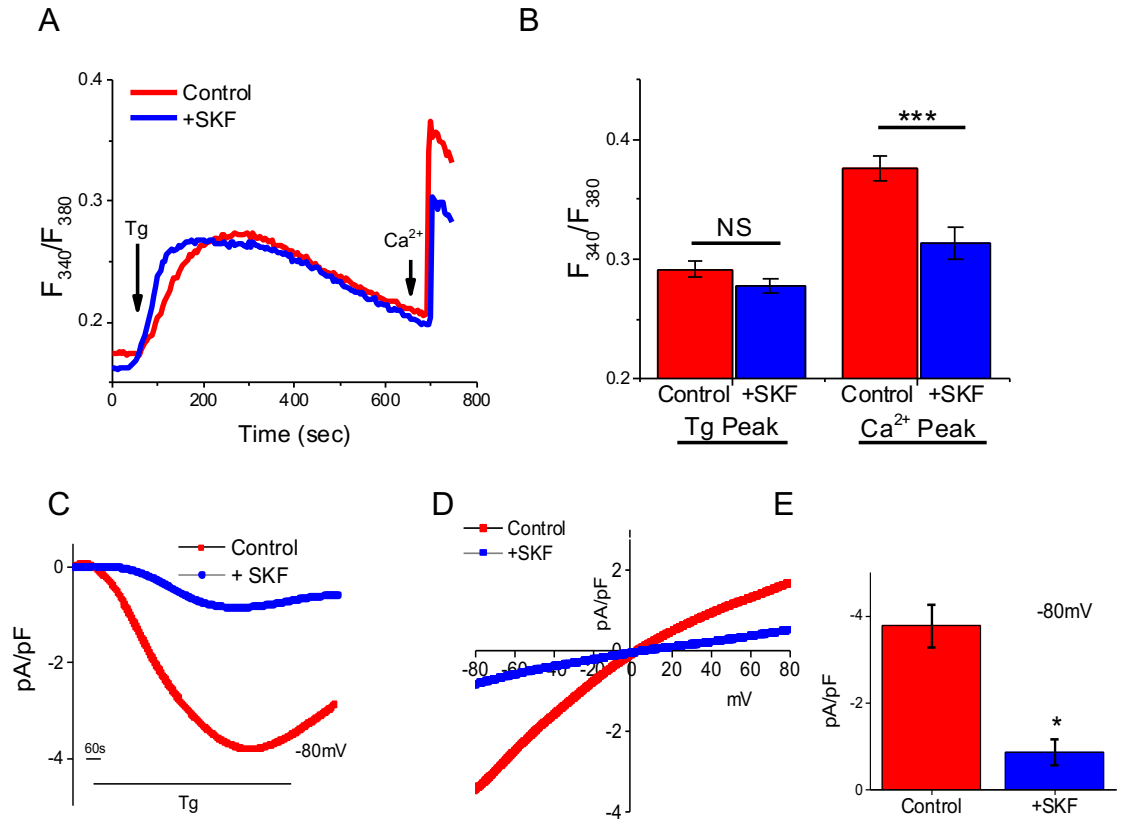

Figure 9 Blockage of SOCE in differentiated Subc AT by SKF

Representative Fura-2 traces showing the transient $[Ca^{2+}]_i$ after addition of 1 μM Tg and 1 mM Ca^{2+} to differentiated Subc AT (A) in control and cells pretreated with 10 μM SKF for 15 min. (B) Bar diagram quantifies Tg-induced ER Ca^{2+} release and Ca^{2+} entry peaks under these conditions. Each bar gives the mean ± SEM of 40–60 cells in three separate experiments. Application 1 μM Tg in bath solution induced inward currents at −80mV in control and SKF treated differentiated Subc AT (C). Respectively IV curves under these conditions are shown in (D). Quantitation (n = 7 recordings) of current intensity at −80 mV is shown in (E). Graphs are mean ± SEM, significance: *, $p < 0.05$; ***, $p < 0.001$.

To confirm that TRPC1 is involved in modulating SOCE, protein expression of TRPC1, STIM1, and ORAI1 in both Subc AT SVF and differentiated Subc AT was analyzed. Consistent with other studies, expression of TRPC1 and STIM1 was increased upon differentiation (Graham et al., 2009; Sukumar et al., 2012); however, there was no change in ORAI1 expression (Figure 10 A, C). Known markers of adipocyte differentiation, FABP4 and perilipin, were used to confirm differentiation.

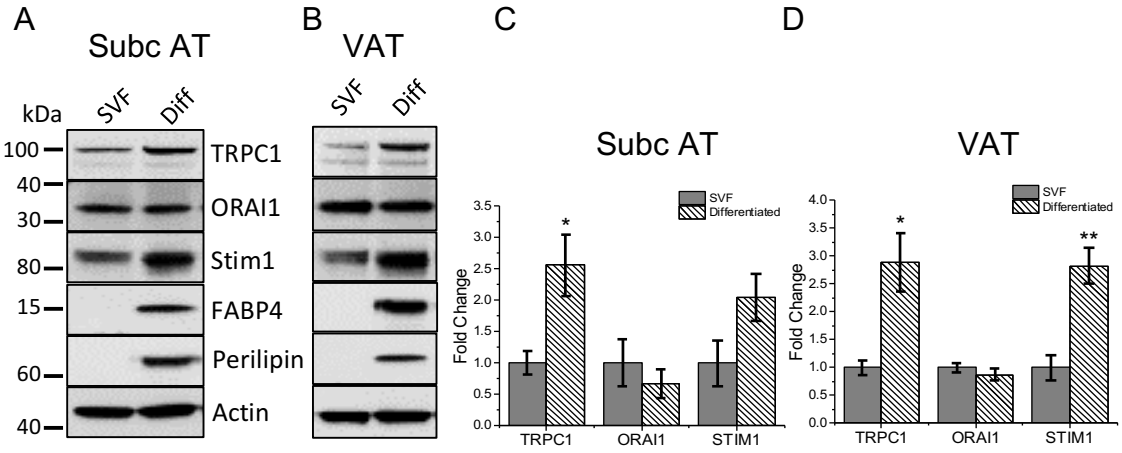

Figure 10 Changes in Ca^{2+} channel expression during differentiation in Subc AT and VAT

Western blot and quantification of TRPC1, ORAI1, Stim1, FAPB4, and perilipin protein expression normalized to actin of Subc AT SVF and differentiated Subc AT (A,C) and VAT SVF and differentiated VAT (B,D). Graphs are mean ± SEM, significance: *, $p < 0.05$; **, $p < 0.01$.

Differentiated visceral adipocytes exhibit increased store-operated Ca^{2+} entry

White AT has different properties based on its location. It is well known that visceral adipose tissue (VAT), when compared with Subc AT, is functionally different in that VAT has higher inflammatory potential (Zhou et al., 2007) due to increased localization of inflammatory and immune cells. VAT has greater oxidative capacity and lipolysis potential than Subc AT and less capacity to differentiate resulting in a greater percentage of large adipocytes as compared to Subc AT (Ibrahim, 2010). To date, it is unknown whether store-mediated changes in $[Ca^{2+}]_i$ leading to adipocyte differentiation is analogous between VAT and Subc AT. Thus, we investigated SOCE from adipocytes derived from the VAT depots. Consistent with Subc AT protein expression, STIM1, ORAI1 and TRPC1 were expressed in both VAT SVF and differentiated VAT adipocytes with increased expression of STIM1 and TRPC1 seen in differentiated VAT, and again no change in ORAI1 expression (Figure 10 B, D).

Measurements of membrane current recordings of VAT SVF adipocytes induced upon the addition of Tg (1mM) showed an inward TRPC1-like current and pretreatment with SKF (10mM) significantly inhibited the nonselective current (Figure 11 A, B). Importantly, after differentiation, the similar TRPC1-like current was observed in VAT cells (Figure 11 D, E) and a ~50% increase in the current amplitude was observed upon differentiation (Figure 11 C, F). Again Tg-induced

currents were inhibited by the addition of SKF in differentiated VAT adipocytes (Figure 11 D, E).

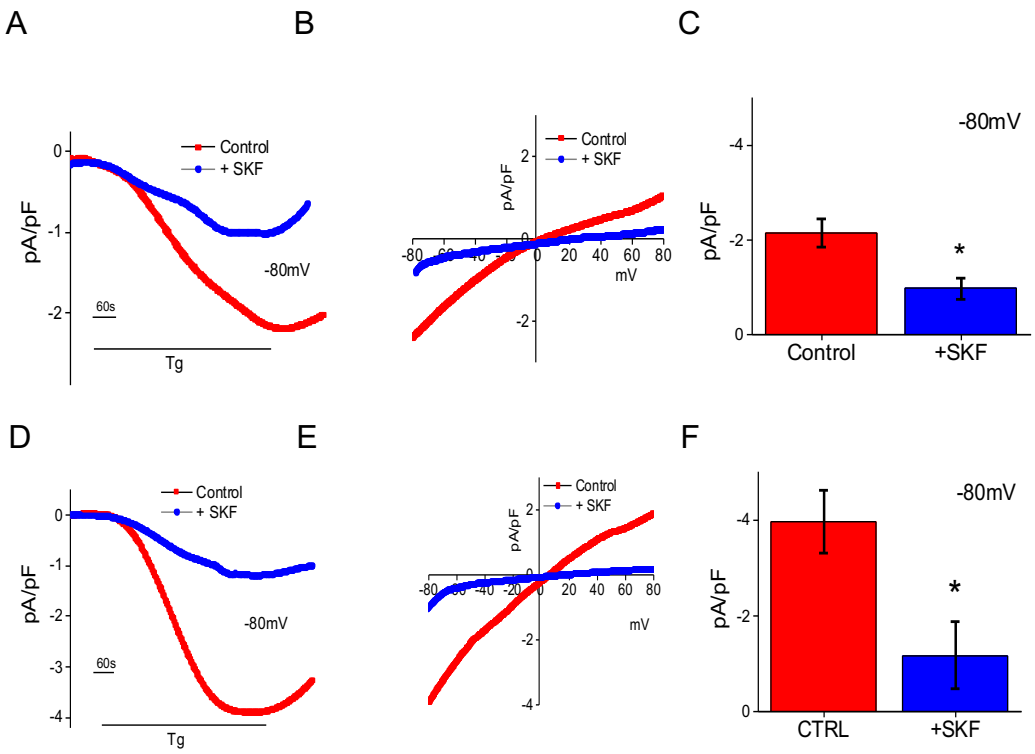

Figure 11 Increased SOCE currents in differentiated VAT

Application of 1 µM Tg in bath solution induced inward currents at −80mV in control and SKF treated VAT SVF cells (A) and differentiated VAT (D). Respectively IV curves under these conditions are shown for VAT SVF in (B) and differentiated VAT in (E). Quantitation (n = 5 recordings) of current intensity at −80 mV is shown for VAT SVF in (C) and differentiated VAT in (F). Graphs are mean ± SEM, significance: *, $p < 0.05$.

Calcium imaging of VAT SVF adipocytes treated with SKF had no change in internal Ca^{2+} release, but had a significant reduction in SOCE upon the addition of 1mM external Ca^{2+} (Figure 12 A, B). However, differentiated VAT adipocytes treated with SKF showed a reduction in both internal Ca^{2+} ER store release upon

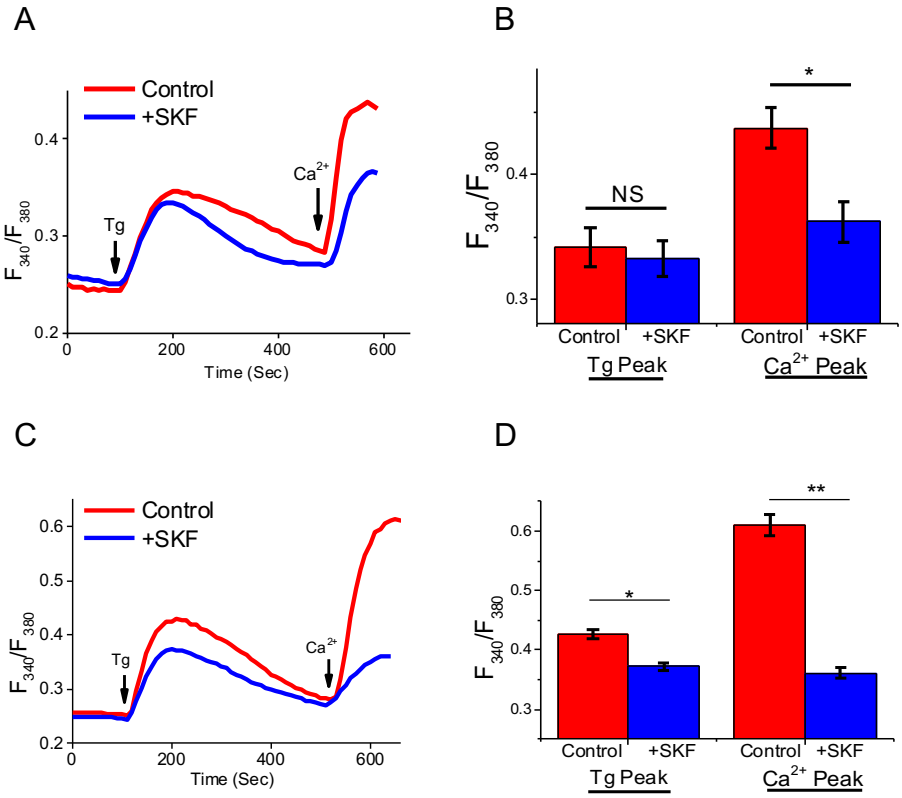

Figure 12 Fura-2 Traces of SVF and differentiated VAT

Representative Fura-2 traces showing the transient increase in $[Ca^{2+}]_i$ after addition of 1 μM Tg and 1 mM Ca^{2+} to VAT SVF cells (A) and differentiated VAT (C) pretreated with 10 μM SKF for 15 min. Bar diagram quantifies Fura-2 Tg and Ca^{2+} peaks for VAT SVF cells (B) and differentiated VAT (D). Each bar gives the mean ± SEM of 40–60 cells in three separate experiments. Graphs are mean ± SEM, significance: *, $p < 0.05$; **, $p < 0.01$.

Tg treatment and SOCE upon addition of external Ca^{2+} which could be attributed to slightly smaller ER stores in the cells sampled or a specific response of differentiated VAT to SKF (Figure 12 C, D). These results indicate that differentiated VAT adipocytes may be more sensitive to alterations in store-operated Ca^{2+} entry than VAT SVF adipocytes, however the properties of both Subc AT and VAT exhibit similar SOCE functionality.

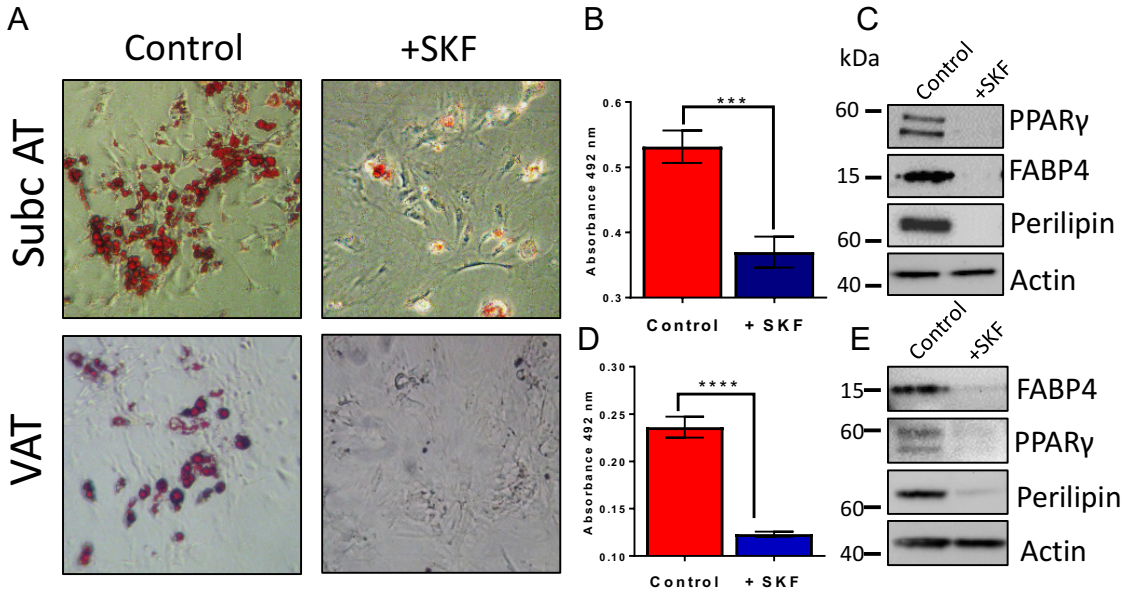

Figure 13 Inhibition of SOCE impairs ability of adipocytes to differentiate

(A) Oil-red-o staining (using 10X objective) of Subc AT and VAT differentiated in the presence of SKF (10 μM) for 7 days. Quantification of absorbance at 492nm of stained lipid droplets using eluted oil-red-o stain for Subc AT (B) and VAT (D). Western blot of PPARγ, FAPB4, and perilipin protein expression of Subc AT (C) and VAT (E) differentiated in the presence of SKF. Graphs are mean ± SEM, significance: ***, $p < 0.001$; ****, $p < 0.0001$.

Inhibition of SOCE impairs ability of adipocytes to differentiate

Impaired differentiation of preadipocytes has been shown in obese subjects (Isakson et al., 2009). Interestingly, altering $[Ca^{2+}]_i$ inhibits differentiation of adipocytes (Jensen et al., 2004; Neal and Clipstone, 2002), however to date, it is unknown whether store-mediated changes in $[Ca^{2+}]_i$ leading to adipocyte differentiation is analogous between VAT and Subc AT. To investigate, we first blocked SOCE by pretreating cells with SKF and then initiated differentiation. Subc AT and VAT SVF adipocytes were differentiated in the continuous presence of SKF (10 mM) for 7 days and lipid accumulation was detected by oil-red-O (Figure 13 A). Oil-red-o stains neutral triglycerides and lipids and the absorbance at 492 nm can be used to quantify total lipid in sample. As such, treatment with SKF significantly reduced the ability of both Subc AT and VAT SVF cells to accumulate intracellular lipids (Figure 13 B, D). Expression of PPARγ, FABP4, and perilipin is absent in undifferentiated preadipocytes, thus measuring their protein expression level is a measurement of adipogenesis. In both Subc AT and VAT, treatment with SKF blocked nearly all expression of FABP4, perilipin, and PPARγ (Figure 13 C, E). These results further indicate the involvement of SOCE mediated Ca^{2+} influx in adipocyte differentiation and that it may be necessary for early stages of transcriptional regulation.

Loss of TRPC1 in adipocytes reduces SOCE

Since TRPC1 is an active member of SOCE mechanisms and is highly expressed in adipocytes, we explored whether TRPC1 is vital to adipocyte differentiation. To do this, SVF cells from TRPC1$^{-/-}$ and WT mice were isolated and differentiated. Analysis by Ca^{2+} imaging of both Subc AT cell types (SVF and differentiated adipocytes) showed TRPC1$^{-/-}$ cells had a reduction in internal ER Ca^{2+} release (first peak) with the addition of Tg as compared to WT (Figure 14 A-D). When 1mM external Ca^{2+} was added, $[Ca^{2+}]_i$ in both SVF and differentiated TRPC1$^{-/-}$ cells was significantly reduced as compared to WT indicating diminished SOCE in TRPC1$^{-/-}$ cells. The TRPC1-like membrane current observed in WT Subc SVF adipocytes upon the addition of Tg (1mM) was significantly reduced in Subc AT SVF from TRPC1$^{-/-}$ mice (Figure 14 E-G). Similar results were observed in differentiated Subc AT, where loss of TRPC1 significantly decreased Tg-mediated Ca^{2+} currents (Figure 14 H-J).

To confirm that lack of TRPC1 alters SOCE mechanisms in differentiated Sub AT, we depleted internal stores through treatment with angiotensin II, which stimulates endogenous G-protein coupled receptors. Addition of angiotensin II resulted in a decrease of Ca^{2+} entry in TRPC1$^{-/-}$ differentiated Subc AT indicating that TRPC1 is the functional store/receptor-operated Ca^{2+} entry (S/ROCE) channel in these cells (Figure 15 A, B). Importantly, basal Ca^{2+} entry (no store depletion) was unaltered in adipocytes from WT or TRPC1$^{-/-}$ mice (Figure 15 C, D).

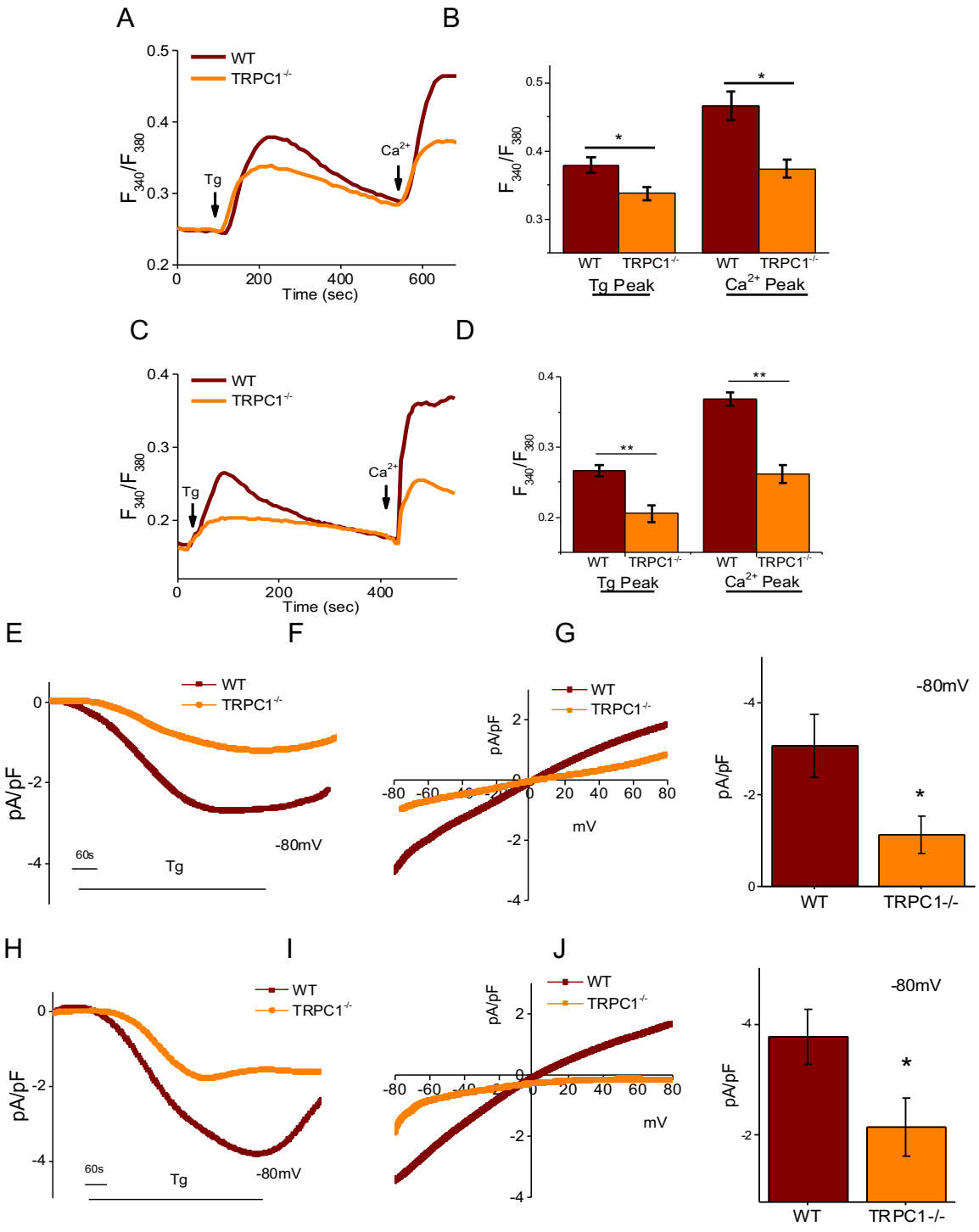

Figure 14 Loss of TRPC1 in adipocytes reduces SOCE

Figure 14 Loss of TRPC1 in adipocytes reduces SOCE

Fura-2 traces and quantification of transient increase in $[Ca^{2+}]i$ after addition of 1 µM Tg and 1 mM Ca^{2+} to WT and $TRPC1^{-/-}$ Subc AT SVF (A, B) and differentiated Subc AT (C, D). Application of 1 µM Tg induced inward currents at −80mV in WT Control and $TRPC1^{-/-}$ Subc AT SVF (E) and differentiated Subc AT (H). Respective IV curves of Subc AT SVF (F) and differentiated Subc AT (I). Quantification (n = 5 recordings) of current intensity at −80 mV is shown for Subc AT SVF in (G) and differentiated Subc AT in (J). Graphs are mean ± SEM, significance: *, $p < 0.05$; **, $p < 0.01$.

Figure 15 Angiotensin II treatment of differentiated Subc AT

Analog plots of Ca^{2+} entry upon addition of angiotensin II in a Ca^{2+} containing media from an average of 30-50 cells isolated from WT or TRPC-/- mice are shown in B. Quantification (mean ± S.D.) of 340/380 ratio under these conditions is shown in B. Basal Ca^{2+} entry (without store-depletion) from an average of 40-50 cells in each condition are shown in C. (D) Quantification (mean ± S.D.) of 340/380 ratio. significance: *, $p < 0.05$; ***, $p < 0.001$.

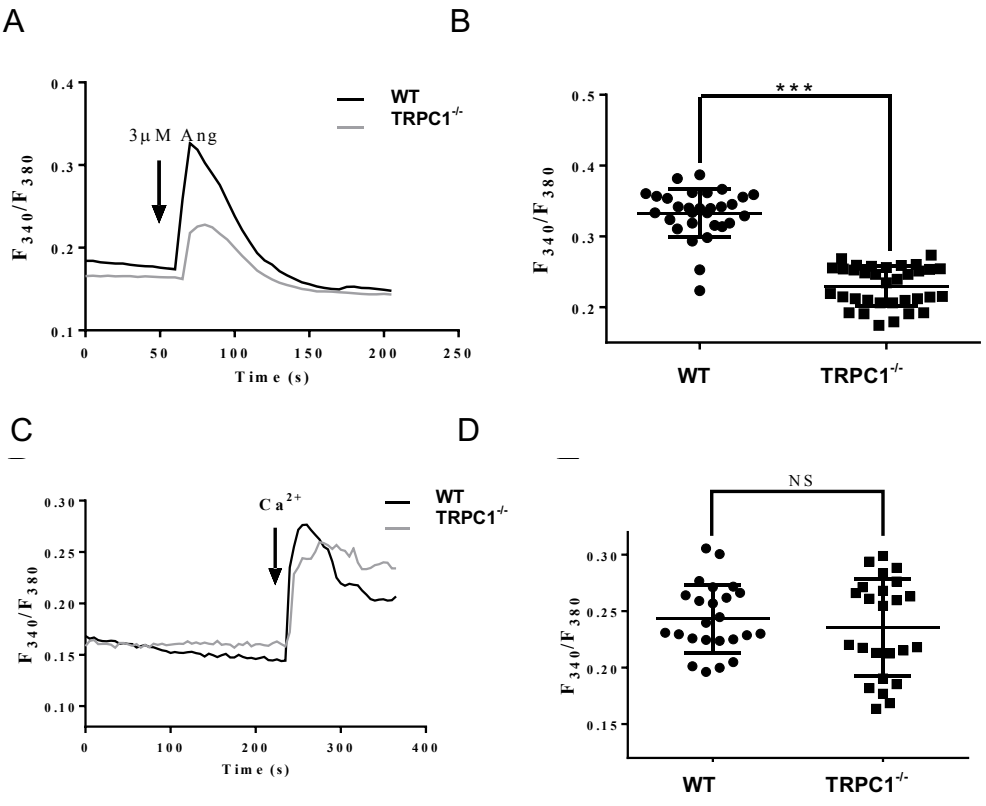

Next, isolated VAT from WT and TRPC1$^{-/-}$ mice was evaluated in the same manner as the Subc AT experiments. Electrophysiological recordings of membrane currents indicate TRPC1 currents were significantly reduced in both VAT SVF TRPC1$^{-/-}$ cells (Figure 16 A-C) and differentiated TRPC1$^{-/-}$ VAT (Figure

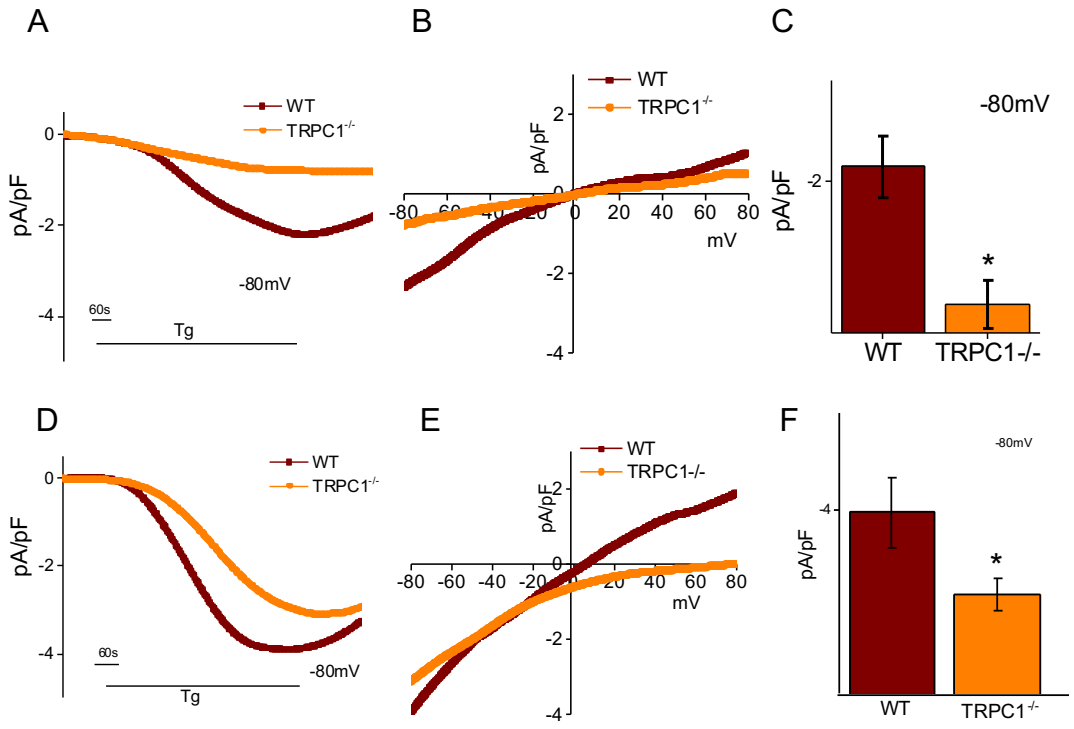

Figure 16 SOCE currents in visceral adipocytes reduced

Application of 1 μM Tg induced inward currents at −80mV in WT Control and TRPC1$^{-/-}$ VAT SVF cells (A) and differentiated VAT (D). Respective IV curves for each cell type are shown for VAT SVF (B) and differentiated VAT (E). Quantitation (n = 5 recordings) of current intensity at −80 mV for VAT SVF (C) and differentiated VAT (F). Graphs are mean ± SEM, significance: *, $p < 0.05$.

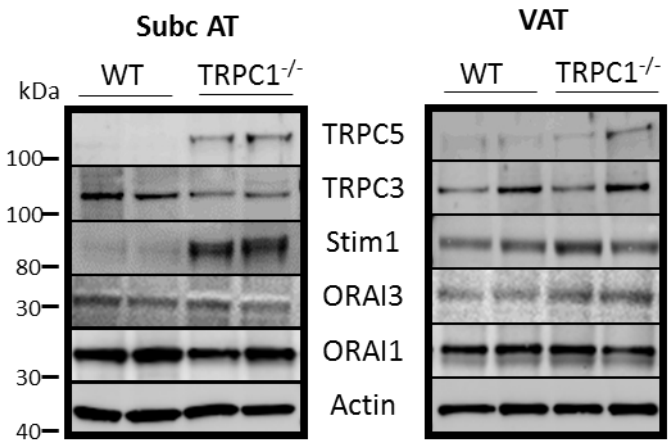

Figure 17 Ca^{2+} channel expression of WT and $TRPC1^{-/-}$ Subc AT and VAT

Western blot of TRPC5, TRPC3, STIM1, ORAI3, and ORAI1 protein expression of WT and $TRPC1^{-/-}$ Subc AT and VAT tissue lysates.

16 D-F). Interestingly, after differentiation, the Ca^{2+} current in $TRPC1^{-/-}$ VAT was more inwardly rectifying and showed properties similar to ORAI1 currents. Analysis of Ca^{2+} influx upon treatment with Tg showed a decrease in internal ER Ca^{2+} release in $TRPC1^{-/-}$ differentiated VAT adipocytes but not in undifferentiated VAT SVF (**Error! Reference source not found.** A-D). Similar to Subc AT, addition of external Ca^{2+} resulted in a reduction in Ca^{2+} influx in both types (SVF and differentiated) of $TRPC1^{-/-}$ VAT as compared to WT control (**Error! Reference source not found.** A-D). Combined data from Subc AT and VAT indicates SOCE mechanisms in SVF and differentiated adipocytes from both depots are impaired due to the loss of TRPC1.

Protein expression analysis of numerous Ca^{2+} regulating proteins in WT and $TRPC1^{-/-}$ Subc AT and VAT was performed to rule out compensation for the lack of TRPC1. As shown in Figure 18, an increase in STIM1 and TRPC5 expression was observed in Subc AT of $TRPC1^{-/-}$ mice which is consistent with our previous

work (Krout et al., 2017). However, no significant change in either STIM1 or TRPC5 was observed in VAT. It is known that TRPC1 forms a C1/C5 heterotetramer with TRPC5 (Shi et al., 2012), however loss of TRPC1 would make TRPC5 inactive and thus not compensate for the loss of TRPC1 in $TRPC1^{-/-}$ mice. Interestingly, increasing STIM1 expression has been shown to have no effect on normal SOCE mechanisms (Gwozdz et al., 2012). The remaining Ca^{2+} channels, TRPC3, ORAI1, and ORAI3, showed no change in protein expression between WT and $TRPC1^{-/-}$ in either tissue type (Figure 18). This indicates the lack of TRPC1 function in adipose tissue most likely does not increase Ca^{2+} entry by altering protein expression of other Ca^{2+} channels.

Lack of TRPC1 mediated Ca^{2+} influx reduces ability to differentiate

We next investigated whether a lack of TRPC1 would alter the ability of Subc and VAT SVF cells to differentiate. Analysis of lipid accumulation via oil-red-o in WT and $TRPC1^{-/-}$ adipocytes after seven days of differentiation revealed a significant reduction in total lipid when TRPC1 is nonfunctional in Subc AT (Figure 19 A, B) and VAT (Figure 19 C, D). This same phenomenon is replicated in the protein expression of perilipin, FABP4, and PPARγ which were also reduced in $TRPC1^{-/-}$ Subc AT (Figure 20 A, B) and VAT (Figure 20 C, D) as compared to WT. To offset the reduced ability to increase $[Ca^{2+}]_i$ of $TRPC1^{-/-}$ cells, Subc AT and VAT SVF cells from WT and $TRPC1^{-/-}$ mice were differentiated with a 2 and 4 fold greater extracellular Ca^{2+} concentration than basal. In WT and $TRPC1^{-/-}$ Subc AT

cells, increasing extracellular Ca^{2+} to both 2 and 4 fold produced no change in lipid accumulation (Figure 19 A, B). No difference in lipid accumulation was observed when extracellular Ca^{2+} concentrations were increased in TRPC1$^{-/-}$ VAT, however WT VAT adipocytes differentiated with a 4 fold greater extracellular Ca^{2+} concentration had significantly less lipid than basal (Figure 19 C, D). We next assessed whether the reduction in lipid accumulation due to increased

extracellular Ca^{2+} was replicated in adipogenetic protein expression. In WT Subc AT there was a significant reduction in expression of PPARγ and perilipin when extracellular Ca^{2+} concentration was raised to 4-fold, however the expression of FABP4 did not seem to be altered in either tissue type (Figure 20 A, B). Raising extracellular Ca^{2+} concentrations in TRPC1$^{-/-}$ Subc AT and VAT had similar results

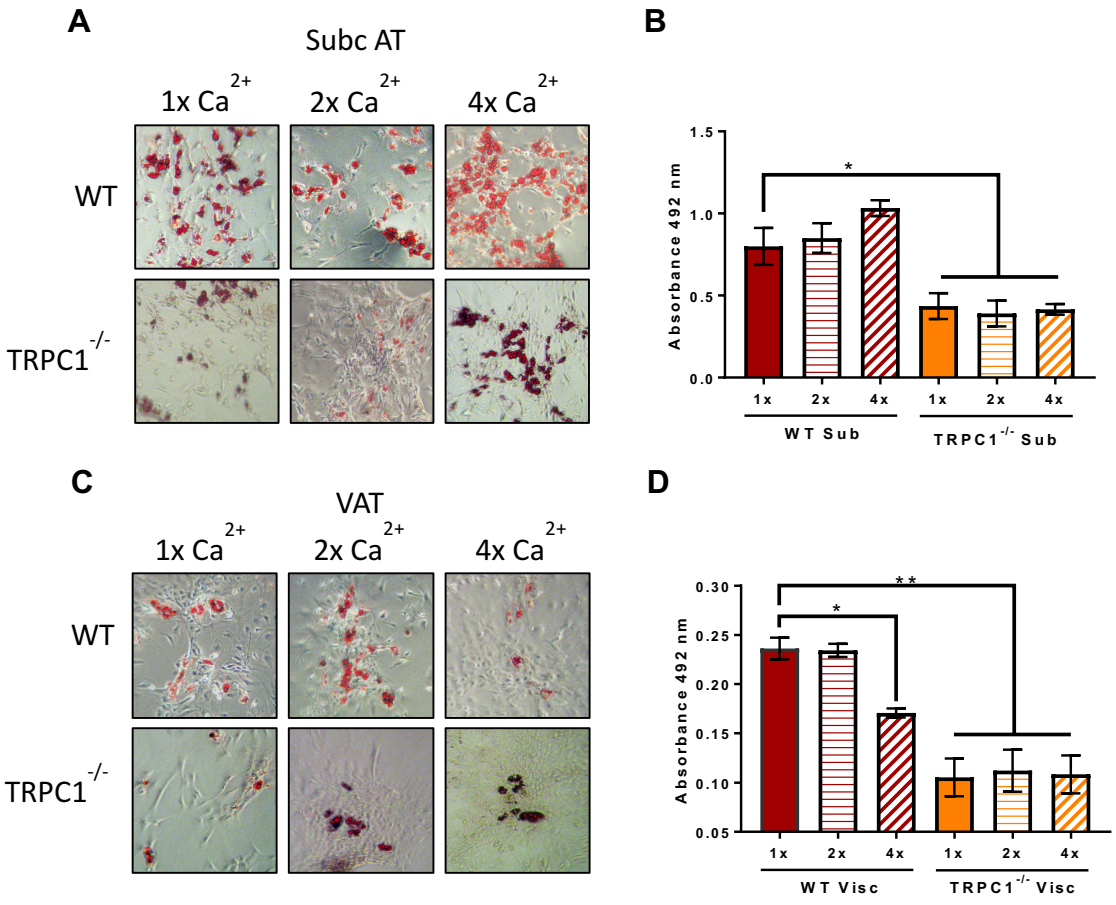

Figure 18 Loss of TRPC1 in adipocytes reduces ability to differentiate

Oil-red-o staining of WT and TRPC1$^{-/-}$ Subc AT (A) and VAT (C) differentiated in 1x (basal), 2x, or 4x extracellular Ca^{2+} for 7 days. Quantification of eluted oil-red-o stain at 492nm of Subc AT (B) and VAT (D). Graphs are mean ± SEM, significance: *, $p < 0.05$; **, $p < 0.01$.

to WT with the greatest expression observed at basal for PPARγ and perilipin. Together these results reveal TRPC1 to be a functional partner in SOCE in both Subc AT and VAT differentiation and may necessary for the early stages of differentiation to promote PPARγ expression. Further, reduced Ca^{2+} influx due to loss of TRPC1 cannot be supplemented by raising extracellular Ca^{2+} concentrations. Finally, increased extracellular Ca^{2+} concentrations diminish lipid accumulation and PPARγ expression in WT Subc AT and VAT, however no substantive change was observed in FABP4 expression.

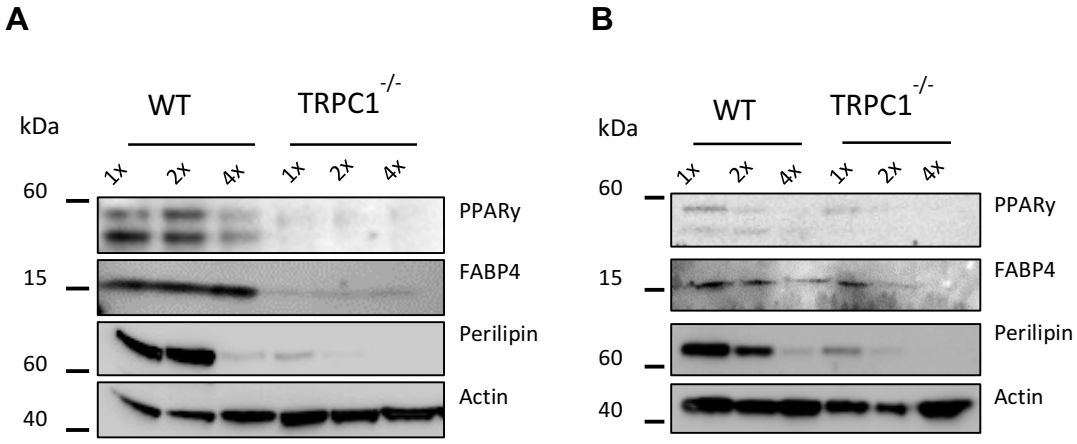

Figure 19 Adipogenetic protein expression in TRPC1$^{-/-}$ adipocytes diminished

Western blot of PPARγ, FAPB4, and perilipin protein expression of WT and TRPC1$^{-/-}$ Subc AT (A) and VAT (B) differentiated in 1x (basal), 2x, or 4x extracellular Ca^{2+}.

TRPC1$^{-/-}$ mice have increased fatty-acid desaturation index and adiposity with age

We have determined that lack of TRPC1 leads to a reduction in lipid accumulation and differentiation in an ex vivo model, leading us to next investigate whether dysfunctional TRPC1 channels could alter overall body composition. Body mass composition analysis was performed on TRPC1$^{-/-}$ and WT mice aged 13-15 months, which resulted in a more than two-fold increase in the ratio of total fat to body weight in TRPC1$^{-/-}$ mice as compared to age matched WT mice (Figure 21 A). Visually this difference in body composition can be seen in Figure 21 B where 9-month-old TRPC1$^{-/-}$ mice have increased Subc AT and VAT volume as compared to its WT counterpart. Interestingly, the increase in total fat observed in TRPC1$^{-/-}$ mice did not translate to an increase in their overall body weight. Within a majority of age groups, no significant difference in the overall body weight was observed in TRPC1$^{-/-}$ mice when compared with WT mice, however younger TRPC1$^{-/-}$ mice, aged 0-3 months, had reduced overall body weight (Figure 21 C). In all ages, TRPC1$^{-/-}$ mice did have lower organ weights (such as hearts and kidneys), which were reduced in size regardless of age and may attribute to the increase in adiposity without an increase in overall body weight (Figure 21 D).

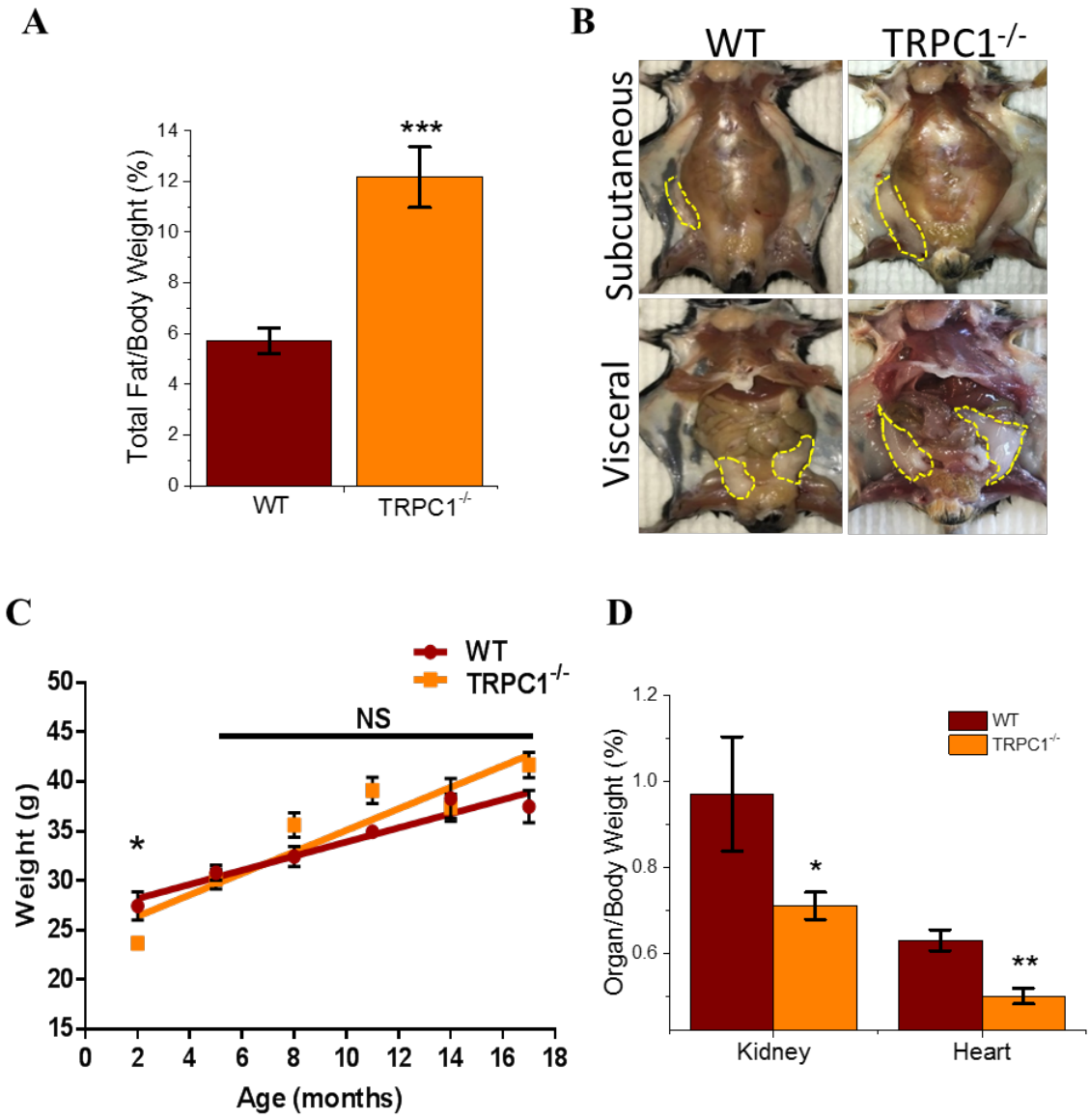

Figure 20 TRPC1$^{-/-}$ mice have increased adiposity with age

(A) Body fat mass measured by EchoMRI and calculated by dividing the fat weight by total body weight of mice aged 13-15 months n=9-11. (B) Exposed Subc AT and Visc AT of WT and TRPC1$^{-/-}$ male mice aged 9 months. (C) Total body weight of WT and TRPC1$^{-/-}$ mice grouped by 3-month increments of age. (D) Ratio of organ to total body weight of WT and TRPC1$^{-/-}$ mice. Graphs are mean ± SEM, significance: *, $p < 0.05$; **, $p < 0.01$; ***, $p < 0.001$.

Obesity is most easily characterized by excess adipose accumulation, however excess lipids are also stored in other organs such as the liver, muscle, and pancreas. To determine whether the increased adiposity observed in TRPC1$^{-/-}$ mice effected important metabolic organs, fatty acid composition of liver samples from WT and TRPC1$^{-/-}$ mice was calculated using gas chromatography/mass spectrometry (GC/MS). Liver fatty acid composition was relatively the same between WT and TRPC1$^{-/-}$ samples with the exception of mono and polyunsaturated fatty acids which were increased in TRPC1$^{-/-}$ (Figure 22 A). These included palmitoleic acid (16:1), oleic acid (18:1), linoleic acid (18:2), eicosenoic acid (20:1), and eicosadienoic acid (20:2). Increased ratios of monounsaturated to saturated fatty acids (desaturation index), particularly palmitoleic to palmitic acid (16:1/16:0) and oleic to stearic acid (18:1/18:0), has been correlated to obesity and insulin resistance (Jeyakumar et al., 2009; Pinnamaneni et al., 2006; Yee et al., 2014). Within our study, we found that both ratios were increased in liver samples from TRPC1$^{-/-}$ mice (Figure 22 B), indicating increased activity of Stearoyl CoA desaturase 1. Together these data suggest that the loss of TRPC1 function attributes to an increase in the accumulation of adipocytes, but not overall weight, and a liver lipid profile similar to an obese phenotype.

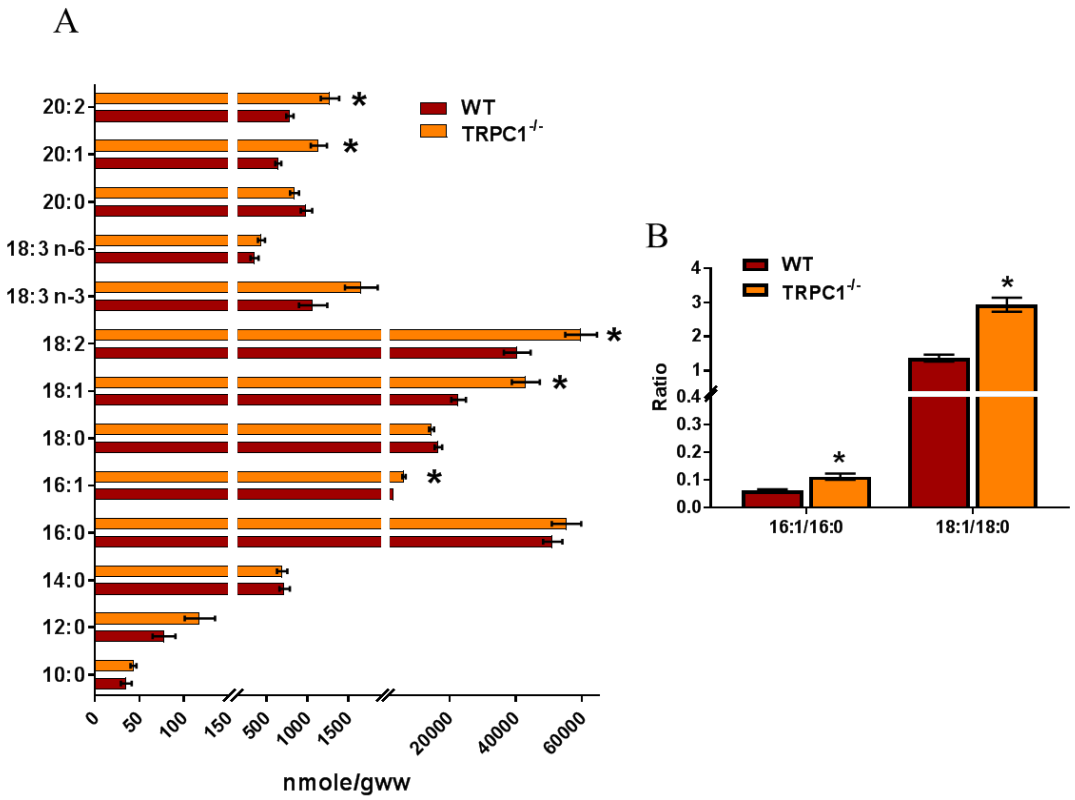

Figure 21 Desaturation of liver fatty acids increased in TRPC1-/- mice

Composition of liver fatty acids of WT and TRPC1$^{-/-}$ mice aged 4 months determined by gas chromatography/mass spectrometry (GC/MS) n=5. (B) Fatty acid desaturation index (16:1/16:0 and 18:1/18:0) calculated from (A). Graphs are mean ± SEM, significance: *, $p < 0.05$.

Conclusion

The incidence of obesity-associated diseases such as type II diabetes, hypertension, cardiovascular risk, and cancer has increased drastically worldwide. Consequently, scientific inquiry into the mechanisms underlying adipose tissue development and the pathology of obesity has gained interest. Though an array of metabolic disorders are linked to alterations of Ca^{2+} homeostasis (Arruda and Hotamisligil, 2015), the study of Ca^{2+} within adipose tissue has been underrepresented. Evidence suggests adipose tissue $[Ca^{2+}]_i$ is partly mediated by SOCE (El Hachmane et al., 2018), thus we focused on the identification of the endogenous Ca^{2+} entry channel and establish its role in adipocyte function. In our study, we identify TRPC1 as a major regulator of adipocyte energy metabolism through mediation of adipocyte differentiation.

SOCE was first identified as a major component of non-excitable cells (Parekh and Putney, 2005), but further research has identified SOCE within a multitude of tissue types. This knowledge has unveiled it to be a ubiquitous Ca^{2+} signaling pathway which regulates numerous cellular functions including those connected with diabetic complications (Chaudhari and Ma, 2016). Identification of SOCE mechanisms within adipocytes may lead to a better understanding of the onset of obesity and metabolic disorders and reveal therapeutic possibilities. Within our study, Ca^{2+} entry was demonstrated to have SOCE properties that could effectively be reduced by the addition of a non-specific Ca^{2+} entry channel blocker SKF in both Subc AT and VAT. This indicates a similar mechanism for Ca^{2+} entry

influx between the tissue types. Furthermore, the current properties observed and blocked by SKF were similar to that of a TRPC1 channel (Liu et al., 2003; Selvaraj et al., 2012). The role of SOCE and the specific Ca^{2+} channel involved within Subc AT and VAT was further confirmed using adipose tissue with a genetic ablation of TRPC1. Loss of TRPC1 showed a significant decrease in Ca^{2+} entry upon treatment with Tg in SVF and differentiated adipocytes of both tissue types. Importantly, although ORAI1 was present, it was not able to compensate for the loss of TRPC1, suggesting that the major Ca^{2+} entry channel in adipocytes is mediated via TRPC1. Interestingly, loss of ORAI1 has been shown to modulate immune function (Ahuja et al., 2017), which also plays a vital role in obesity. Within our study, TRPC5 expression is increased upon adipocyte differentiation; however as TRPC1 forms C1/C5 heterotetramers (Shi et al., 2012), loss of TRPC1 would inactivate TRPC5 and thus could not compensate in $TRPC1^{-/-}$ mice. Upon differentiation, a higher amplitude of TRPC1-like current in both Subc AT and VAT was observed which is most likely attributable to the more than 2-fold upregulation of TRPC1 expression. In addition, current properties in differentiated VAT cells, especially in $TRPC1^{-/-}$, were similar to that observed with ORAI1. This suggests that ORAI1 could play a role in VAT tissues, however further research is needed to fully establish the role of ORAI1 in these cells.

Adipocyte differentiation is a complex process and dysregulation can lead to lipid accumulation and altered energy and metabolic regulation. Though the process is not fully understood, several studies have identified Ca^{2+} dependency

within adipocyte differentiation (Jensen et al., 2004; Neal and Clipstone, 2002; Pramme-Steinwachs et al., 2017; Shi et al., 2000). Our study is the first to use both genetic and pharmacological inhibitors to show that Ca^{2+} entry via TRPC1 is critical for adipocyte differentiation. Our results are consistent with other studies that have identified modulators such as STIM1 expression changes (Graham et al., 2009) and calcineurin, a calcium and calmodulin dependent serine/threonine protein phosphatase, activation (Neal and Clipstone, 2002) as important for the maturation of adipocyte precursor cells. Use of SKF to block store-mediated Ca^{2+} entry during differentiation not only impaired lipid droplet formation in WT Subc AT and VAT SVF, but also inhibited the expression of lipid mobilization proteins FABP4 and perilipin and transcription factor PPARγ.

The transcription factor PPARγ is essentially expressed during early differentiation stages and regulates a number of adipocyte marker genes, including FABP4 and perilipin (Farmer, 2006; Wu et al., 1999). Here we show blockage of Ca^{2+} influx by SKF suppresses PPARγ expression indicating Subc AT and VAT SVF may be unable to induce the initial processes of differentiation when SOCE is inhibited. Suppression of SOCE by TRPC1 loss, as seen in $TRPC1^{-/-}$ Subc and VAT cells, resulted in a reduction but not a complete impairment of lipid accumulation in both tissue types. Correspondingly, $TRPC1^{-/-}$ Subc and VAT differentiated adipocyte expression of FABP4, perilipin, and PPARγ was reduced when compared to WT indicating TRPC1 may be involved in the initial stages of PPARγ mediated differentiation. In the next chapter, we will discuss adipocyte size

more, however it was found that TRPC1$^{-/-}$ had a lower quantity of large adipocytes in Subc AT and VAT as compared to WT which may be attributed to partial differentiation dysfunction.

In contrast to Ca^{2+} blockage, continuous exposure to high external Ca^{2+} has been shown to inhibit preadipocyte differentiation (Jensen et al., 2004) and block adipocyte lipid accumulation and expression of adipogenic transcription factors (Pramme-Steinwachs et al., 2017; Shi et al., 2000). The relationship between serum and extracellular Ca^{2+} is tightly regulated and kept at relatively similar concentrations (Hofer and Brown, 2003). Interestingly, increased serum Ca^{2+} has been associated with obesity (Ren et al., 2013) and type II diabetes (Lorenzo et al., 2014) and could denote a correlative increased extracellular Ca^{2+} concentration. Within our study, increasing normal extracellular Ca^{2+} concentrations by 4-fold decreased differentiation in WT VAT but had no effect on Subc AT. Interestingly, a slight difference in lipid accumulation was observed between WT Subc AT and WT VAT at all Ca^{2+} concentrations. Subc AT is known to have greater differentiation potential and proliferative ability when compared to VAT (Baglioni et al., 2012), which most likely explains the differences observed in WT Subc and VAT lipid accumulations. Subc AT was able to overcome the inhibitory effect of the increased extracellular Ca^{2+} to sustain lipid accumulation, whereas VAT adipocytes were not. Though increasing extracellular Ca^{2+} concentrations had no effect on lipid accumulation in Subc AT, protein expression of key differentiation factors reduced when Ca^{2+} increased which is similar to that

of VAT. This may confirm what other studies have shown that extended exposure to high Ca^{2+} concentrations inhibits differentiation of adipocytes, particularly in VAT.

Impaired adipogenesis can lead to a multitude of different outcomes with the most common being an unhealthy expansion of adipose tissue. This phenomenon is generally seen in adult obesity which is hypertrophic in nature and the reason why PPARγ agonists such as TZDs are useful in obesity (Choe et al., 2016). Interestingly, hypertrophic adipocytes from obese mice were observed to have increased Ca^{2+} deposits surrounding lipid droplets possibly indicating increased $[Ca^{2+}]_i$ (Giordano et al., 2013). Within our study, TRPC1$^{-/-}$ mice exhibited increased adipose tissue accumulation as they aged; however overall body weight did not significantly increase relative to WT mice. This increase in adipose accumulation could be due to dysfunctional adipose differentiation which in time results in a hypertrophic expansion. Another important finding was that organ weights were reduced, which could be due to the fact that TRPC1 has been shown to play a critical role in cell proliferation (Alonso-Carbajo et al., 2017) and may be a reason for the increase in adipose accumulation without an increase in body weight.

Though differentiation may contribute to the increased adiposity, there could be other explanations including a reduction of lipolysis. If this is the case, fatty acids are not mobilized from triacylglycerol stores properly, which in turn would expand adipose tissue volume over time. Furthermore, deletion of FABP4

has been shown to reduce lipolysis and FABP4 knockout mice have increased white AT mass on a high-fat diet (Hotamisligil et al., 1996). In our model, lack of TRPC1 may inhibit the expression FABP4 thus reducing lipolysis. Another possibility is that TRPC1 could be involved in store-operated Ca^{2+} entry necessary to induce lipolysis. Lack of store-operated Ca^{2+} entry proteins have shown to disrupt regulators of lipid metabolism and results in increased organ lipid droplet formation (Maus et al., 2017). Together, these results indicate that SOCE via TRPC1 may be involved in the initial stages of adipocyte differentiation of both Subc AT and VAT and result in increased adipose tissue volume over time, however more research needs to be done to determine the exact mechanism.

CHAPTER IV

THE TRPC1 Ca^{2+}-PERMEABLE CHANNEL INHIBITS EXERCISE-INDUCED PROTECTION AGAINST HIGH-FAT DIET-INDUCED OBESITY AND TYPE II DIABETES

Introduction

Obesity is a hallmark of metabolic syndrome and a key feature of obesity is the disruption of metabolic homeostasis leading to excess adipose accumulation (Blüher, 2009; Claycombe et al., 2013; Claycombe et al., 2016; Claycombe et al., 2015), thus therapeutic targeting of proteins involved in these pathways could be essential for slowing or preventing the development of obesity and obesity-related health problems, including insulin resistance and type II diabetes. As shown in Chapter one along with other reports (Sukumar et al., 2012), TRPC1 gene expression is induced in differentiated adipocytes, yet no data are currently available on whether TRPC1 has a role in adipocyte energy metabolism regulation by altering mitochondrial energy oxidation, adipocyte lipid storage and size, and adipose tissue weight.

A possible way that TRPC channels may control energy metabolism and adiposity is by acting as sensors for chemical factors necessary in adipocyte biology (Sukumar et al., 2012). Dietary saturated fat intake promotes obesity and

type II diabetes (Holzer et al., 2011) whereas n-3 polyunsaturated fatty acids (PUFAs) mainly found in fish oil produce opposite effects (Kuda et al., 2016; Ouguerram et al., 2006). Treatment of human embryonic kidney cells (HEK 293) with n-3 PUFAs such as linolenicdocosahexaenoic, and eicosapentaenoic acids inhibit Ca^{+2} entry via TRPC5 homomeric and TRPC1–TRPC heteromeric channels. Interestingly, the PUFA concentrations used in this study were within the physiologically achievable range of the human diet (Sukumar et al., 2012). Whether high dietary saturated fat intake modulates adipocyte energy metabolism via TRPC1-mediated signaling is not yet known.

Moreover, experimental evidence indicates that several TRP channels play an important role in the onset of diabetes (Graham et al., 2009; Hu et al., 2009; Sabourin et al., 2015) or diet-induced obesity (Ye et al., 2012); however, the role of TRPC1 in these circumstances is not yet established. Exercise regulates body energy stores and insulin resistance by reducing adipocyte size and lipid content (Craig et al., 1981; Gollisch et al., 2009) and by regulating serum glucose homeostasis through inducing GLUT4 (glucose transporter type 4) protein expression (Stanford et al., 2015). Interestingly, treadmill running prevents Ca^{+2} dysregulation and diabetic dyslipidemia in high-fat (HF) fed swine (Witczak et al., 2006). TRPC1 knock-out (KO or $TRPC1^{-/-}$) mice with attenuated Ca^{+2} entry (Liu et al., 2007) experienced reduced muscular endurance due in part to reduced force production and a greater rate of muscle fatigue (Zanou et al., 2010). However, whether a HF diet could exacerbate reduced exercise tolerance in TRPC1 KO mice

or contribute to mitochondrial energy metabolism dysfunction is also not yet known. Currently, no other studies have investigated the effects of dietary HF and exercise on adipocyte energy metabolism alteration via TRPC1 protein regulation of intracellular Ca^{+2} homeostasis.

The regulation of adipocyte size and longevity may also be an area of involvement for TRPC1. It has been shown that increased subcutaneous adipocyte size is predictive to the development of insulin resistance and type II diabetes (Lundgren et al., 2007; Skurk et al., 2007; Weyer et al., 2000). Further, there is a negative correlation between adipocyte size and insulin sensitivity and a positive correlation with proinflammatory adipocytokine secretion (Lönn et al., 2010; Yang et al., 2012). It has also been reported that adipose mass along with differentiation is regulated by a process called autophagy (Singh et al., 2009; Zhang et al., 2009). Interestingly, there is an increase in autophagy in obese subjects, particularly in VAT depots (Kovsan et al., 2011) along with an increase in apoptotic pathways (Alkhouri et al., 2010; Sorisky et al., 2000). Autophagy deficient mice exhibit reduced efficiency in adipogenesis (Baerga et al., 2009) with altered morphology (Wang and Peng, 2012).

Autophagy is described as a cellular process responsible for the delivery of proteins or organelles to lysosomes for degradation. Cells encountering stressful situations can either try to survive using the beneficial process of autophagy or by activating a programmed cell death program called apoptosis (Decuypere et al., 2011; East and Campanella, 2013; Kondratskyi et al., 2013). To date, three types

of autophagy exist; macroautophagy, microautophagy and chaperone-mediated autophagy (CMA) (Decuypere et al., 2011; Kato et al., 2014). Cellular stress conditions including nutrient starvation, hypoxia conditions, invading microbes, and tumor formation have been shown to induce autophagy and allows cell survival in these stressful or pathological situations (Kato et al., 2014). In addition, autophagy also recycles existing cytoplasmic components that are required to sustain vital cellular functions (Zhang and Calderwood, 2011). Although autophagy and apoptosis are mechanistically different cellular processes, there are some common regulatory proteins that intervene in both, such as the anti-apoptotic/anti-autophagy regulators B-cell lymphoma 2 (Bcl-2) and B-cell lymphoma-X large (Bcl-XL) and Ca^{2+} signaling. Bcl-2 and Bcl-XL are known to inhibit apoptosis by binding to Bcl-2–associated X (Bax) or Bcl-2 homologous antagonist/killer (Bak) but also suppress autophagy by binding to Beclin-1 (Lindqvist et al., 2014).

Intracellular Ca^{2+} is known to play an important role in autophagy in both basal and induced models (Cárdenas et al., 2010; Høyer-Hansen et al., 2007), however the mechanism by which Ca^{2+} regulates autophagy remains controversial (Decuypere et al., 2011). This is due to the previous studies showing both an activating and inhibitory role in autophagy (Cárdenas et al., 2010; Su et al., 2013). A commonality to these different studies is the focus on IP3R which is important for SOCE mechanisms (Figure 23). With regards to channel identity, our laboratory has shown in numerous studies indicating TRPC1 has a role in cell survival and apoptosis (Bollimuntha et al., 2006; Pani et al., 2006; Selvaraj et al., 2009).

Recently our lab has shown that TRPC1 is a key regulator in hypoxia and nutrient depletion dependent autophagy (Sukumaran et al., 2015). Specifically, that an increase in intracellular Ca^{2+} via TRPC1 regulates autophagy, thereby preventing cell death in two morphologically distinct cells lines (Sukumaran et al., 2016).

The present study investigated the involvement of TRPC1 in diet-induced obesity and type II diabetes. Additionally, regulation of adipocyte formation under normal-fat (Stanford et al., 2015) or HF diet and control cage or voluntary exercise conditions was also evaluated to determine how optimal dietary treatments and exercise promote a healthy body weight. Our data indicate that TRPC1 KO mice fed a HF diet and exercised are protected from diet-induced obesity and type II diabetes risk due to decreased autophagy and increased apoptosis resulting from loss of Ca^{+2} influx through TRPC1.

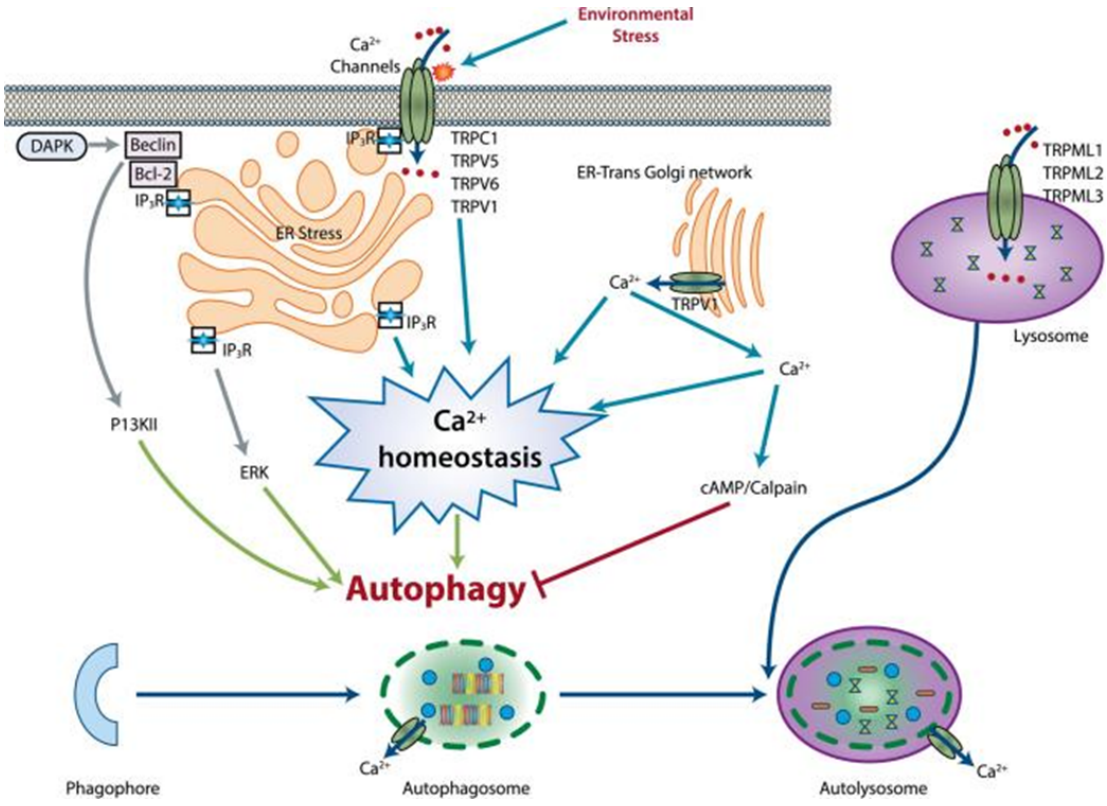

Figure 22 Role of intracellular Ca^{2+} and Ca^{2+} permeable channels in autophagy

Schematic diagram showing intracellular Ca^{2+} and Ca^{2+} permeable channels in the control of autophagy. Stimulation of Ca^{2+} permeable channels are activated both excited and non-excited Ca^{2+} channels and results in release of the store Ca^{2+} from the ER and Golgi bodies. These results in ER stress and disturbed Ca^{2+} homeostasis in the cells; which via various Ca^{2+} regulated proteins like ERK, calpains, cAMP regulates the autophagy processes. Reprinted from “Functional role of TRP channels in modulating ER stress and Autophagy” by P. Sukumaran, 2016, *Cell Calcium*, 60, 123-132. Copyright 2016 by Elsevier. Reprinted with permission.

Results

Body fat mass is decreased in TRPC1 KO mice fed a HF diet and exercised

For 12 weeks, mice were fed diets containing either 16% (normal-fat, NF) or 45% fat (high-fat, HF) for 12 weeks and subjected to voluntary wheel running

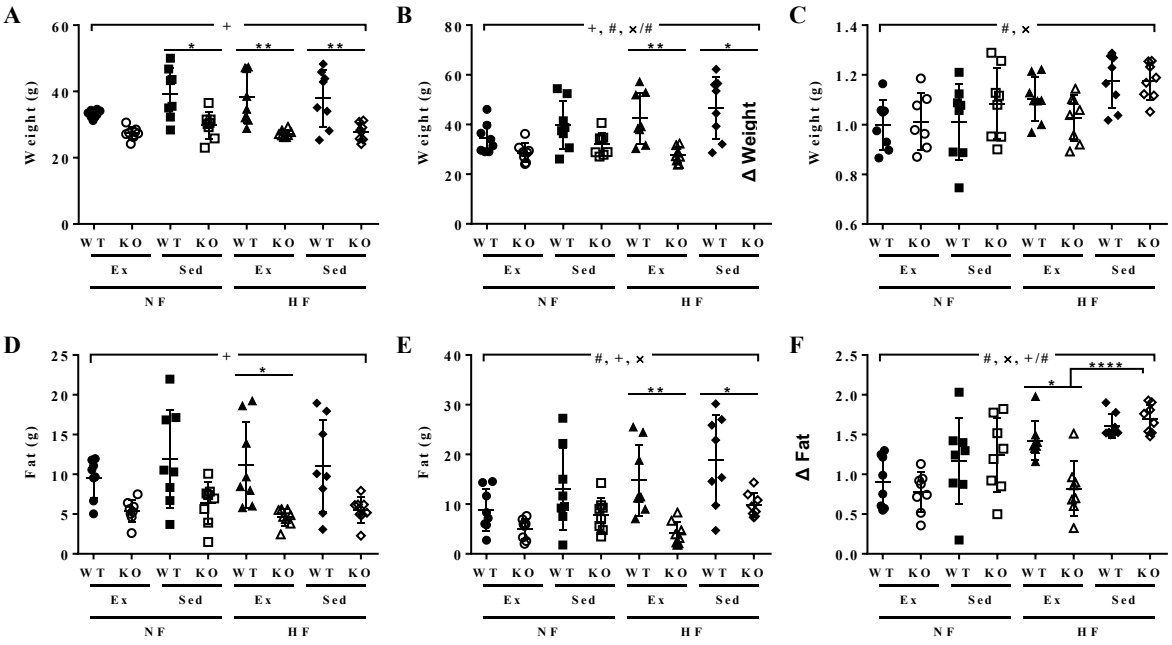

Figure 23 TRPC1 KO mice fed a HF diet and exercised have decreased body fat mass

A and *B*, body weight was measured at week 0 (*A*) and week 12 (*B*). *C*, body weight change was calculated by dividing the body weight at week 12 by the body weight at week 0. *D* and *E*, body fat mass was measured by EchoMRI at week 0 (*D*) and week 12 (*E*). *F*, body fat change was calculated by dividing the fat weight at week 12 by the fat weight at week 0. Data are presented as mean ± S.D., n = 6–8. Significant ($p < 0.05$) effects from 3-way ANOVA are indicated by + (mouse type), × (diet), and # (exercise).

exercise. TRPC1 KO mice had lower body weight (Figure 24 A) and body fat mass (Figure 24 D) at the start of the study and after 12 weeks of diet and exercise (Figure 24 B, E) when compared to WT mice. However, when calculated as a fold change, there was no change in body weight when comparing WT to TRPC1 KO mice (Figure 24 C). Within groups, change in body fat mass was significantly decreased in TRPC1 KO mice fed a HF diet and exercised compared to WT mice fed a HF diet and exercised (Figure 24 F). Furthermore, TRPC1 KO mice fed a HF diet and exercised had less change in body fat mass than TRPC1 KO mice fed a

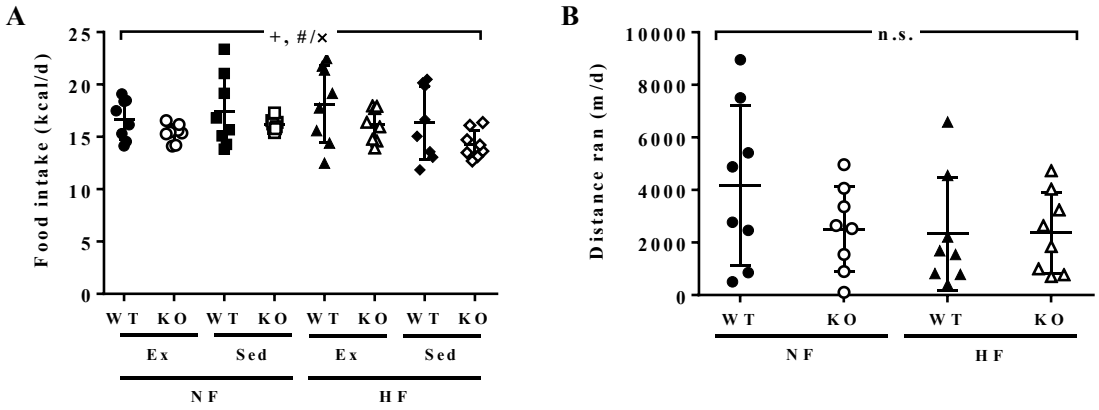

Figure 24 Daily food intake and exercise is unaltered

Food consumption and exercise were measured biweekly from WT and TRPC1 KO mice over the course of 12 weeks. Data are presented as means ± S.D., n = 7-8. Significant ($p < 0.05$) effects from 3-way ANOVA are indicated by + (mouse type), × (diet), and # (exercise).

HF diet and subjected to sedentary cage activity (Figure 24 F). Though food intake variation was influenced by the type of mouse and an exercise x diet interaction, altered body composition was not a result of group differences in food consumption or exercise (Figure 25 A, B). As we saw from the data presented in Chapter One, TRPC1 is the major Ca^{2+} entry channel in adipocytes and the new data presented here shows that loss of TRPC1 decreases obesity risk in HF fed mice that exercise.

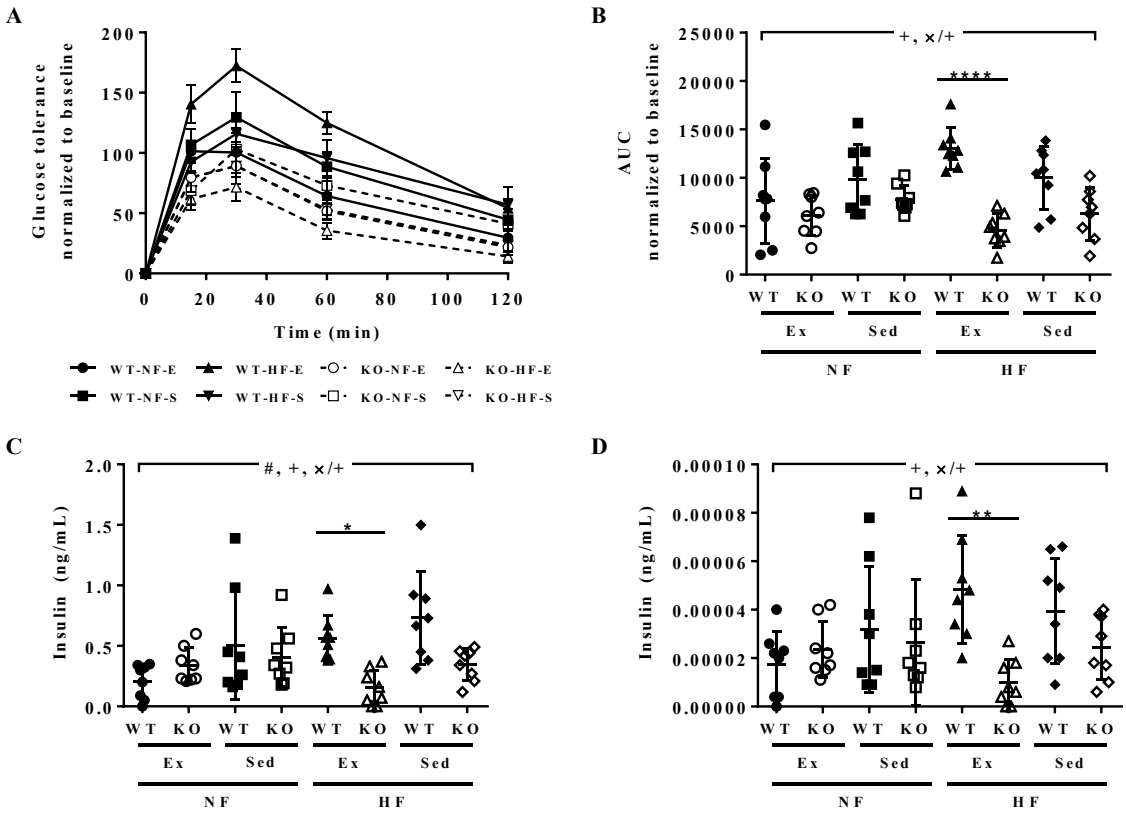

Figure 25 TRPC1 KO mice fed a HF diet and exercised have reduced insulin resistance

A–D, blood glucose (*A* and *B*), plasma insulin (*C*), and calculated homeostatic model assessment of insulin resistance (*D*) were measured from WT and TRPC1 KO mice fasted overnight after 12 weeks of diet and exercise. Data are presented as mean ± S.E. (*A*) or S.D. (*B–D*), $n = 7–8$. Significant ($p < 0.05$) effects from 3-way ANOVA are indicated by + (mouse type), × (diet), and # (exercise).

TRPC1 KO mice fed a HF diet and exercised are protected from type II diabetes risk

The data provided above show an important role for TRPC1 in the onset of metabolic syndrome. Thus, glucose concentrations were next evaluated under these conditions. Maximum blood glucose concentrations occurred 15-30 min after intraperitoneal injection of glucose in all groups (Figure 26 A). Interestingly, overall TRPC1 KO mice had reduced blood glucose concentrations as compared to WT, however, within groups, blood glucose concentrations were only decreased in TRPC1 KO mice fed a HF diet and exercised when compared to WT mice fed a HF diet and exercised (Figure 26 B). Similarly, serum insulin concentrations were overall decreased in TRPC1 KO mice and the group TRPC1 fed a HF diet and exercised was decreased as compared to WT mice fed a HF diet and exercised (Figure 26 C). Using a homeostatic model assessment of insulin resistance (HOMA IR) to assess the fasting blood glucose/insulin ratio, we found that, once more, TRPC1 KO mice were overall less insulin resistant than WT and the TRPC1 KO group fed a HF diet and exercised were less insulin resistant than WT mice fed a HF diet and exercised (Figure 26 D). It was confirmed that this difference was not due to altered expression of GLUT4 in the subcutaneous adipose tissue (Figure 27 A) or skeletal muscle (Figure 27 B). These studies suggest that loss of TRPC1 decreases insulin resistance and risk of diabetes thereby inhibiting metabolic syndrome.

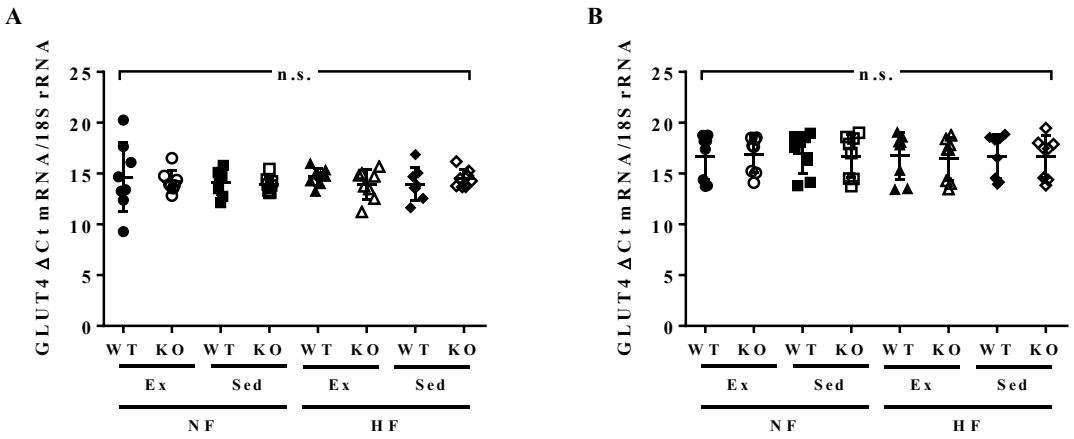

Figure 26 GLUT4 expression is unaltered in Subc AT and skeletal muscle

A and *B*, GLUT4 expression in subcutaneous adipose tissue (*A*) and hind leg biceps femoris skeletal muscle (*B*) was measured from WT and TRPC1 KO mice following 12 weeks of diet and exercise. Data are presented as mean ± S.D., *n* = 7–8.

Adipocyte numbers are decreased in TRPC1 KO mice fed a HF diet and exercised

To establish if adipocyte number or size is varied under these conditions, we counted the number of adipocytes present in adipose tissue depots and determined the adipocyte size. In the subcutaneous and visceral adipose tissue depots, adipocytes with size ranges of 80-160 μm were decreased in TRPC1 KO mice fed a HF diet and exercised compared to WT mice fed a HF diet and exercised but not in the smaller size range of 20-80 μm (Figure 28). In addition, TRPC1 KO mice fed a HF diet and subjected to sedentary cage activity had decreased adipocytes from 160-200 μm when compared to WT mice fed a HF diet and subjected to sedentary cage activity (Figure 28) This data suggests that loss of TRPC1 combined with a HF diet decreases the number of larger adipocytes, which could explain the decreased fat mass observed in Figure 24.

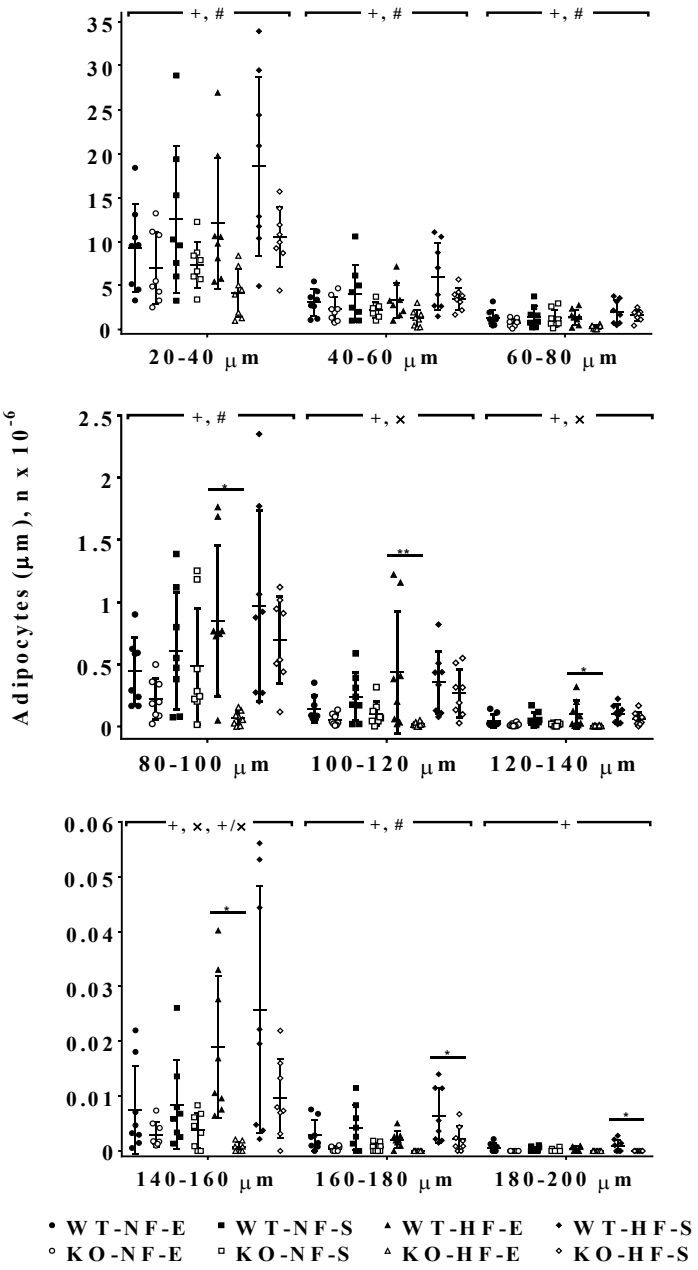

Figure 27 TRPC1 KO mice fed a HF diet and exercised have fewer adipocytes

Adipose tissue harvested from WT and TRPC1 KO mice following 12 weeks of diet and exercise was measured by a Multisizer. Data are presented as mean ± S.D., n = 6–8. Significant ($p < 0.05$) effects from 3-way ANOVA are indicated by + (mouse type), × (diet), and # (exercise).

Autophagy marker expression is decreased while apoptosis marker expression is increased in TRPC1 KO mice fed a HF diet and exercised

To determine whether reduced adipocyte numbers in adipose depots of TRPC1 KO mice fed a HF diet and exercised seen in Figure 28 were due to apoptosis or reduced differentiation of adipocytes, we measured mRNA of key markers for adipogenesis (PPARγ), beiging (FGF21), hypoxia (HIF1α), and autophagy (MAP1LC3A, BECN1). Though there was no altered mRNA expression of PPARγ, FGF21, HIF1α, or BECN1 in subcutaneous adipose tissue (Figure 30 A-D), expression of the autophagy marker MAP1LC3A was decreased (as indicated by an increased Ct value) in TRPC1 KO mice fed a HF diet and exercised compared to WT mice fed a HF diet and exercised (Figure 29 A). To confirm that our mRNA expression was replicated on the protein level, we examined protein expression of autophagy (LC3A, p62) and apoptosis (Bax, Bcl-xl) regulating proteins in WT and KO mice fed a HF diet and exercised. LC3A expression was decreased along with an increase in p62 expression in samples from TRPC1 KO mice that were fed a HF diet and exercised when compared with WT mice fed a HF diet and exercised indicating a deficiency in autophagy (Figure 30 B, C). Conversely, increased expression of Bax and an increased Bax to Bcl-xl ratio, which is an indication of increased apoptosis, was observed in the TRPC1 KO mice fed a HF diet and exercised compared to WT mice fed a HF diet and exercised (Figure 29 B-D). Together, these results suggest that loss of TRPC1 decreases autophagy, a survival mechanism, and increases apoptosis, which

could promote loss of larger adipocytes. In addition, loss of TRPC1 significantly decreased phosphorylation of ERK2, whereas no change in the phosphorylation of ERK1 and AMPK was observed (Figure 31). These data further indicate that loss of TRPC1 inhibits ERK2 phosphorylation, which has been shown to interact with ATG proteins and thus could modulate autophagy in these cells.

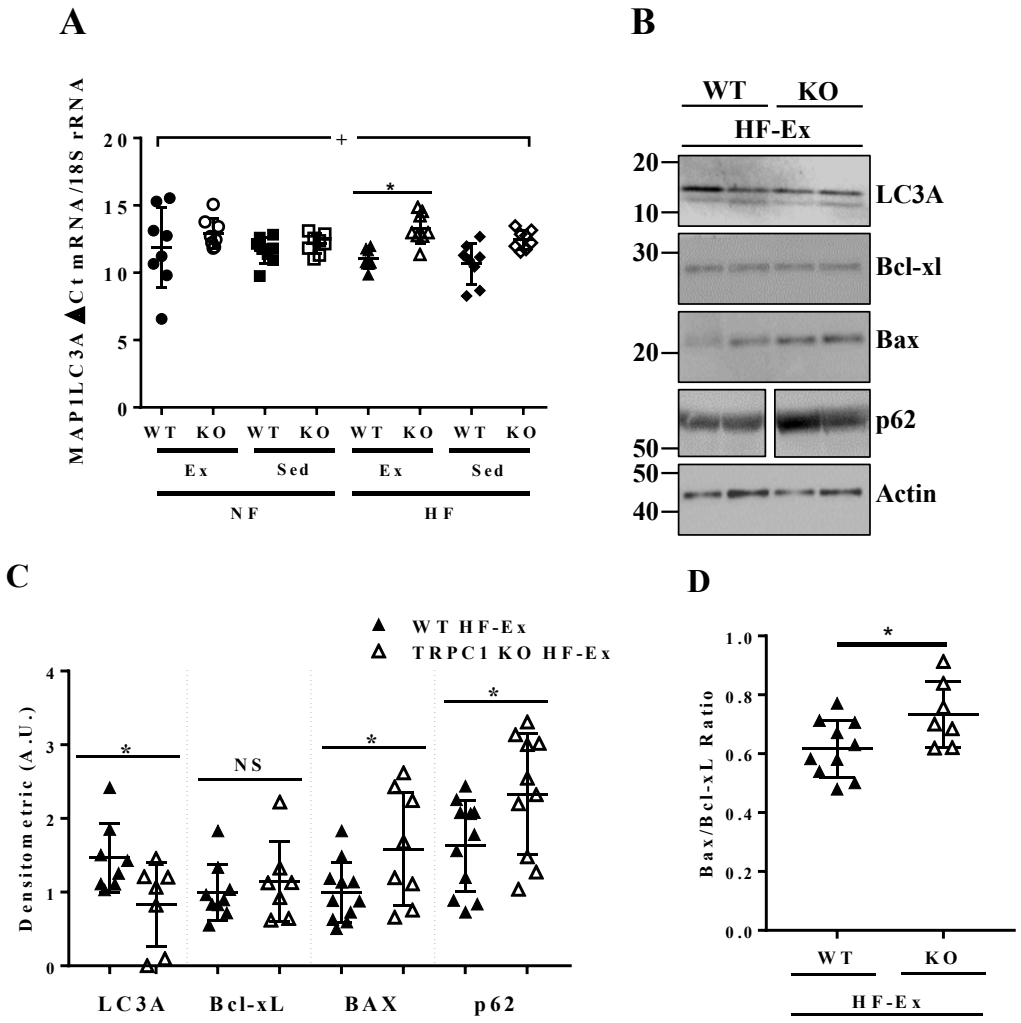

Figure 28 Autophagy marker expression is decreased whereas apoptosis marker expression is increased in TRPC1 KO mice fed a HF diet and exercised

A, MAP1LC3A mRNA expression was measured from subc adipose tissue taken from WT and TRPC1 KO mice following 12 weeks of diet and exercise. Data are presented as mean ± S.D., *n* = 6–8. *B*, subc adipose tissue from WT and TRPC1 KO mice fed a HF diet and exercised was resolved and analyzed by Western blotting using antibodies labeled in the figure. Quantification of each protein is shown in *C*. Data are presented as mean ± S.D., *n* = 7–11. *D*, ratio of Bax/Bcl-xl is presented as a fold increase of TRPC1 KO over WT values.

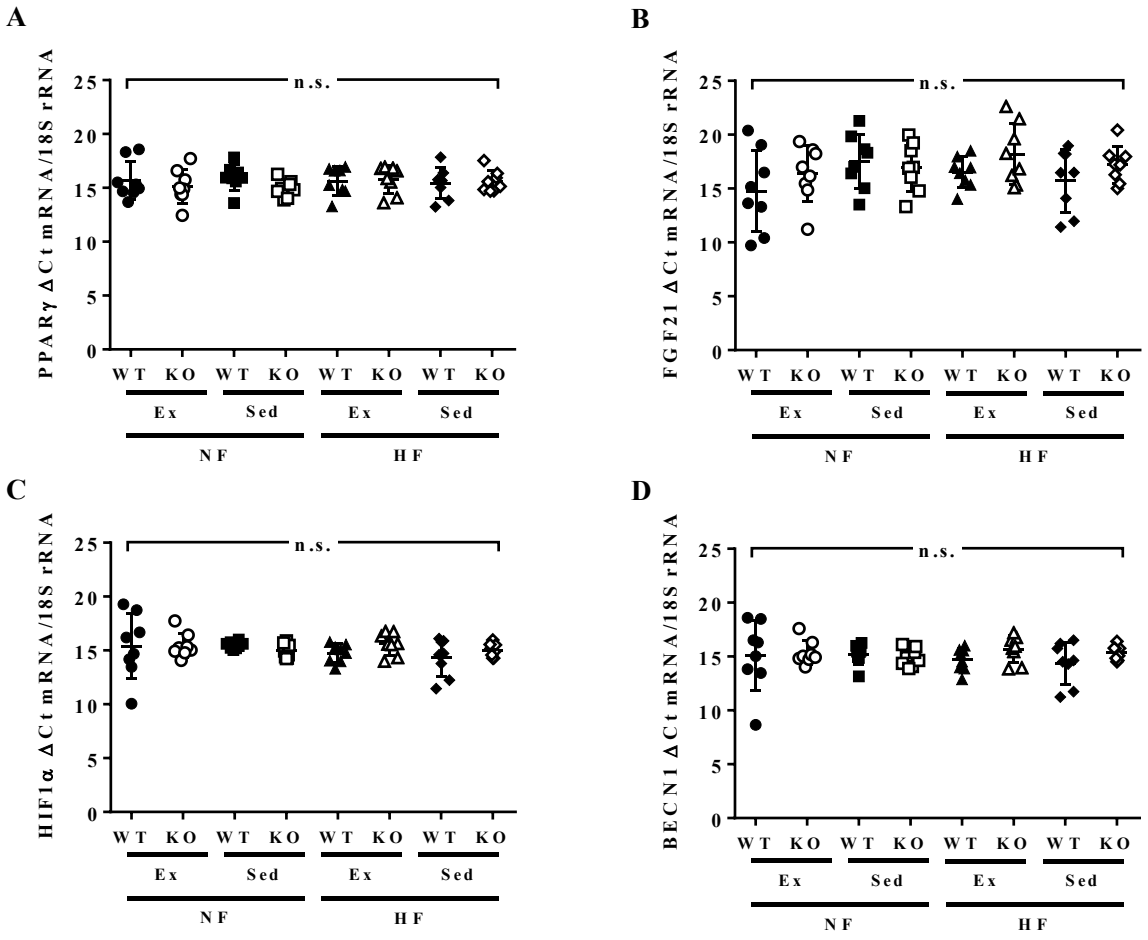

Figure 29 Expression of markers for adipogenesis, beiging, and hypoxia were unaltered in subcutaneous adipose tissue

mRNA expression of PPARγ (adipogenesis) (A), FGF21 (beiging) (B), HIFIα (hypoxia) (C), and BECN1 (autophagy) (D) was measured from subcutaneous adipose tissue taken from WT and TRPC1 KO mice following 12 weeks of diet and exercise. Data are presented as means ± S.D., n = 6-8.

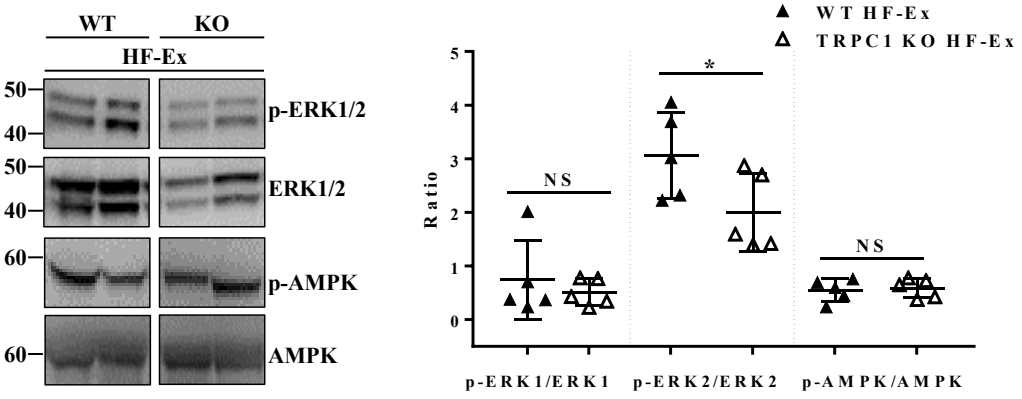

Figure 30 Reduced ERK2 phosphorylation observed in in TRPC1 KO mice fed a HF diet and exercised

Subc adipose tissue isolated from WT and TRPC1 KO mice fed a HF diet and exercised was resolved on SDS-PAGE gels and analyzed using different antibodies as labeled in the figure with quantification of the phosphorylated to non-phosphorylated form of each protein. Data are presented as mean ± S.D., n = 5.

Conclusion

This study is the first to show that TRPC1 KO mice that exercise are protected from HF diet-induced obesity and type II diabetes risk due to decreased adipose tissue mass and adipocyte number as a result of reduced autophagy and increased apoptosis. Thus, in combination, exercise, HF diet, and loss of TRPC1 reduce adiposity through a yet undefined mechanism. Given that TRPC1 is involved in Ca^{2+} entry following depletion of internal Ca^{2+} stores in the ER, TRPC1 KO results in decreased Ca^{2+} entry in a variety of cell types including adipocytes (Sukumar et al., 2012), skeletal muscle (Zanou et al., 2010), neuronal (Fiorio Pla et al., 2005), intestinal epithelial cells (Rao et al., 2006), and salivary glands (Liu et al., 2007; Liu et al., 2000). Thus, based on our data, it is probable that reduced Ca^{2+} entry due to TRPC1 KO is influenced further by HF diet and exercise, suggestive of a relationship between Ca^{2+} entry, diet, and exercise. Although expression of Orai1 and STIM1 was observed in adipocytes, the properties of the endogenous channel was similar to that observed with TRPC1-mediated I_{SOC} (Liu et al., 2007; Liu et al., 2000) and not as observed with ICRAC channels (Peinelt et al., 2006; Yuan et al., 2009). Similarly, the increased expression of TRPC5 in adipocytes did not alter Ca^{2+} influx as current-voltage recordings were distinctly different from TRPC5 homologs and TRPC1/TRPC5 heteromeric channels would be non-functional due to the loss of TRPC1 function (Strübing et al., 2001; Wu et al., 2010). Furthermore, TRPC1 KO mice showed exercise-mediated inhibition of adiposity and decreased insulin resistance in the absence of TRPC1 suggesting

that TRPC1 might be the dominant Ca^{2+} channel in these cells. However, additional studies will be needed to determine the role of Orai1 channels in exercise-mediated regulation of metabolic syndrome.

The present study demonstrated that fat mass was reduced in TRPC1 KO mice compared to WT mice following twelve weeks of HF diet and exercise. Similarly, previous studies have shown that TRPV4 KO mice (another Ca^{2+} entry channel from the TRPV family) are also protected from obesity and metabolic dysfunction with exposure to HF diet (Ye et al., 2012) suggesting that Ca^{2+} channels negatively regulate obesity. This is in contrast to the expectations that HF-fed mice develop obesity and glucose intolerance (Kalupahana et al., 2010) since TRPC1 KO mice fed a HF-diet and exercised were less insulin resistant than their WT counterpart, indicative of protection from type II diabetes risk, yet GLUT4 expression was unaltered in hind leg biceps femoris skeletal muscle or subcutaneous adipose tissue. Furthermore, the number and size of subcutaneous and visceral adipocytes are decreased in TRPC1 KO mice compared to WT mice when fed a HF diet and exercised. Because TRPC1 plays a key role in cell survival and apoptosis (Bollimuntha et al., 2006; Pani et al., 2006; Selvaraj et al., 2009), it was hypothesized that TRPC1 KO mice would alter expression patterns of key markers for adipogenesis, apoptosis, or autophagy in subcutaneous adipose tissue. TRPC1 KO mice fed a HF diet and exercised had decreased expression of the autophagy marker MAP1LC3A and increased p62 expression along with an increase in apoptosis markers (particularly the ratio of Bax/Bcl-xl). This is in

agreement with our previous findings that silencing of TRPC1 decreased autophagy and increased cell death (Sukumaran et al., 2015). Loss of TRPC1 also decreased phosphorylation of ERK2, which is consistent with previous studies where activation of Ca^{2+} channels in adipocytes increased ERK2 phosphorylation (Ye et al., 2012). In addition, loss of TRPC1 decreased the number of larger adipocytes. These findings suggest that elimination of TRPC1-mediated Ca^{2+} entry in TRPC1 KO mice promotes suppression of autophagy in HF diet-fed and exercised mice resulting in increased adipocyte cell death. These results are consistent with previous studies where patients with metabolic syndrome also have higher serum Ca^{2+} levels (Saltevo et al., 2011; Sorva and Tilvis, 1990), which could be due to the loss of TRPC1 or other Ca^{2+} channels that mediate Ca^{2+} entry in adipocyte cells, thereby increasing serum Ca^{2+} levels. Interestingly, in skeletal muscle, even though contraction does not depend on extracellular Ca^{2+} (Armstrong et al., 1972), Ca^{2+} entry through TRPC1 is essential for maintaining force during sustained repeated contractions. TRPC1 KO mice experience muscle fatigue during endurance exercise though spontaneous wheel running activity is unchanged (Zanou et al., 2010). Our data is in agreement as we showed no alteration in voluntary exercise. However, a reduction in endurance exercise might be expected because loss of TRPC1 could impact mitochondrial respiration by altering Ca^{2+} homeostasis, due to an increase in total mitochondrial protein stimulated by exercise training (Holloszy, 1967; Scalzo et al., 2014), and Ca^{2+} is needed for proper functioning of mitochondria (Chan et al., 2009). In addition, ER

stress resulting from reduced Ca^{2+} entry could increase translocation of apoptotic factors into mitochondria thus permeabilizing the membrane, causing release of cytochrome c and activation of caspases, leading to mitochondrial-mediated cell death (Budihardjo et al., 1999; Pan et al., 2001; Selvaraj et al., 2009; Wei et al., 2001). These findings demonstrate that loss of TRPC1 disrupts Ca^{2+} homeostasis potentially resulting in mitochondrial-mediated cell death of adipocytes. Although a previous study has shown that knockdown of TRPC1 only attenuated non-stimulated Ca^{2+} influx in breast cancer cells (Davis et al., 2012), our results using adipocytes did not show any decrease in basal Ca^{2+} entry. These results suggest that while in breast cancer cells other Ca^{2+} influx channels (Orai1) might be more important for SOCE, TRPC1 is essential for adipocyte function, especially in blocking the effects of exercise in HF diet-induced obesity. The mechanism by which TRPC1 KO mice fed a HF diet and exercised are protected from obesity and type II diabetes risk needs further investigation. However, our study and another published study (Ye et al., 2012) indicate that loss of Ca^{2+} might be the main factor that inhibits the formation of metabolic syndrome.

CHAPTER V

TRPC1 TRANSPORTS Ca^{2+} INVOLVED IN SNARE COMPLEX FORMATION DURING ADIPONECTIN SECRETION

Introduction

Adipose tissue was initially considered to be an inert fat storage depot until the discovery of linkages between obesity and inflammation. Currently, adipose tissue is considered a complex endocrine organ secreting over 600 bioactive factors (Lehr et al., 2012; MacDougald and Burant, 2007), termed adipokines. These adipokines influence diverse physiological processes by relaying information to other metabolically active organs such as muscle, liver, pancreas, and brain, thereby modulating systemic metabolism (Ouchi et al., 2011). Importantly, increased adipose accumulation, as seen in obesity, correlates to dysregulation of adipokine secretion (Arita et al., 1999; Matsuzawa, 2010; Maury and Brichard, 2010) and increases susceptibility to other diseases (Rasouli and Kern, 2008). Altering levels of the adipokines, mainly adiponectin (Fruebis et al., 2001; Okada-Iwabu et al., 2013) and leptin (Stern et al., 2016), have shown to improve energy homeostasis and offset diet-induced obesity. Thus, adipokines have potential to be therapeutic targets to combat/counter or reduce obesity and

other metabolic diseases, however, a full understanding of the mechanisms and intracellular mediators that modulate adipokine secretion within adipose tissue is first required.

Adiponectin is a cytokine primarily secreted from mature adipocytes, however it has been shown to be expressed in other tissues including human and murine osteoblasts, liver, myocytes, epithelial cells, and placental tissue (Achari and Jain, 2017). Adiponectin is known to have an anti-inflammatory effect as it inhibits the expression of vascular adhesion molecules, scavenger receptors, is an antagonist of toll like receptors (TLR) and their ligands, and pro-inflammatory cytokines TNFα, IL-6 and IL-1β in various tissues types (Fantuzzi, 2013; Tsatsanis et al., 2005; Turer and Scherer, 2012). Anti-oxidant properties have also been attributed to adiponectin which are mediated by the cyclic AMP/protein kinase A pathway (Ebrahimi-Mamaeghani et al., 2015; Scherer et al., 1995; Yamauchi and Kadowaki, 2013). Adiponectin has garnered interest as a metabolic therapeutic due to its positive effect on lipid and glucose metabolism in kidney, liver and muscle. Utilizing the AMPK pathway, adiponectin is known to increase fatty acid oxidation, mitochondria biogenesis, and insulin sensitivity (Achari and Jain, 2017; Komai et al., 2014).

Adiponectin is one of the most abundant circulating cytokine accounting for roughly 0.01% of total serum protein (Villarreal-Molina and Antuna-Puente, 2012). Normal human serum adiponectin concentrations are 3 to 30 μg/mL (Ouchi et al., 2003), however concentrations have been found to be negatively correlated to

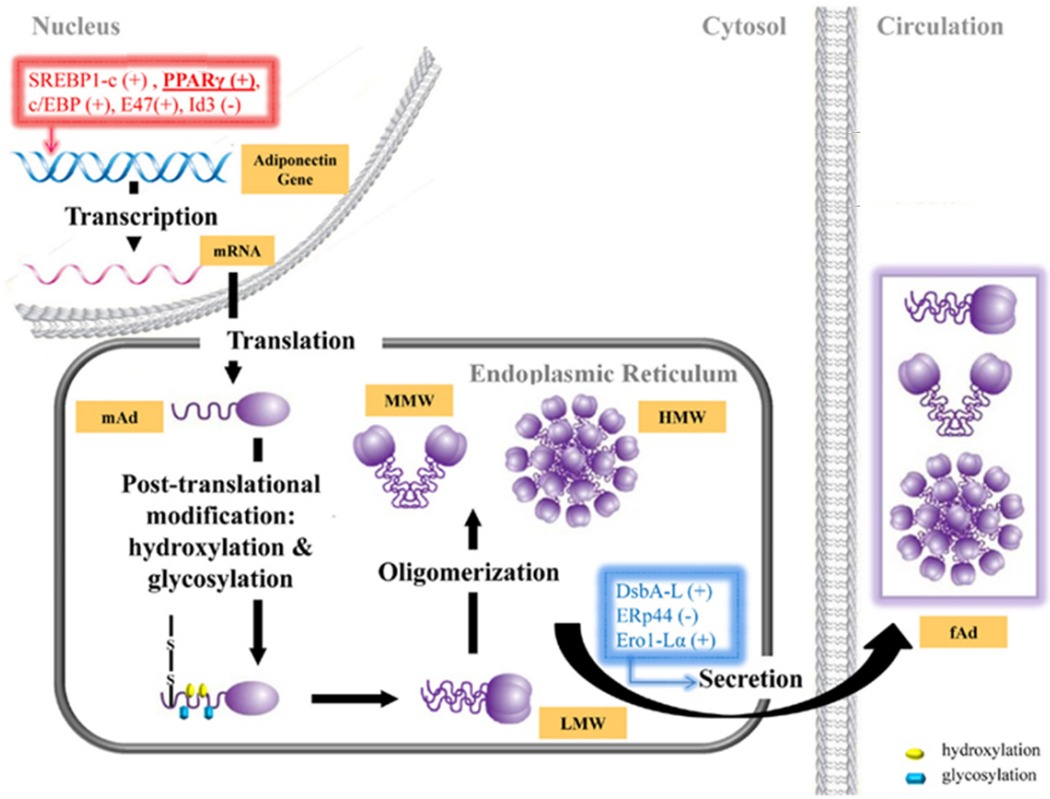

Figure 31 Adiponectin synthesis

Schematic representation of the steps involved in the production and secretion of adiponectin**.** Monomeric adiponectin (mAd) is the initial form and post-translationally modified and oligomerized into trimers (low molecular weight, LMW), hexamers (medium, MMW) and oligomeric (high, HMW) forms. Reprinted from “Adiponectin action: A combination of endocrine and autocrine/paracrine effects” K. Dadson, 2011, Frontiers in Endorcinology, 2011;2-62. Copyright 2011 by Frontiers Media SA. Reprinted with permission.

obesity and positively correlated to insulin sensitivity (Achari and Jain, 2017; Kadowaki et al., 2006; Kovacova et al., 2012). Decreases in blood concentrations during obesity have been attributed to disturbances in both production and

secretion of adiponectin from adipose tissue (Hoffstedt et al., 2004; Kovacova et al., 2012; Liu and Liu, 2009). Interestingly, mice fed a high-fat diet and treated with a synthetic small-molecule adiponectin receptor (AdipoRon) agonist ameliorated insulin resistance and glucose intolerance (Okada-Iwabu et al., 2013). Moreover, treatment with this synthetic adiponectin inhibited the onset of diabetes in genetically obese rodent model db/db mice further highlighting the prospect of using adiponectin as a therapeutic target for metabolic disorders.

Adiponectin is initially synthesized as a monomeric pre-hormone (Figure 32), then oligomerized into three isoforms and packaged in vesicles until stimulated for release (Dadson et al., 2011). Expression is transcriptionally regulated by the transcription factors C/EBPs, sterol regulatory element binding protein 1c (SREBP1c), and nuclear receptor peroxisome proliferator-activated receptors γ (PPARγ) which is induced by the thiazolidinedione (TZD) family of drugs (Dadson et al., 2011; Liu and Liu, 2009; Yamauchi and Kadowaki, 2013). Adiponectin is first formed as a 30 kDa monomer that is assembled within the ER into complex isoforms such as high (HMW 300 kDa), medium (MMW 140 kDa), and low (LMW 67 kDa) molecular weights (Figure 32). The HMW isoform is thought to be the most biologically active and Ca^{2+} has been implicated as important for its formation (Banga et al., 2008; Rosen and Spiegelman, 2014). Interestingly, the ratio of plasma HMW adiponectin to total adiponectin appears to be a stronger indicator of insulin resistance than measuring total adiponectin levels alone due to its high correlation with glucose and insulin levels (Lara-Castro et al., 2006).

Release of adiponectin from adipocytes has been shown to be insulin and Ca^{2+} dependent (Bogan and Lodish, 1999; Cong et al., 2007; Komai et al., 2014; Xie et al., 2008) and a high-Ca^{2+} diet has been shown to stimulate the expression of adipokines along with inhibition of pro-inflammatory factors (Sun and Zemel, 2007). The mechanism of secretion is mediated by golgi-localized, gamma adaptin ear-containing, ARF-binding protein 1 (GGA1)-coated vesicles originating at the Golgi with exocytosis being regulated through protein kinase A (PKA)-independent cAMP stimulation in both a Ca^{2+} dependent and independent process (Komai et al., 2014; Xie et al., 2008). Though Ca^{2+} dependency has been shown in adiponectin exocytosis, the specific Ca^{2+} channel involved has yet to be determined. We've shown in previous chapters the high expression and importance of TRPC1 in adipocyte function, thus TRPC1 could likely be involved in the Ca^{2+} dependent mode of adiponectin secretion (Baboota et al., 2014; Bishnoi et al., 2013; Sukumar et al., 2012).

Regulated exocytosis in adipocytes mediates key functions, exemplified by insulin-stimulated secretion of peptides such as adiponectin and recycling of intracellular membranes containing GLUT4 glucose transporters to the cell surface (Bogan and Lodish, 1999). Plasma membrane synaptosomal-associated protein 25 (SNAP-25) and syntaxin-1, termed t-SNAREs, and secretory vesicle-associated protein 2 (VAMP-2 or v-SNARE), are part of the conserved protein complex involved in the fusion of opposing membranes necessary for exocytosis (Söllner et al., 1993; Trimble et al., 1988; Zhang et al., 2016) (Figure 33). An

important feature of each of these proteins is a stretch of heptad repeats, termed SNARE motifs, which serve as co-binding locations (Fasshauer et al., 1998; Weimbs et al., 1997). Syntaxin-1 and VAMP-2 each contain a single SNARE motif while SNAP-25 contains two. During the initial stage of exocytosis, the vesicle approaches the PM and VAMP-2, syntaxin-1, and SNAP25 interact with each other via SNARE motifs to form quaternary bundles of α-helices called SNARE complexes. It has been well demonstrated that Ca^{2+} provides the final event needed for vesicle fusion and release of its content, however channel specificity is still elusive (Di Giovanni et al., 2010; Südhof and Rothman, 2009). Our laboratory has shown an interaction between VAMP-2 and TRPC3 in neuronal and epithelial cells was necessary for exocytosis (Singh et al., 2004). Interestingly, there is data implying an interaction between SNAP-25 and TRPC1 in human platelets during TRPC1 trafficking (Redondo et al., 2004) which could suggest a more involved role for the two proteins in SNARE complex formation.

As shown in Chapter 2, $TRPC1^{-/-}$ adipose tissue has reduce SOCE function and differentiation leading us to investigate whether other adipose functions are impaired. Ca^{2+} has been shown in numerous studies to be involved in the secretion of adipokines from adipose tissue (Komai et al., 2014; Sukumar et al., 2012; Ye et al., 2010), however the Ca^{2+} channel(s) involved have not been identified. The aim of this study was to identify the endogenous Ca^{2+} entry channel in adipocytes necessary for adipokine production and secretion. We report that loss of TRPC1 function reduces serum adiponectin concentrations in $TRPC1^{-/-}$ mice due to

impaired exocytosis of adiponectin from adipocytes. We further show TRPC1-mediated Ca^{2+} is necessary for SNARE complex formation necessary for adiponectin loaded vesicle fusion.

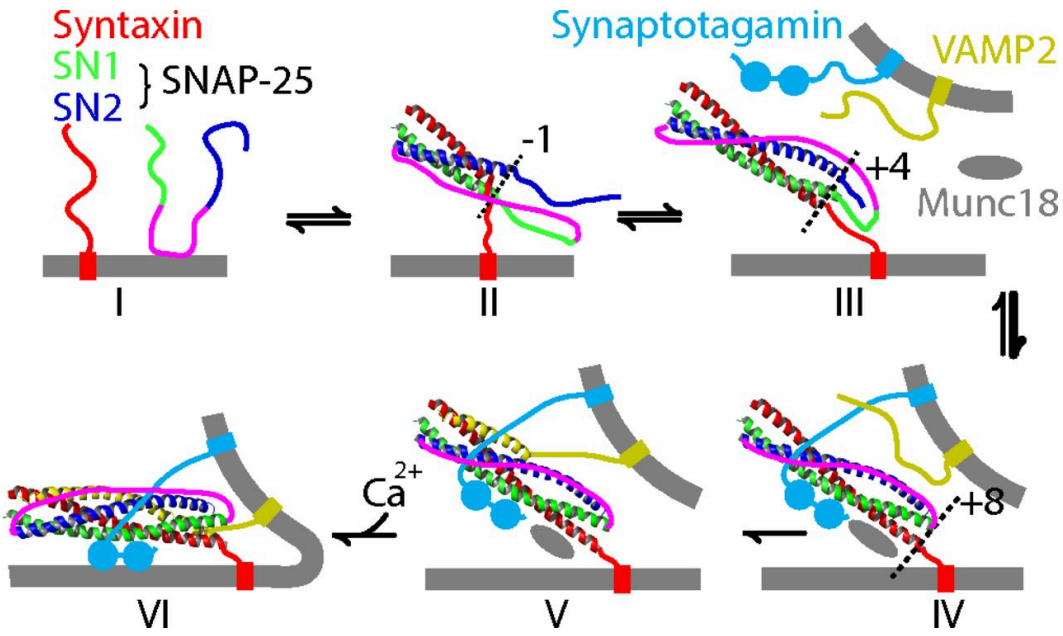

Figure 32 SNARE complex formation

Assembly of SNARE complex formation depicting the steps involved with vesicle fusion and exocytosis. (I) monomeric t-SNAREs SNAP-25 and syntaxin located on the PM, (II) partial assembly of t-SNARE complex, (III) the folded t-SNARE complex and introduction of vesicle associated proteins synaptotagamin and VAMP2 along with Munc-18, (IV) activated SNARE complex, (V) partially zippered trans-SNARE complex, (VI) introduction of Ca^{2+} completes the zippered SNARE complex and exocytosis occurs. Reprinted from “Single-molecule study of t-SNARE complex” by X. Zhang, 2016, Proceedings of the National Academy of Sciences, 113(50) E8031-E8040. Copyright 2016 by Proceedings of the National Academy of Science. Reprinted with permission.

Results

Serum adipokines levels are reduced in TRPC1$^{-/-}$ mice

To determine whether the reduction in Ca^{2+} influx in TRPC1$^{-/-}$ adipose tissue alters adipokine levels, we assessed serum adiponectin and leptin concentrations of WT and TRPC1$^{-/-}$ mice. Elisa assessed serum concentrations of both adiponectin and leptin were significantly reduced in TRPC1$^{-/-}$ mice as compared to their WT counterpart (Figure 34 A, B), whereas no change in food intake was observed (Figure 25). Adiponectin and leptin are almost entirely produced by adipocytes which led us to question whether the reduction in serum concentrations seen in TRPC1$^{-/-}$ mice was due to a decrease in overall production. To assess this,

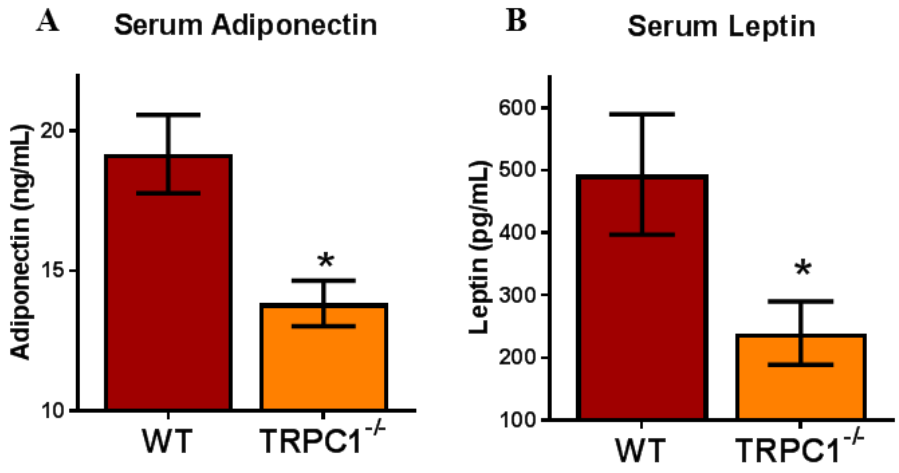

Figure 33 Serum adipokines are altered in TRPC1-/- mice.

Elisa assessed total serum APN (A) and leptin (B) of WT and TRPC1$^{-/-}$ mice aged 3-9 months, APN n=6, leptin n=8. Graphs are mean ± SEM, significance: *, $p < 0.05$

Subc AT and VAT lysates from WT and TRPC1$^{-/-}$ mice were evaluated for adiponectin and leptin protein expression. No difference was observed in either adiponectin or leptin expression between adipose tissue obtained from TRPC1$^{-/-}$ or their WT counter parts indicating loss of serum concentrations is most likely not

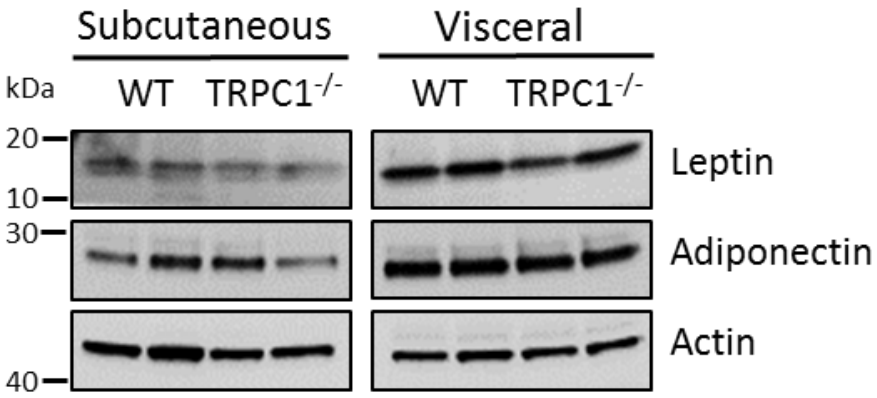

	Subcutaneous	
	WT	TRPC1$^{-/-}$
Leptin	0.733 ± 0.051	0.753 ± 0.024
Adiponectin	0.572 ± 0.051	0.456 ± 0.129

	Visceral	
	WT	TRPC1-/-
Leptin	1.569 ± 0.009	1.366 ± 0.114
Adiponectin	1.765 ± 0.093	1.752 ± 0.119

Figure 34 No difference in leptin and adiponectin concentrations within adipose tissue

Western blot and quantification of leptin and adiponectin protein expression normalized to actin of WT and TRPC1$^{-/-}$ tissue lysates of Subc AT and VAT and quantified.

due to a malfunction in production (Figure 35). Interestingly, both WT and TRPC1$^{-/-}$ VAT samples contained higher levels of both adiponectin and leptin than Subc AT samples possibly indicating VAT may play a larger role as a distributor of adipokines. These results suggest that reduced serum adiponectin and leptin concentrations in TRPC1$^{-/-}$ mice are not likely a consequence of lower adipose tissue production.

Exercise recovers diminished serum adiponectin concentrations in TRPC1$^{-/-}$ mice

Exercise is known to increase circulating adiponectin concentrations (Kriketos et al., 2004; Lee et al., 2011; Wang et al., 2015), however there are conflicting views on the effect of a high-fat diet on serum adiponectin concentrations (Barnea et al., 2006; Bullen et al., 2007). This lead us to investigate whether a high-fat diet and exercise would alter serum adipokine concentrations in TRPC1$^{-/-}$ mice. WT and TRPC1$^{-/-}$ mice were placed on a diet of either normal-chow (16% fat) or high-fat (45% fat) diet for 12 weeks and subjected to voluntary wheel running exercise. At the end of the 12 weeks, serum adiponectin concentrations were assessed. Within WT groups, adiponectin concentrations were increased in sedentary WT mice fed a high-fat diet and in exercised WT mice fed a normal-chow diet as compared to WT sedentary mice fed a high-fat diet, however, the combination of high-fat diet and exercise had no effect on adiponectin concentrations (Figure 36). Similar to Figure 34, sedentary TRPC1$^{-/-}$ mice feed a

normal-chow diet had significantly reduced adiponectin concentrations as compared to their WT counterparts which was replicated in sedentary TRPC1$^{-/-}$ mice feed a high-fat diet indicating the increase in adiponectin due to high-fat diet is impaired in TRPC1$^{-/-}$ mice. Notably, reduced adiponectin concentrations in TRPC1$^{-/-}$ mice fed either normal-chow diet or high-fat diet was offset by the addition

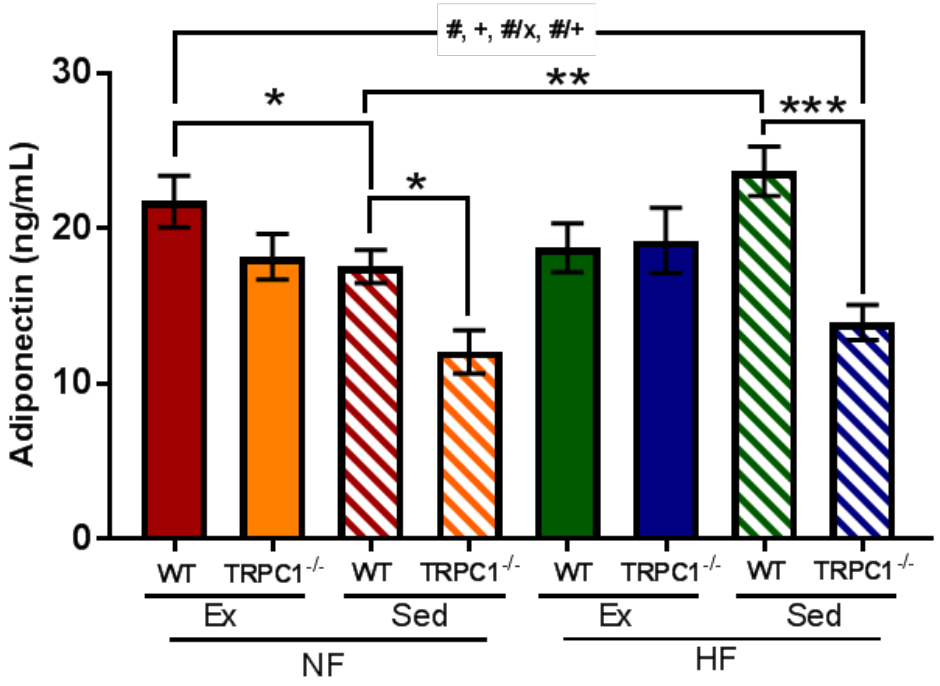

Figure 35 Reduced serum adiponectin concentrations in TRPC1$^{-/-}$ mice recovered when exercised

Total serum adiponectin from WT and TRPC1$^{-/-}$ mice fasted overnight after 12 weeks on normal-chow (16% fat) or high-fat (45% fat), n=8 mice. Normal-chow (NF), High-fat (HF). Significant (p < 0.05) effects from 3-way ANOVA are indicated by + (mouse type), × (diet), and # (exercise). Graphs are mean ± SEM, significance: *, p < 0.05; **, p < 0.01.; ***, p < 0.001.

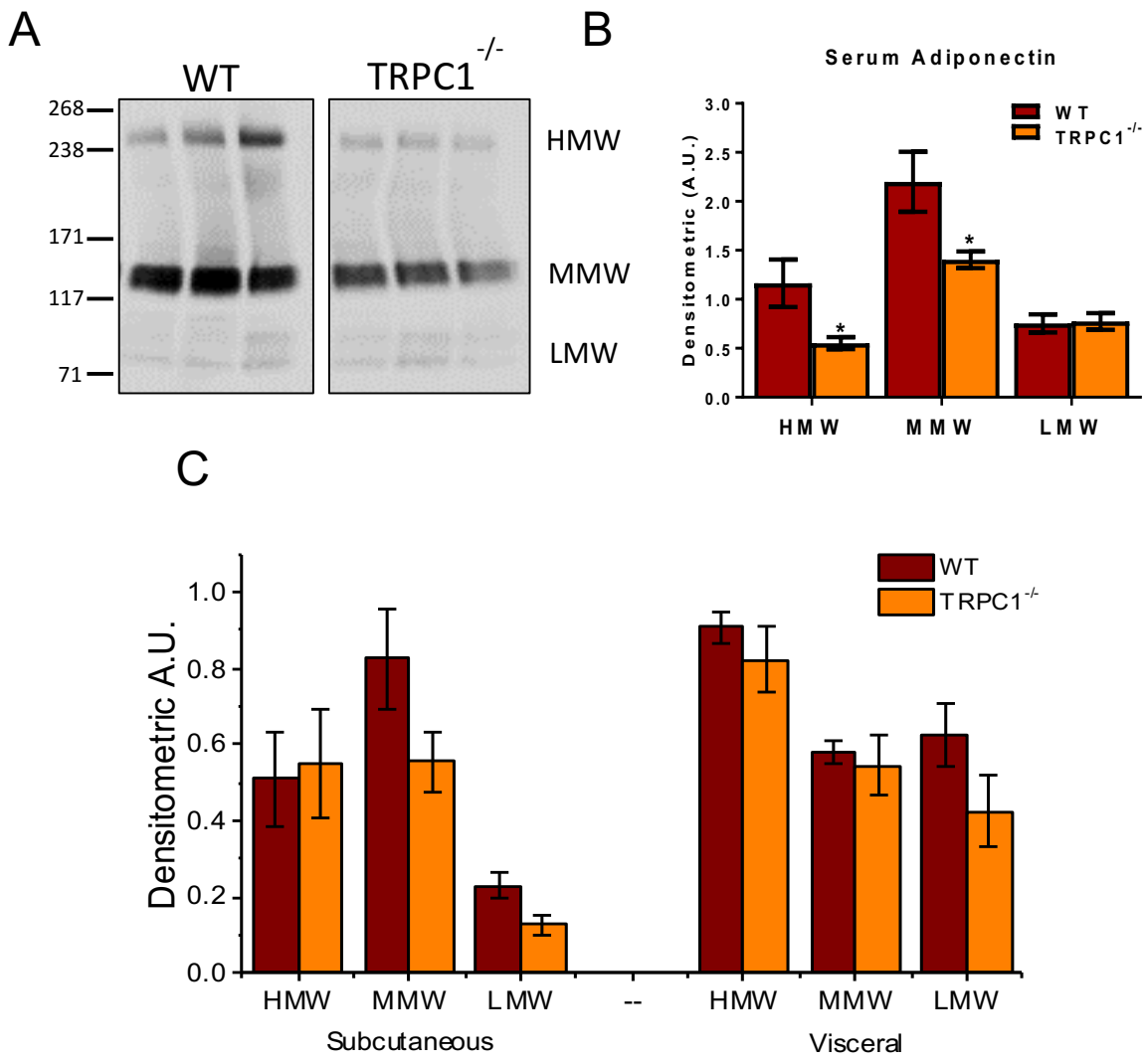

Figure 36 Serum adiponectin isoforms altered in TRPC1$^{-/-}$ mice

Serum adiponectin isoforms (A) assessed by non-denaturing PAGE. Optical density of each isoform (HMW (high molecular weight), MMW (middle molecular weight), LMW (low molecular weight)) normalized to total protein from respective Ponceau S stains and quantified (B). (C) Non-denaturing PAGE of Subc AT and VAT protein tissue lysates and quantified. Graphs are mean ± SEM, significance: *, $p < 0.05$; **, $p < 0.01$.

of exercise. Overall this indicates that serum adiponectin concentrations in TRPC1$^{-/-}$ mice are affected by the addition of exercise, but a high-fat diet results in no change.

Adiponectin isoforms are altered in TRPC1$^{-/-}$ mice

The isoform composition of total serum adiponectin has been shown to be important to overall health assessment due to its correlation with glucose and insulin levels (Lara-Castro et al., 2006), thus we assessed the composition of serum samples from Figure 34. Evaluation of serum adiponectin from WT and TRPC1$^{-/-}$ mice by non-denaturing gel electrophoresis indicated a significant reduction in both HMW and MMW isoforms with no difference in LMW (Figure 37 A, B). To understand whether the reduction of HMW and MMW isoforms in TRPC1$^{-/-}$ mouse serum is due to an issue in adiponectin production and folding within adipose tissue, Subc AT and VAT adiponectin isoform composition was assessed. In all three isoforms, there was no difference observed between WT and TRPC1$^{-/-}$ in either Subc AT or VAT indicating isoform assembly is not a likely candidate for differences in serum levels (Figure 37 C). Within these studies, we observed TRPC1$^{-/-}$ mouse serum contains significantly less of the biologically active form of adiponectin (HMW) than WT mice, which does not correspond to intracellular tissue quantities.

Diminished adiponectin secretion in Subc AT from TRPC1$^{-/-}$ mice

Secretion of adiponectin from adipose tissue can be triggered by insulin (Bogan and Lodish, 1999; Cong et al., 2007). To mimic this process ex vivo, fresh Subc AT and VAT from WT and TRPC1$^{-/-}$ mice was cut into 8-15 mg pieces, suspended in media, and stimulated with insulin (100 nM) for 6 hours. The media was then examined via ELISA and normalized to mg of tissue to determine total adiponectin concentrations. Upon insulin stimulation, secreted adiponectin concentrations from WT Subc AT were significantly increased compared to non-treated control (Figure 38 A). Importantly, treatment of TRPC1$^{-/-}$ Subc AT with

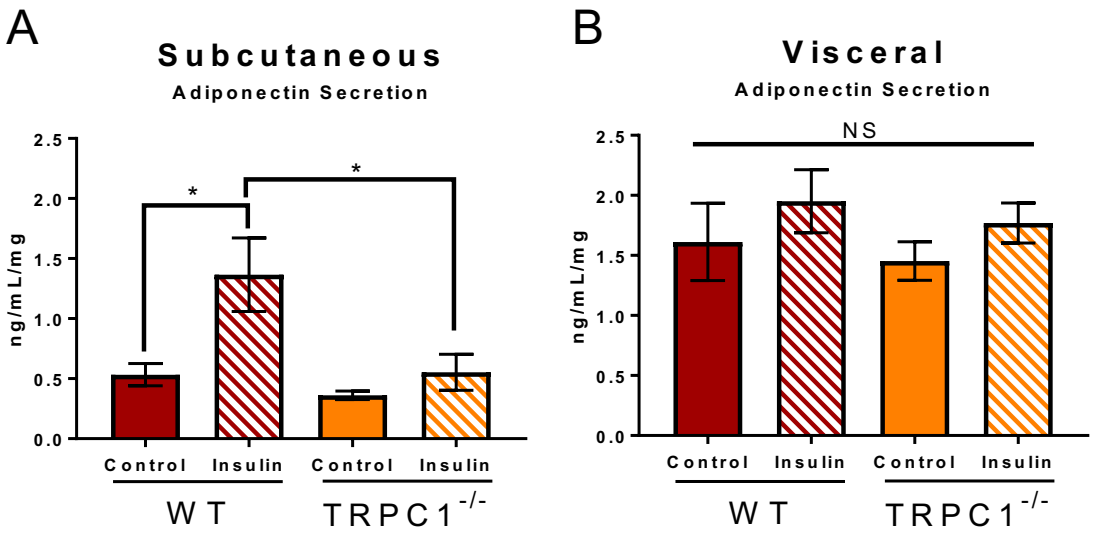

Figure 37 Insulin stimulated secretion diminished in TRPC1$^{-/-}$ Subc AT

Elisa assessed adiponectin secreted from Subc AT (A) and VAT (B) samples in 8-15 mg pieces from WT and TRPC1$^{-/-}$ stimulated with insulin (100 nM) for 6 hours, n=9. Concentration of adiponectin normalized to tissue size (mg). Graphs are mean ± SEM, significance: *, $p < 0.05$.

insulin did not result in a significant increase in adiponectin secretion as seen in the WT Subc AT, but was significantly lower that WT Subc AT stimulated with insulin (Figure 38 A). Interestingly, insulin stimulation of VAT from both WT and TRPC1$^{-/-}$ mice did not result in a significant increase in adiponectin secretion (Figure 38 B), however all VAT samples secreted roughly 2-fold more adiponectin than Subc AT samples. This could be attributed to the increased endogenous levels seen in VAT (Figure 35) and possibly indicate non-stimulated secretion from VAT is higher than Subc AT.

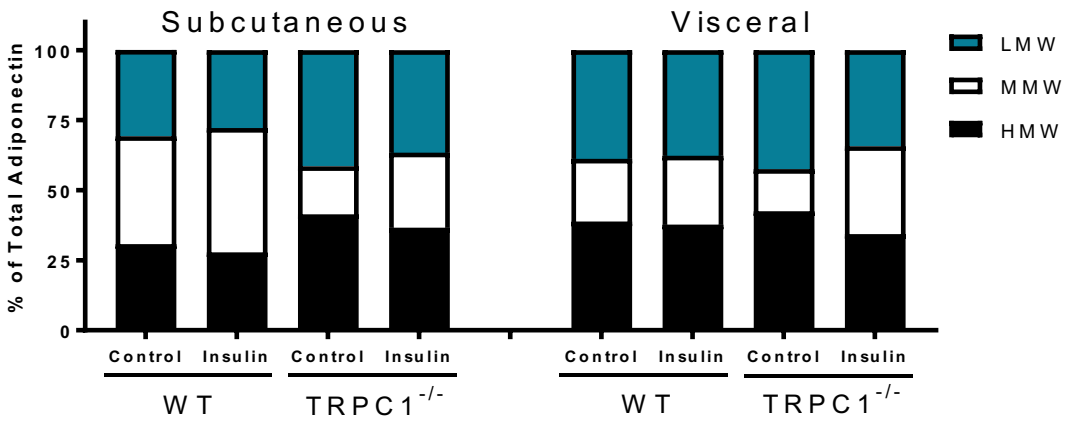

Figure 38 Distribution of adiponectin isoforms from secretion samples

Analysis of adiponectin isoforms from Figure 37 assessed by non-denaturing PAGE. Optical density of each isoform (HMW (high molecular weight), MMW (middle molecular weight), LMW (low molecular weight)) is shown as a percentage of total adiponectin for each lane. No significance was determined for all samples.

Analysis of adiponectin isoforms upon insulin stimulation showed a slight increase in MMW secretion in Subc AT from both WT and TRPC1$^{-/-}$, however no significance was determined. Overall the distribution of adiponectin isoforms was similar in all tissue types and animals (Figure 38). This data indicates adipocytes with TRPC1 deficiency have a reduced response to insulin–stimulated secretion of adiponectin, but it does not affect the overall distribution of isoforms secreted.

Reduced SNARE protein interactions in TRPC1$^{-/-}$ adipose tissue

Our lab has shown that a functional interaction between SNARE family proteins and Ca^{2+} influx is required for intracellular vesicle fusion (Singh et al., 2004), thus we investigated whether impairment of adiponectin secretion may be due to diminished SNARE interactions due to TRPC1 loss. VAMP-2 is found within the plasma membrane of intracellular vesicles and is involved in the docking of the vesicles to the plasma membrane by interacting with plasma membrane SNARE proteins, such as syntaxin-1 and SNAP 25. To assess whether TRPC1 may be involved in SNARE complex formation needed to exocytose adipokine vesicles from adipose tissue, co-immunoprecipitation was performed on fresh adipose samples. Subc AT and VAT were isolated from WT and TRPC1$^{-/-}$ mice, homogenized, quantified, and incubated with insulin (100 nM), SKF (10 mM), or Tg (1 mM) for 30 min. In this model, insulin treatment mimics the initial stages of adiponectin secretion (as seen in Figure 38) and SKF treatment was used to determine whether blocking store-mediated Ca^{2+} influx channels would reduce

insulin-induced SNARE interactions. As shown in Figure 40, plasma membrane SNARE components syntaxin-1 and SNAP-25 co-immunoprecipitated with VAMP2 in both WT and TRPC1$^{-/-}$ control samples. Upon treatment with insulin, the interaction of VAMP-2 with syntaxin-1 and SNAP-25 increased in WT samples, however no change was observed in TRPC1$^{-/-}$ samples. Pretreatment with SKF prior to insulin did not alter interactions of SNAP-25 with VAMP-2 in WT adipose tissue, however it did reduce interactions of VAMP-2 with syntaxin-1. Treatment of TRPC1$^{-/-}$ adipose tissue cells with SKF had no effect on interactions of either syntaxin-1 or SNAP-25 with VAMP-2. Raising $[Ca^{2+}]_i$ and initiating SOCE through treatment with Tg increased SNAP-25 and VAMP-2 interactions in WT adipose tissue, however it did not result in a change in WT VAMP-2 and syntaxin-1 interactions. Further, no variation in interactions between VAMP-2 and SNAP-25 or syntaxin-1 was observed upon treatment with Tg within TRPC1$^{-/-}$ adipose tissue indicating depletion of the ER and initiation of SOCE mechanisms is not enough to overcome the loss of TRPC1. Together these results indicate insulin stimulated SNARE complex formation in adipose tissue involves TRPC1-mediated Ca^{2+} entry, which is needed for exocytosis of adiponectin.

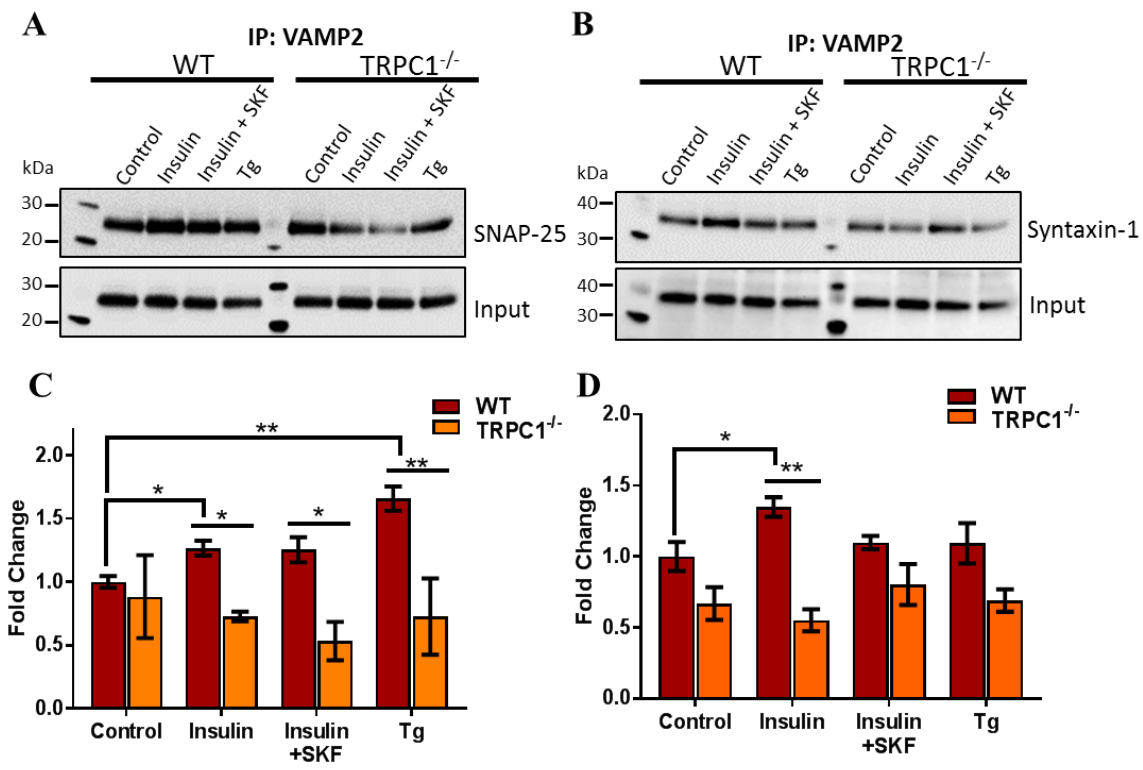

Figure 39 Reduced SNARE protein interactions in TRPC1$^{-/-}$ adipose tissue

Co-immunoprecipitation assay of SNARE complex proteins in combined Subc AT and VAT tissue lysates from WT and TRPC1-/- upon stimulation with insulin (100 nM), SKF (20 µM), or Tg (2 µM). Western blot analysis was performed using anti-Vamp2 antibody and immunoprecipitating with anti-SNAP25 (A,C) and anti-Syntaxin-1 (B,D) antibodies. Graphs are mean ± SEM, significance: *, $p < 0.05$; **, $p < 0.01$.

Conclusion

Reduced secretion of adiponectin resulting in low serum concentrations is a common feature of obesity (Kovacova et al., 2012), whereas low serum leptin can be used as an indicator of malnutrition (Amirkalali et al., 2010). TRPC1$^{-/-}$ mice present both reduced serum adiponectin and leptin concentrations, however TRPC1$^{-/-}$ mice do not display either of these phenotypes. Food consumption and weight measurements of TRPC1$^{-/-}$ mice were similar to WT throughout their lifetime (Figure 25), however as we saw previously (Figure 21), as TRPC1$^{-/-}$ mice age, their volume of adipose deposits increases. This increase in adiposity later in life is could be attributed to decreased differentiation as discussed in Chapter III or to suppressed adiponectin secretion which lowers overall body metabolism. Importantly, equal concentrations of adiponectin and leptin were observed within the Subc AT and VAT samples of WT and TRPC1$^{-/-}$ mice, which is contrary to the reduced serum concentrations in TRPC1$^{-/-}$ mice (Figure 35). This indicates that there is no reduction in adipokine production, but rather the release of adipokines is affected in TRPC1$^{-/-}$ mice.

When challenging both WT and TRPC1$^{-/-}$ mice with a high-fat diet and exercise for 12 weeks, we observed an increase in total serum adiponectin concentrations in sedentary WT mice feed a high-fat diet and exercised WT mice on a normal-chow. It has been well established that exercise increases circulating adiponectin concentrations (Kriketos et al., 2004; Lee et al., 2011; Wang et al., 2015), however the effect of a high-fat diet on serum adiponectin is still debated.

Differing studies have shown both increases and decreases in serum adiponectin concentrations when mice are fed a high-fat diet (Barnea et al., 2006; Bullen et al., 2007; Chaolu et al., 2011) and may be reflective of acute versus long-term feeding. This discrepancy in results after high-fat feeding may explain why WT mice feed a high-fat diet and exercised did not display an increase in adiponectin concentrations as compared to sedentary WT mice on a normal-chow diet. Importantly, the results of the 12 week study confirmed our previous result that sedentary TRPC1$^{-/-}$ mice on a normal-chow diet have significantly decreased serum adiponectin concentrations and as we saw in Figure 24, sedentary TRPC1$^{-/-}$ mice fed normal-chow did not display a difference in overall body weight or fat mass as compared to WT. This indicates reduced serum adiponectin concentrations in TRPC1$^{-/-}$ mice is not a result of increased adiposity further indicating a dysfunction in adiponectin secretion. It is also notable that the high-fat diet had no effect on sedentary TRPC1$^{-/-}$ mice, however the addition of exercise did result in differences in both TRPC1$^{-/-}$ mice feed a high-fat and normal-chow diet.

Exercise is thought to increase circulating adiponectin concentrations through a multitude of processes including increased expression of adiponectin receptors in muscle (Tsuchida et al., 2004; Zeng et al., 2007), increased secretion of adiponectin from muscle through PPARy activation (Amin et al., 2010), and release of adiponectin from adipose tissue due to exercise induced fat mass loss (Wang et al., 2015). The theory that increased serum adiponectin is due to release

of adiponectin stores from exercise induced fat mass loss is most likely not occurring in our study as the only animal that had reduced weight and fat mass was TRPC1$^{-/-}$ mice that were fed a high-fat diet and exercised (Figure 24). If this theory was correct, we would expect the increased serum adiponectin concentrations in exercised WT mice on normal-chow to be correlated to a decrease in fat mass, which was not seen. The more probable explanation would be increases in either adiponectin receptors or secretion from muscle, which could compensate for the reduced adiponectin secretion from adipose tissue due to TRPC1 loss.

Interestingly, it has been found that the greatest reduction in serum adiponectin in obese subjects is from Subc AT and the metabolically active isoform HMW (Kovacova et al., 2012). Analysis of serum adiponectin isoforms in our study indicates a similar reduction in HMW with the addition of MMW, however internal adipose tissue concentrations of adiponectin were similar between WT and TRPC1$^{-/-}$. This reduction in TRPC1$^{-/-}$ serum HMW isoform is most likely due to increased utilization by downstream targets, such as muscle and liver, since overall abundance is diminished. However, due to the lack of understanding of the purpose and distribution of adiponectin isoforms, more investigation is needed.

The dependence on Ca^{2+} for the secretion of adipokines has been shown in numerous studies (Bogan and Lodish, 1999; El Hachmane et al., 2018; Komai et al., 2014; Levy et al., 2000; Sukumar et al., 2012; Ye et al., 2010), however the Ca^{2+} channel(s) involved have not been identified. The most extensive work has

shown that cAMP stimulates exocytosis of adiponectin-containing vesicles in a Ca^{2+} dependent and independent manner (Komai et al., 2014), but no channel specificity was determined. Within the study by Sukumar et al., alterations in adiponectin secretion due to blockage of TRPC1 and TRPC5 in differentiated 3T3-L1 adipose cells through use of antibodies and siRNA was investigated. Contrary to our findings, their results showed an increase in adiponectin in the extracellular media indicating increased secretion, however no measurement of changes in internal adiponectin production, basal internal concentrations, or agonist mediated release were determined. Also, the 3T3-L1 cell line originates from a single clone, resulting in a cell line incomparable to the characteristics of primary cell culture models (Ruiz-Ojeda et al., 2016). Because of this, we do not feel the 3T3-L1 cell line is a precise model of the in vivo state, thus we believe our usage of primary cell lines from SVF and ex vivo tissue stimulation is a more accurate representation.

It has been well documented that regulated exocytotic events including the fusion of intracellular organelles such as synaptic vesicles, secretory vesicles/granules, or lysosomes with the plasma membrane are Ca^{2+}-dependent (Reddy et al., 2001; Royle and Murrell-Lagnado, 2003). In particular, TRPC channels have been implicated in the GPR40 signaling pathway of glucose-stimulated insulin secretion in pancreatic beta-cell (Yamada et al., 2016). Within secretory pathways, it has been suggested that increases in $[Ca^{2+}]_i$ is needed in the vicinity of organelles (Barclay et al., 2005; Burgoyne and Clague, 2003), thus

our lab began investigation into the recruitment of Ca^{2+} channels to the site of fusion. Our lab previously demonstrated a functionally significant interaction between TRPC3 and SNARE proteins involved in intracellular vesicles fusion (Singh et al., 2004). Within this study, TRPC3 was observed to colocalize and co-immunoprecipitate with VAMP-2 in neuronal cells, thus we theorized that this phenomenon may not be isolated to TRPC3. Utilizing this theory, we investigated whether TRPC1 may be important for SNARE complex formation adipocytes. To understand the mechanisms as to how TRPC1 regulates adipokine secretion, we stimulated fresh homogenized WT and $TRPC1^{-/-}$ adipose tissue with various agents and measured the interactions of VAMP-2 with SNAP-25 and syntaxin-1. Insulin stimulation induced the secretion of adiponectin and increased interactions of VAMP-2 with both SNAP-25 and syntaxin-1 in WT adipose tissue indicating a possible mechanistic action for adiponectin secretion. Treatment of adipocytes with Tg has shown both an increase and a decrease in adiponectin secretion in a time dependent manner (Torre-Villalvazo et al., 2018), thus we explored whether short term treatment with Tg would alter SNARE interactions. As seen in Figure 40, a 30 min treatment with Tg increased VAMP-2 and SNAP-25 interactions only in WT adipose tissue. Interestingly, neither insulin or Tg resulted in changes in VAMP-2 interactions with either SNAP-25 and syntaxin-1 within $TRPC1^{-/-}$ adipose tissue which indicates a role for TRPC1 in insulin stimulated vesicle fusion. We believe these results provide enough evidence to state that insulin stimulated TRPC1 mediated Ca^{2+} influx is involved in fusion of VAMP-2 with SNAP25 and

syntaxin1, thus necessary for proper secretion of adipokines. Overall, our results provide evidence that TRPC1 not only plays a key role in adipocytes differentiation, but is essential for adipokine secretion, and dysfunction in these vital processes could lead to obesity and metabolic syndrome.

CHAPTER VI

LOSS OF TRPC1 IS LIKELY NOT THE CAUSE OF REDUCED ADIPONECTIN SIGNALING IN SKELETAL MUSCLE

Introduction

As discussed in Chapter V, adiponectin is known to regulate lipid metabolism and mitochondrial biogenesis in a number of target organs including muscle and liver (Achari and Jain, 2017). The effects of adiponectin are mediated in these tissues primarily via the action of two plasma membrane bound atypical seven-transmembrane domain receptors, named AdipoR1 and AdipoR2 (Yamauchi et al., 2003) (Figure 41). Both receptors contain an intracellular N-termini and extracellular C-termini and are significantly homologous with 67% amino acid identity (Kadowaki et al., 2006). AdipoR1 is ubiquitously expressed with the highest abundance in skeletal muscle, while AdipoR2 is predominantly expressed in the liver (Wang et al., 2009; Yamauchi and Kadowaki, 2013). Differences between AdipoR1 and AdipoR2 have been identified in binding properties (Yamauchi et al., 2003), cell surface expression (Heiker et al., 2010; Keshvari et al., 2017), and temporal signaling profiles (Keshvari and Whitehead, 2015). Interestingly, a deficiency in AdipoR1, AdipoR2, or both receptors produced

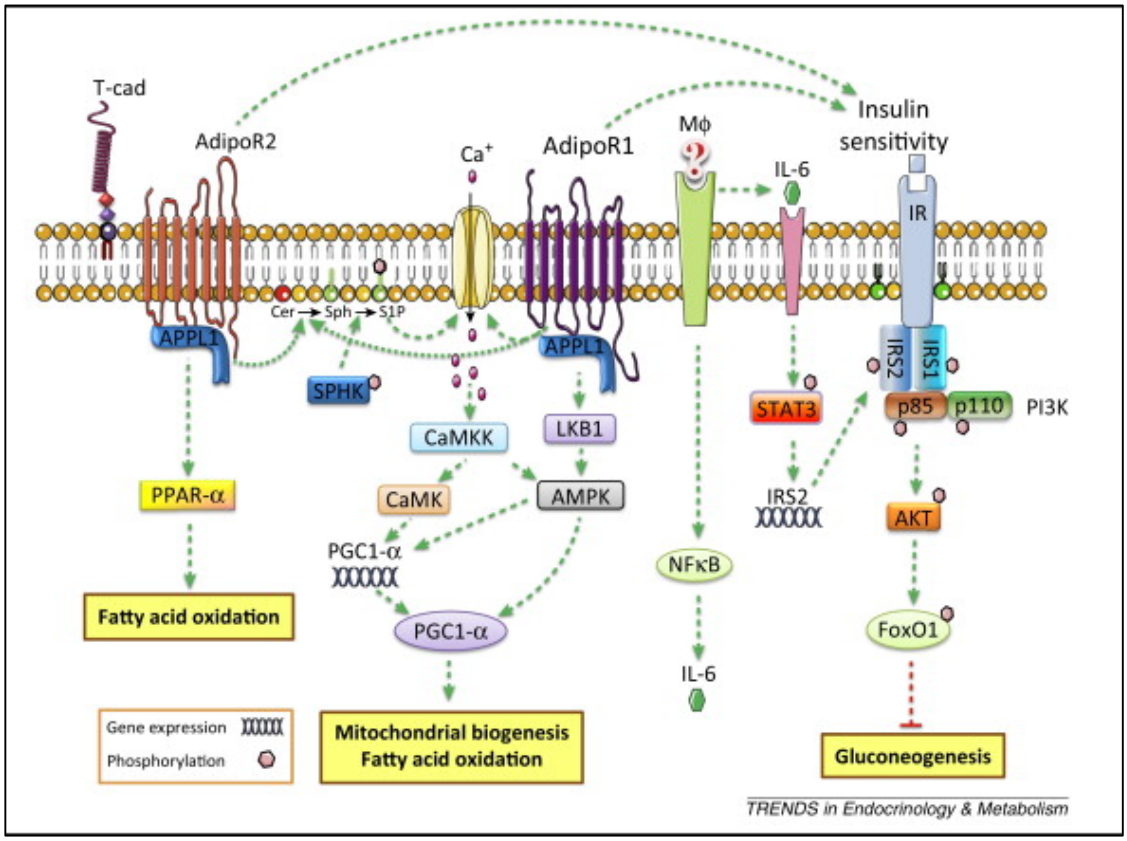

Figure 40 Adiponectin signaling through AdipoR1 and AdipoR2

Adiponectin has three known receptors of AdipoR1, AdipoR2, and T-cadherin (T-cad). AdipoR1/2 can interact with adaptor protein containing pleckstrin homology domain, phosphotyrosine-binding domain, and leucine zipper motif (APPL1). AdipoR1 increases Ca^{2+} influx to activate Ca^{2+}/calmodulin-dependent protein kinase kinase (CaMKK) and subsequent downstream kinases. Ca^{2+}/calmodulin-dependent protein kinase (CaMK) and AMP-activated protein kinase (AMPK) can increase peroxisome proliferator-activated receptor (PPAR) gamma coactivator 1 alpha (PGC-1α) mRNA expression thereby increasing mitochondrial biogenesis and fatty acid oxidation. AdipoR1 activates liver kinase B1 (LKB1) and AMPK. AdipoR2 is predominantly expressed in the liver and can activate PPARα to increase FA oxidation and insulin sensitivity. Reprinted from “The multifaceted and controversial immunometabolic actions of adiponectin” by S. Esmaili, 2014, Trends in Endocrinology and Metabolism, 25(9), 444-451. Copyright 2014 by Elsevier. Reprinted with permission.

glucose intolerance in a diet-induced obesity mouse model (Yamauchi et al., 2007), while muscle-specific AdipoR1-KO mice also display metabolic dysfunction (Iwabu et al., 2010). Overexpression of AdipoR1 in rat skeletal muscle has been shown to improve insulin resistance and promote glucose uptake (Patel et al., 2012). Recently, overexpression of AdipoR1 or AdipoR2 in mouse tibialis anterior muscle increased adiponectin signaling, however the effects were diminished in obese mice despite no reduction in circulating adiponectin levels (Keshvari et al., 2017). The overexpression of AdipoR1 or AdipoR2 had no effect on circulating adiponectin concentrations, however, knockouts of the receptors had differing phenotypes. Mice deficient of AdipoR1 had increased fat mass, decreased glucose tolerance, and no change in plasma adiponectin concentrations while AdipoR2 deficient mice were lean, had improved glucose tolerance, and increased plasma adiponectin concentrations (Bjursell et al., 2007). Much is still to be understood about adiponectin signaling, but evidence suggests the receptors AdipoR1 and AdipoR2 may play differing roles.

Another adiponectin-binding partner is T-cadherin which has been identified in C2C12 myoblasts and skeletal muscle. Though T-cadherin has a high binding affinity for hexameric and HMW forms (Hug et al., 2004), it is not thought to have the same receptor properties as AdipoR1 and AdipoR2 as T-cadherin does not contain an intracellular domain. Interestingly, deficiency of T-cadherin in mice leads to a major upregulation of circulating adiponectin levels indicating some sort of role in adiponectin signaling (Williams et al., 2012).

Bound to both AdipoR1 and AdipoR2 is adaptor protein containing pleckstrin homology domain, phosphor-tyrosine domain, and leucine zipper domain 1 (APPL1) which is known to positively modulate adiponectin signaling (Figure 41). Specifically, suppression of APPL1 reduces adiponectin signaling while overexpression increases downstream events (Cheng et al., 2007; Mao et al., 2006). The downstream targets of AdipoR1 and AdipoR2 are contrasting and result in different outcomes. AdipoR1, through APPL1, is known to promote AMP-activated protein kinase (AMPK) activation and a subsequent increase in expression of master regulator peroxisome proliferator-activated receptor γ coactivator-1α (PGC-1α), whereas AdipoR2 mediates activation of peroxisome proliferator-activated receptor alpha (PPARα), both of which are involved in fatty acid oxidation (Jäger et al., 2007; Yamauchi et al., 2007). Another interesting difference between AdipoR1 and AdipoR2, is the involvement in Ca^{2+} influx in AdipoR1 signaling. Iwabu et al., 2010 showed that adiponectin binding to AdipoR1 induces a Ca^{2+} influx, which activates Ca^{2+}/calmodulin-dependent protein kinase kinase β (CaMKKβ) and subsequent AMPK. Within this study, downregulation of AdipoR1 by siRNA reduced the influx of Ca^{2+} and chelating Ca^{2+} with EGTA reduced phosphorylation of AMPK. Though there is strong evidence to suggest that Ca^{2+} is a component of the adiponectin signaling pathway, no work has been done to determine the channel responsible for its influx.

It has been demonstrated that SOCE partially contributes to the Ca^{2+} supply necessary for the maintenance of skeletal muscle contraction, however it has been

determined that it is not required for the initiation of muscle contraction (Cho et al., 2017; Stiber et al., 2008). In skeletal muscle, SOCE is modulated much faster than non-excitable cells with activation occurring within a second whereas non-excitable cells require tens of seconds (Nakipova et al., 2017). The fast kinetics of skeletal muscle SOCE is likely due to the pre-coupling of STIM1 to ORAI1 (Dirksen, 2009; Stiber et al., 2008). Very little has been investigated regarding TRPC1 involvement in SOCE within skeletal muscle, but TRPCs have been shown to have important roles in skeletal muscle in other ways. In particular, TRPC1 has been shown to be important for skeletal muscle migration and differentiation (Louis et al., 2008; Zanou et al., 2012). Further, skeletal muscles from TRPC1$^{-/-}$ mice display smaller myofibre cross-sectional areas resulting in reduced contractional force over time (Zanou et al., 2010).

Within this study, we investigate the involvement of TRPC1 in adiponectin signaling pathway in muscle to determine whether loss of TRPC1 has an effect on downstream targets and upstream adiponectin serum concentrations due to failed signaling. We report that SOCE mechanisms are exhibited in both C2C12 muscle cell line and primary Extensor Digitorum Longus (EDL) muscle. Additionally, activation of AdipoR1 with the agonist AdipoRon results in an influx of Ca^{2+} which can be blocked by SKF and 2APB, however this blockage has no effect on the downstream targets of AMPK and PGC1α. Further, loss of TRPC1 in EDL muscle does not reduce the influx of Ca^{2+} due to AdipoRon treatment or PGC1α expression, however it does reduce the phosphorylation of AMPK. Together this

data indicates TRPC1 is most likely not a target channel for adiponectin signaling and loss TRPC1 does not affect downstream effects.

Results

Reduced expression of adiponectin targets in TRPC1$^{-/-}$ muscle

Our first step was to determine whether reduced serum adiponectin concentrations in TRPC1$^{-/-}$ mice had an effect on the expression of genes targeted by adiponectin in liver and muscle. These included PGC1α, lipid metabolism genes of medium-chain acyl-CoA dehydrogenase (ACADM), fatty acid synthase (FASN), and acetyl-CoA carboxylase (ACC) along with mitochondrial biogenesis genes nuclear-encoded NRF1 (nuclear respiratory factor 1), mitochondrial transcription factor A (TFAM), and estrogen-related receptor alpha (ERRα). Interestingly, the two tissue types had differing expression levels even though they are both adiponectin targets (Figure 42). Liver showed no change in PGC1α or mitochondrial biogenesis genes, however TRPC1$^{-/-}$ mice had a significant increase in the lipid metabolism genes FASN and ACC as compared to WT mice. Conversely, muscle expression levels of TRPC1$^{-/-}$ mice were decreased in PGC1α, lipid metabolism ACC and FASN mRNA, and mitochondrial biogenesis NRF1 and ERRα. The muscle mRNA profile is similar to those reported due to decreases in serum adiponectin concentrations (Civitarese et al., 2006), however more investigation is needed to confirm.

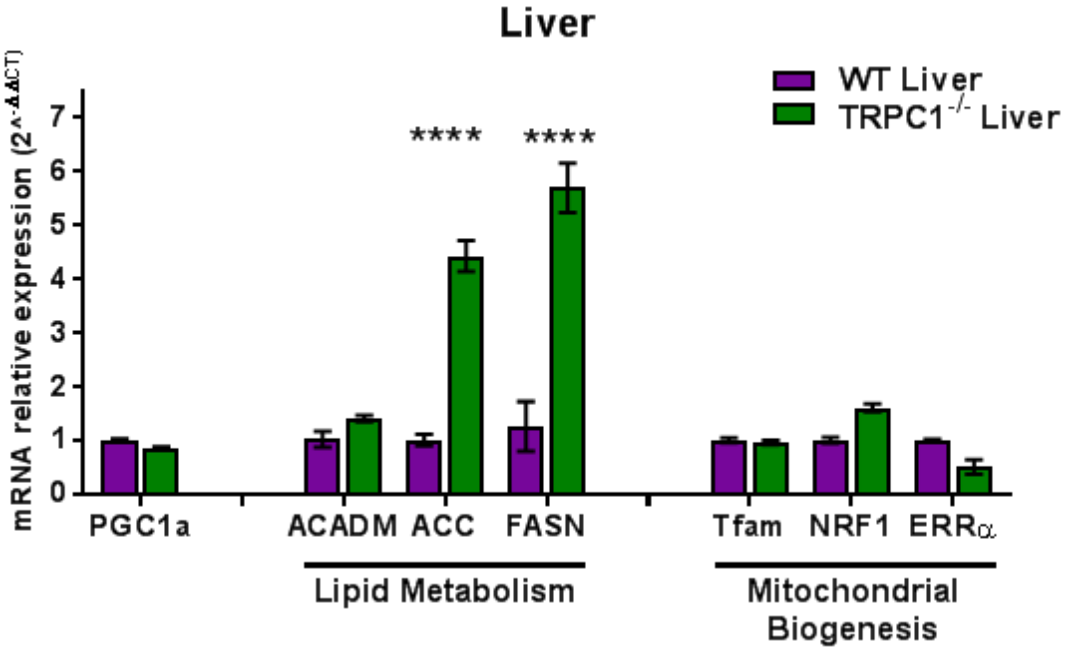
Liver
WT Liver
TRPC1-/- Liver
mRNA relative expression (2^-ΔΔCT)
7
6
5
4
3
2
1
0
****
****
PGC1a
ACADM
ACC
FASN
Tfam
NRF1
ERRα
Lipid Metabolism
Mitochondrial Biogenesis

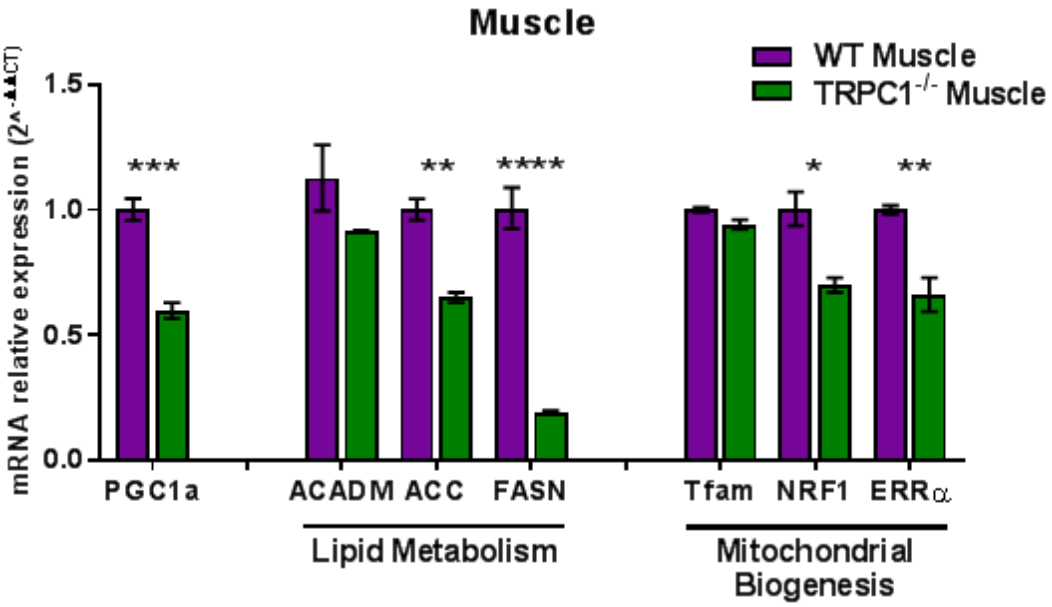
Muscle
WT Muscle
TRPC1-/- Muscle
mRNA relative expression (2^-ΔΔCT)
1.5
1.0
0.5
0.0
***
**
****
*
**
PGC1a
ACADM
ACC
FASN
Tfam
NRF1
ERRα
Lipid Metabolism
Mitochondrial Biogenesis

Figure 41 mRNA expression of lipid metabolism and mitochondrial biogenesis genes in liver and muscle

Isolated mRNA from liver and bicep femoris muscle of WT and TRPC1$^{-/-}$ mice were measured for the expression of peroxisome proliferator-activated receptor γ coactivator 1α (PGC1α), lipid metabolism genes of medium-chain acyl-CoA dehydrogenase (ACADM), fatty acid synthase (FASN), and acetyl-CoA carboxylase (ACC) along with mitochondrial biogenesis genes nuclear-encoded NRF1 (nuclear respiratory factor 1), mitochondrial transcription factor A (TFAM), and estrogen-related receptor alpha (ERRα), n= 3. Graphs are mean ± SEM, significance: *, $p < 0.05$; **, $p < 0.01$; ***, $p < 0.001$; ****, $p < 0.0001$.

Differentiated muscle cell line exhibits SOCE characteristics

Since muscle mRNA was reduced in TRPC1$^{-/-}$ mice, we investigated whether this was a result of reduced adiponectin signaling in muscle due to a lack of TRPC1 mediated Ca^{2+} influx. Before analyzing TRPC1 directly we first utilized the C2C12 muscle cell line and differentiated the cells into mature myotubes and measured Ca^{2+} influx and protein expression of SOCE proteins. Calcium imaging results indicated a reduction in $[Ca^{2+}]_i$ peak upon treatment of Tg (release of ER stores) when cells were treated with either (10 uM) SKF or (100 uM) 2-Aminoethoxydiphenyl borate (2-APB, an inhibitor of IP3 receptors and TRP

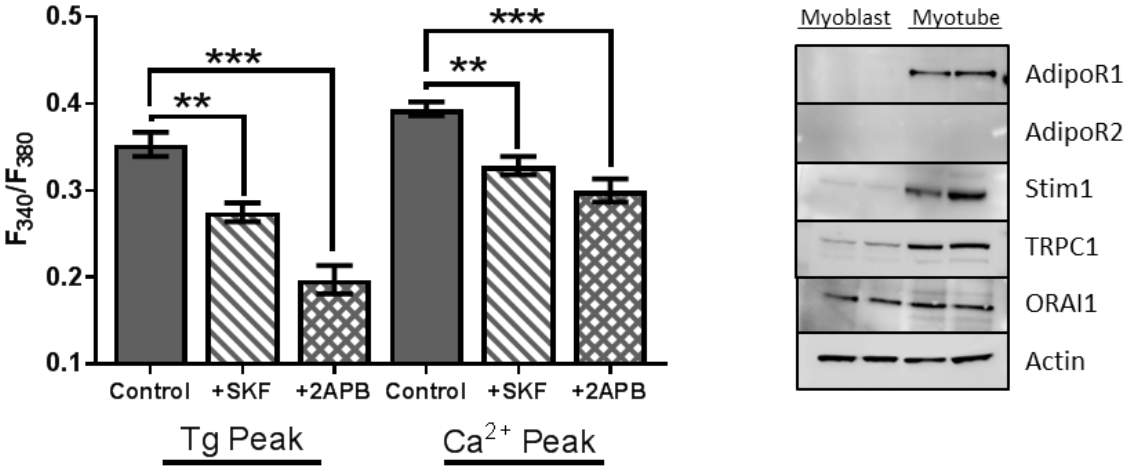

Figure 42 C2C12 myotubes exhibit SOCE properties

Quantification of Fura-2 trace peaks of $[Ca^{2+}]_i$ after addition of 1 μM Tg and 1 mM Ca^{2+} to differentiated C2C12 myotubes treated with either 10 uM SKF or 100 uM 2APB. Protein expression of SOCE proteins Stim1, TRPC1, and ORAI1 and adiponectin receptors AdipoR1 and AdipoR2 in C2C12 myoblasts and myotubes. Graphs are mean ± SEM, significance: **, $p < 0.01$; ***, $p < 0.001$.

channels) (Figure 43). Upon the addition of 1 mM extracellular Ca^{2+}, a reduction in Ca^{2+} influx was observed in both SKF and 2APB treatments. This data confirms earlier reports that SOCE is displayed within C2C12 myotubes (Stiber et al., 2008), however, the administration of SKF and 2APB adversely affect ER store release. To confirm the presence of SOCE in C2C12 myotubes, protein expression of SOCE channels including STIM1, TRPC1, and ORAI1 was measured. Expression of all three SOCE proteins was highly evident in differentiated C2C12 myotubes, however expression of STIM1 and TRPC1 was minimal in undifferentiated C2C12 myoblasts (Figure 43). Together this data indicates mature C2C12 myotubes exhibit SOCE characteristics and the STIM1, ORAI1, and TRPC1 complex may be involved.

Blockage of SOCE reduces AdipoRon Ca^{2+} influx,

but not downstream targets

To test whether SOCE was involved in adiponectin signaling pathway in muscle, we first confirmed the expression of the adiponectin receptors AdipoR1 and AdipoR2 in C2C12 cells. As shown, neither receptor is expressed in C2C12 myoblasts and only the AdipoR1 receptor is expressed in mature C2C12 myotubes (Figure 43). Utilizing the synthetic adiponectin receptor agonist AdipoRon, we measured the Ca^{2+} influx when SOCE channels are blocked. Administration of (50 uM) AdipoRon resulted in an immediate influx of Ca^{2+} in C2C12 myotubes which

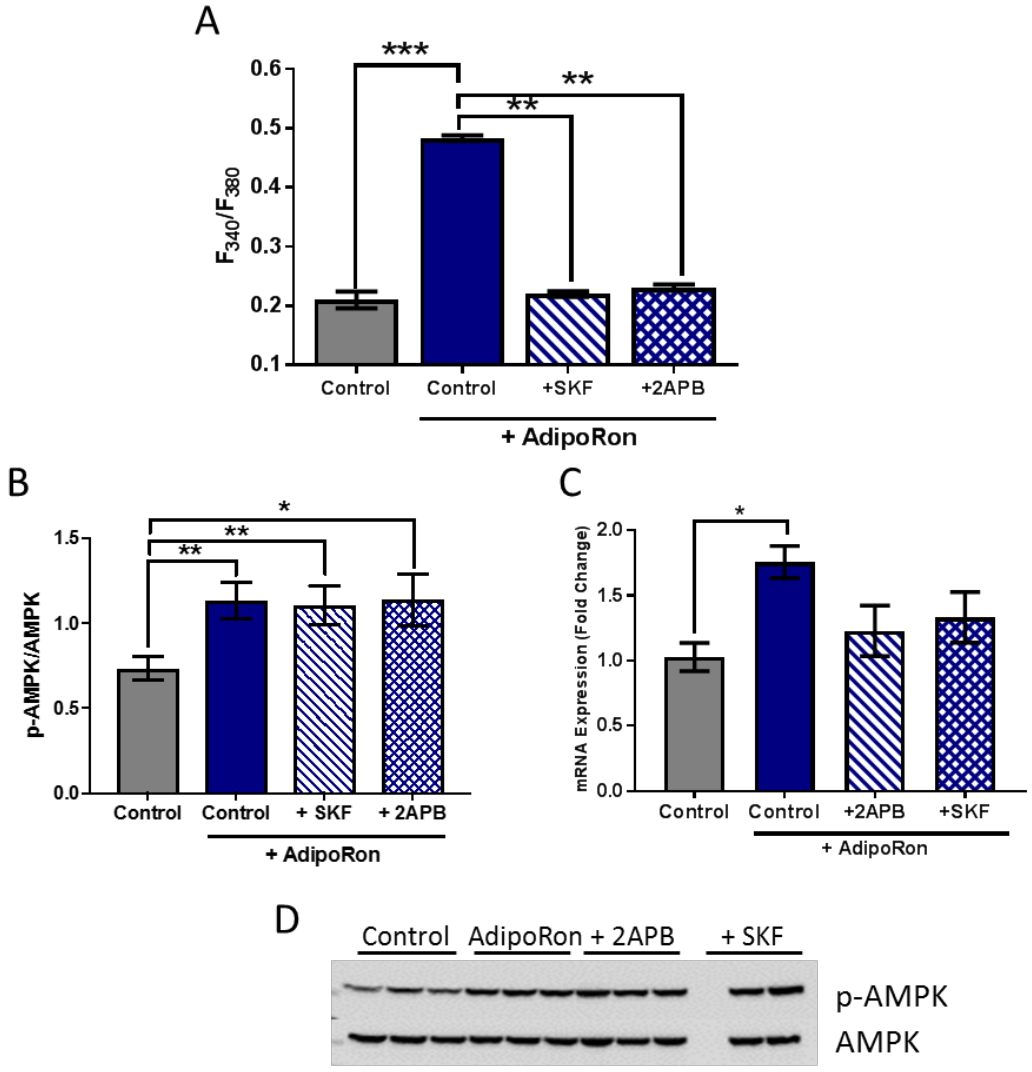

Figure 43 Blockage of SOCE reduces AdipoRon Ca2+ influx, but not downstream targets in C2C12 myotubes

(A) Quantification of Fura-2 trace peaks of $[Ca^{2+}]_i$ after addition of 50 uM AdipoRon to differentiated C2C12 myotubes treated with either 10 uM SKF or 100 uM 2APB in a Ca^{2+} buffer. (B) Western blot quantification of ratio of p-AMPK to AMPK after 5 min treatment with 50 uM AdipoRon with representative blot in (D) n=7-13. (C) Relative mRNA expression of PGC1α after 90 min treatment with 50 uM AdipoRon quantified by RT-PCR, n=6. Graphs are mean ± SEM, significance: *, $p < 0.05$, **, $p < 0.01$; ***, $p < 0.001$

was completely diminished with treatment of (10 uM) SKF or (100 uM) 2APB (Figure 44 A). We next tested whether this reduction in Ca^{2+} influx due to SKF and 2APB would alter the downstream signaling targets of AdipoR1 of AMPK and PGC1α. C2C12 cells were pretreated with (10 uM) SKF and (100 uM) 2APB for 10 min and then treated with (50 uM) AdipoRon for an additional 5 min and activating phosphorylation of AMPK was measured (Figure 44 B, D). As shown, AdipoRon induced a significant increase in AMPK phosphorylation, however treatment with SKF or 2APB had no effect. AdipoRon is known to induce increased expression of PGC1α mRNA after 90 min (Okada-Iwabu et al., 2013), thus we quantified PGC1α mRNA expression after pretreatment with (10 uM) SKF and (100 uM) 2APB for 10 min. Results are inconclusive as treatment with SKF and 2APB on PGC1α mRNA is neither significantly increased from control or decreased from AdipoRon treatment (Figure 44). Overall, these data suggest that adiponectin receptor activation results in SOCE like Ca^{2+} influx, however blockage of SOCE is not detrimental to the progression of the signaling cascade.

SOCE not diminished in primary muscle due to loss of TRPC1

Even though the downstream targets of AdipoR1 were not affected by blockage of SOCE in C2C12 myotubes, we were still interested in whether TRPC1 may be involved in adiponectin signaling in either a SOCE or SOCE independent manner. First, WT EDL muscle fibers were isolated and individually cultured to activate muscle satellite cells. Upon confluence, EDL myoblasts will naturally

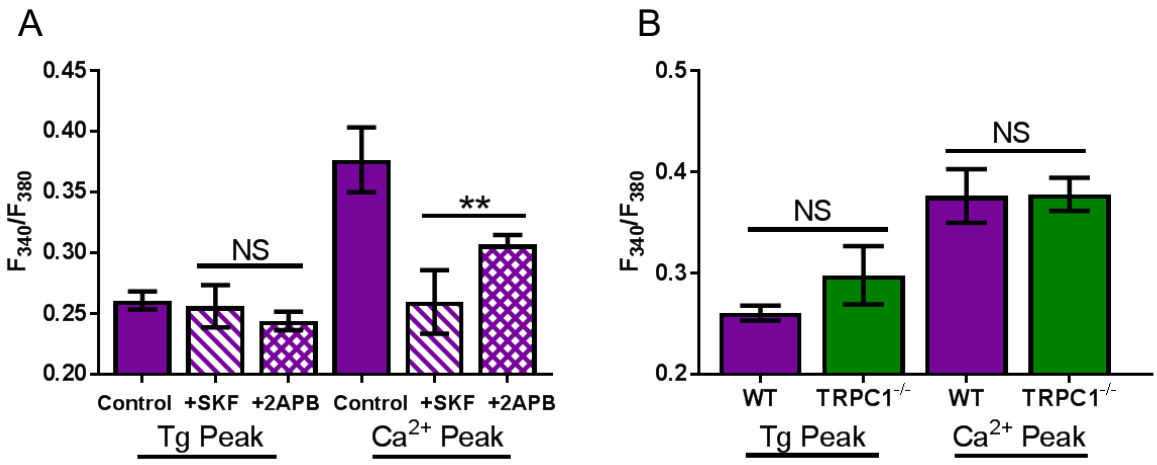

Figure 44 WT EDL muscle exhibits SOCE mediated Ca^{2+} influx which is not diminished by loss of TRPC1

EDL muscle was isolated from WT and TRPC1$^{-/-}$, cultured, and differentiated into mature EDL myotubes as described in Methods. (A) Quantification of Fura-2 trace peaks of $[Ca^{2+}]_i$ after addition of 1 μM Tg and 1 mM Ca^{2+} to WT EDL myotubes treated with either 10 uM SKF or 100 uM 2APB. (B) Quantification of Fura-2 trace peaks of $[Ca^{2+}]_i$ after addition of 1 μM Tg and 1 mM Ca^{2+} to WT and TRPC1$^{-/-}$ EDL myotubes treated with either 10 uM SKF or 100 uM 2APB. Graphs are mean ± SEM, significance: **, $p < 0.01$.

differentiate into myotubes with twitching observed around day 7. We first established whether primary WT EDL muscle cultures exhibit the same SOCE mechanisms as C2C12 cells by blocking SOCE channels with SKF or 2APB. As seen in Figure 45 A, WT EDL efflux relatively the same from ER stores upon treatment with Tg, however treatment with either (10 uM) SKF or (100 uM) 2APB reduced the influx of Ca^{2+} upon addition of 1 mM Ca^{2+}. We next tested TRPC1$^{-/-}$

EDL in the same manner. As compared to WT EDL, TRPC1$^{-/-}$ displayed no significant change in either ER store efflux due to Tg or Ca^{2+} influx due to addition of 1 mM Ca^{2+} to the extracellular solution (Figure 45 B). Together this indicates that EDL muscle do exhibit SOCE mechanisms, however loss of TRPC1 does not affect it.

Initial influx of Ca^{2+} due to treatment with AdipoRon is not TRPC1 dependent

To determine the involvement of TRPC1 in adiponectin signaling, we first confirmed the expression of AdipoR1 in both WT and TRPC1$^{-/-}$ EDL. Neither WT or TRPC1$^{-/-}$ EDL express AdipoR2 and no difference of AdipoR1 expression was observed between WT and TRPC1$^{-/-}$ EDL (Figure 46, B). The next step was to measure the response of WT EDL to AdipoRon when SOCE mechanisms are blocked. AdipoRon administration resulted in a significant increase in Ca^{2+} influx which was blocked when treated with (10 uM) SKF or (100 uM) 2APB (Figure 46 A). Comparison of Ca^{2+} influx upon treatment of AdipoRon resulted in no significant difference between WT and TRPC1$^{-/-}$ EDL (Figure 46 C). So far, this data indicates that treatment with the adiponectin receptor AdipoRon does not initiate a Ca^{2+} influx via TRPC1.

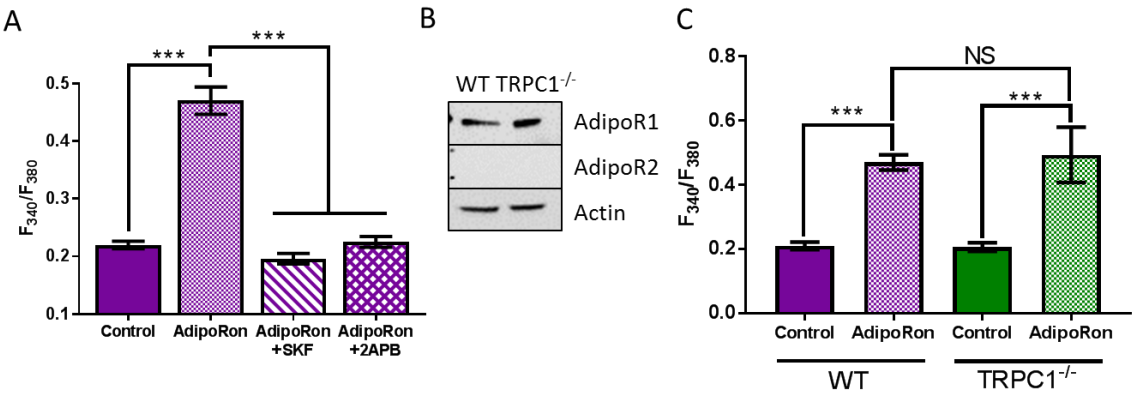

Figure 45 AdipoRon initiated Ca^{2+} influx is not TRPC1 dependent

(A) Quantification of Fura-2 trace peaks of $[Ca^{2+}]_i$ after addition of 50 uM AdipoRon to differentiated WT EDL myotubes treated with either 10 uM SKF or 100 uM 2APB in a Ca^{2+} buffer. (B) Protein expression of AdipoR1 and AdipoR2 in WT and TRPC1$^{-/-}$ EDL. (B) Quantification of Fura-2 trace peaks of $[Ca^{2+}]_i$ after addition of 50 uM AdipoRon to differentiated WT and TRPC1$^{-/-}$ EDL myotubes in a Ca^{2+} buffer. Graphs are mean ± SEM, significance: ***, $p < 0.001$.

Loss of TRPC1 in EDL impairs the ability of AdipoRon to initiate downstream targets of adiponectin signaling

The final step to determine involvement of TRPC1 in adiponectin signaling was to monitor the effects of AdipoRon on downstream targets of AMPK and PGC1α in TRPC1$^{-/-}$ EDL. Addition of AdipoRon to WT EDL resulted in a more than 2 fold increase in phosphorylation of AMPK after 5 minutes (Figure 47 A, B). When the same treatment was applied to TRPC1$^{-/-}$ EDL, there was a slight increase in

phosphorylation of AMPK, however it was not enough to be significant. Moreover, comparison of TRPC1$^{-/-}$ to WT indicated loss of TRPC1 significantly reduced phosphorylation of AMPK initiated by AdipoRon treatment (Figure 47 A, B). Expression changes of PGC1α mRNA were next examined and found that loss of TRPC1 in EDL myotubes reduced the ability of AdipoRon signaling. Significant increases in PGC1α mRNA observed in WT EDL upon AdipoRon treatment were not observed in TRPC1$^{-/-}$ EDL (Figure 47 C). The combined results of activation of p-AMPK and PGC1α indicates that TRPC1 may be indirectly involved with in the function of adiponectin signaling.

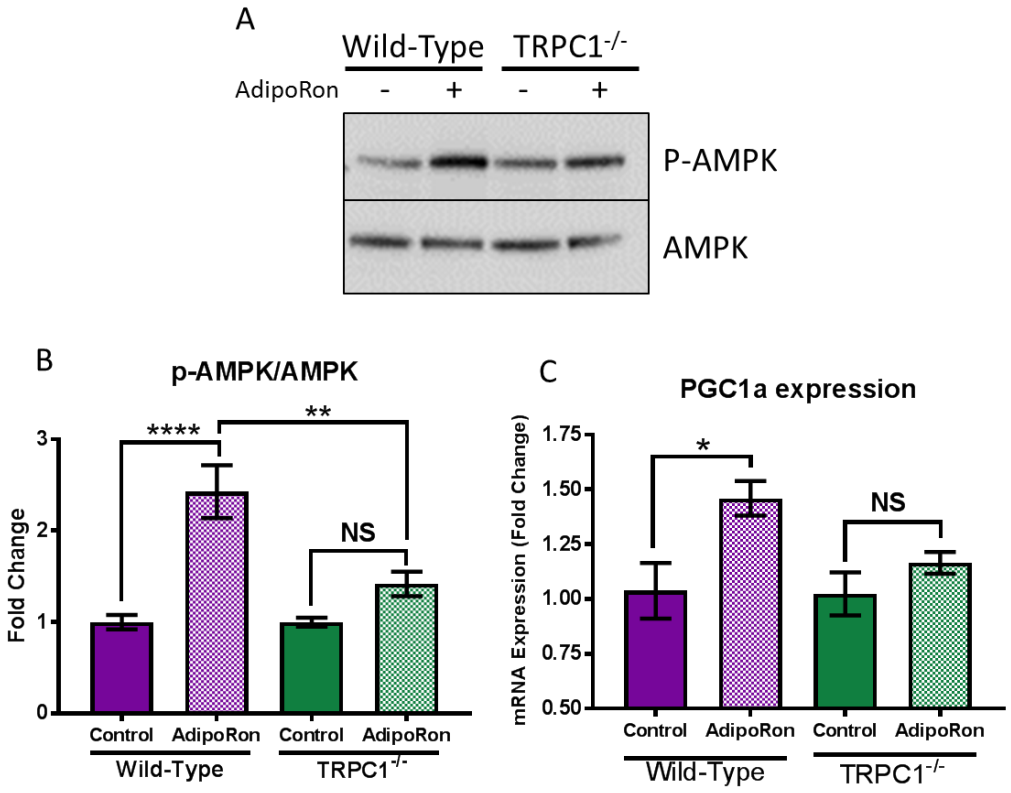

Figure 46 Loss of TRPC1 in EDL impairs the ability of AdipoRon to activate AMPK

(B) Western blot quantification of ratio of p-AMPK to AMPK in WT and TRPC1$^{-/-}$ EDL after 5 min treatment with 50 uM AdipoRon n=6, representative blot in (A). (C) Relative mRNA expression of PGC1α in WT and TRPC1$^{-/-}$ after 90 min treatment with 50 uM AdipoRon quantified by RT-PCR n=6. Graphs are mean ± SEM, significance: *, $p < 0.05$, **, $p < 0.01$; ****, $p < 0.0001$.

Conclusion

Within this study our aim was to extend the understanding of Ca^{2+} involvement, specifically SOCE, in adiponectin signaling to determine whether decreases in PGC1α expression and other targets in TRPC1$^{-/-}$ muscle are a result of decreased signaling capabilities. We employed the use of both the immortalized cell line C2C12 and primary EDL skeletal muscle to determine the role of SOCE activation due to AdipoR1 activation. Here we are the first to show that AdipoRon initiates Ca^{2+} influx that can be blocked by SKF and 2APB, however these treatments do not affect downstream targets. Finally, we were able to determine that loss of TRPC1 does not inhibit the influx of Ca^{2+} due to AdipoRon, but does diminish AMPK phosphorylation. Collectively, these results identify SOCE involvement in adiponectin, but TRPC1 may not be playing a role.

Increased hepatic lipogenesis is a common feature of obesity. Elevated expression of both FASN and ACC have been correlated to obesity (Beaven et al., 2013; Dentin et al., 2006), with the enzyme FASN considered a determinant of maximal tissue capacity of lipid storage (Postic and Girard, 2008) and blockage of ACC has been shown to reduce excess liver lipid accumulation in mice on a high-fat diet (Savage et al., 2006). Within our model, the increased expression of FASN and ACC observed in TRPC1$^{-/-}$ liver indicates an increase in lipogenesis and could be indicative of an obese phenotype. Multiple theories have surfaced as to why increased liver lipogenesis is observed in an obese state. These include the absence of functional adipocytes resulting in an increase of fatty acids being

pushed to the liver (Yki-Järvinen, 2005) and low serum adiponectin concentrations negatively affecting liver functionality (Viganò et al., 2011). Further investigation is needed to determine the cause of reduced FASN and ACC in TRPC1$^{-/-}$ which could be due to dysfunctional adipocytes or liver.

Muscle is similarly affected by the onset of obesity. Accumulation of lipid in skeletal muscle due to high levels of adipose tissue lipolysis or impaired blood lipid clearance by adipose tissue is known to result in insulin resistance and hyperglycemia in skeletal muscle (Stern et al., 2016). Adiponectin is known to offset the negative effects of obesity by encouraging fatty acid oxidation in skeletal muscle thereby decreasing intramuscular lipid accumulation and improving insulin sensitivity (Civitarese et al., 2006; Fruebis et al., 2001; Yamauchi et al., 2002). Similar to adiponectin KO mice (Civitarese et al., 2006), we observed a decrease in PGC1α, lipid metabolism, and mitochondrial biogenesis genes in TRPC1$^{-/-}$ muscle. This lead us to investigate whether this phenomenon is due to decreased circulating adiponectin concentration(s) or decreased adiponectin signaling.

The small molecule agonist AdipoRon was developed by Okada-Iwabu et al. in 2013 which is orally active and binds and activates both AdipoR1 and AdipoR2. AdipoRon is known to increase AMPK phosphorylation, PGC1α, and mitochondrial content making it a useful tool in studying adiponectin signaling. Interestingly, knockdown of AdipoR1/2 or blockage of Ca^{2+} by EGTA diminishes the benefits of AdipoRon in muscle (Okada-Iwabu et al., 2013). Within our study, the combination of SKF or 2APB with AdipoRon in C2C12 cells completely

abolished the immediate influx of Ca^{2+} seen in the AdipoRon only cells. However, blockage of SOCE currents had no effect on p-AMPK or PGC1α most likely indicating a Ca^{2+} independent mechanism within adiponectin signaling. As seen in Figure 41, liver kinase B1 (LKB1) is also known to phosphorylate AMPK and in our model, could be compensating for the lack of Ca^{2+} normally seen. More investigation is needed to determine whether LKB1 is compensating for blocked Ca^{2+}, however we can determine from our data that SOCE is a partial but not a mandatory component of AdipoR1 signaling.

Examination of WT EDL produced similar results to the C2C12 myotubes where SOCE was initiated by treatment with AdipoRon and blocked by SKF and 2APB. When comparing AdipoRon induced Ca^{2+} influx in TRPC1$^{-/-}$ to WT EDL, we saw no change due to the loss of TRPC1. Importantly, expression in AdipoR1 in WT and TRPC1$^{-/-}$ EDL muscle was similar indicating increased or decreased binding of AdipoRon to AdipoR1 due to receptor expression changes had no effect on the amplitude of Ca^{2+} influx. This is relevant as muscle and hepatic protein levels of AdipoR1 are significantly reduced in obesity (Lustig et al., 2014), further indicating that reduced expression of downstream targets of adiponectin signaling in TRPC1$^{-/-}$ muscle is due to substrate loss. Interestingly, though there is no change in AdipoRon mediated Ca^{2+} influx due to TRPC1 loss, we did observe reduced AMPK phosphorylation. This reduction in AMPK phosphorylation may still be linked to loss of TRPC1, however through a different mechanism. Calcium entry via TRPCs has been found to be necessary for thrombin-induced nuclear factor

kappa-light-chain-enhancer of activated B cells (NF-κB) through AMPK phosphorylation in endothelial cells (Bair et al., 2009) which may be relevant to muscle function. Whether TRPC1 is linked to the reduced phosphorylation of AMPK in our EDL muscle, does not explain how loss of TRPC1 failed to reduce or increase PGC1α expression significantly. The evidence of this study suggests that TRPC1 does not have a role in AdipoRon mediated SOCE and TRPC1 loss in muscle is most likely not the cause of reduced PGC1α, lipid metabolism and mitochondrial biogenesis mRNA expression.

CHAPTER VII

DISCUSSION

The role of Ca^{2+} homeostasis in adipose tissue biology has garnered increased attention in recent years due to its connection with metabolic disorders (Arruda and Hotamisligil, 2015). The purpose of this dissertation is to expand this knowledge base with hopes that the information can someday be used for therapeutic interventions. The evidence provided highlights a central role for TRPC1 in regulating the Ca^{2+} dependent processes of differentiation, autophagy, and adipokine secretion in adipose tissue.

TRPC1 and SOCE mechanisms in adipose tissue have recently been identified in the 3T3-L1 cell line (El Hachmane et al., 2018; Sukumar et al., 2012), however no work has been done to confirm this in vivo. The work provided here is the first to identify TRPC1 dependent SOCE in primary cell cultures from isolated mouse Subc AT and VAT SVF. In both tissue types, it was identified that SOCE was present in SVF with TRPC1-like currents and that upon differentiation, these currents were amplified with concurrent increases in STIM1 and TRPC1 protein expression. Genetic ablation of TRPC1 reduced SOCE in both Subc AT and VAT SVF and differentiated adipocytes further confirming its

role in SOCE. In differentiated VAT, an ORAI1-like current was observed, however there was no change in ORAI1 protein expression and ORAI1 was not able to compensate for the loss of TRPC1, suggesting that the major Ca^{2+} entry channel in adipocytes is mediated via TRPC1.

By focusing on adipose tissue function, we've identified multiple metabolic regulatory functions to be dependent on TRPC1-mediated Ca^{2+} influx. Herein, it was shown that loss of TRPC1 impaired adipocyte differentiation which seems to be a result of inhibited PPARy expression. Further, $TRPC1^{-/-}$ animals fed a high-fat diet and exercised exhibited a reduction in autophagy with a concurrent increase in apoptosis. Together these phenomena may be linked as it has been shown that a reduction in autophagy impairs adipogenesis (Baerga et al., 2009; Singh et al., 2009), however these studies suggest that later transcriptional events such as the upregulation of FABP4 and perilipin to be more severely impacted by decreased autophagy rather than PPARy in early adipogenesis. Overall the data suggests that $TRPC1^{-/-}$ mice have impaired adipogenesis which in the long-term may result in hypertrophic obesity, however if the animals are stressed through diet and exercise, adipogenesis is further impaired by TRPC1-mediated reduction in autophagy resulting in apoptosis and fat mass loss.

The other portion of this dissertation which contributes to the metabolic dysfunction due to TRPC1 loss in adipose tissue is the investigation of adiponectin secretion. Ex-vivo experimentation of insulin-stimulated adiponectin secretion from $TRPC1^{-/-}$ adipose tissue revealed that decreased secretion is

likely due to the lack of TRPC1-mediated Ca^{2+} influx necessary for SNARE complex formation and not reduced internal adipose tissue adiponectin stores. Further, analysis of serum adiponectin revealed TRPC1$^{-/-}$ mice to have reduced concentrations when fed either a high-fat or normal-fat diet as compared to WT. Additionally, these same mice had no change in fat mass, blood glucose, insulin, or insulin resistance as calculated by HOMA IR. This is contrary to a multitude of studies that show a correlation between reduced serum adiponectin concentrations and increased fat mass, blood glucose, insulin, and insulin resistance typically observed in obesity (Abdelgadir et al., 2013; Berg et al., 2001; Kou et al., 2018). Together, this data further indicates a non-obesity induced reduction in serum adiponectin. Exercise was able to recover serum adiponectin concentrations in TRPC1$^{-/-}$ fed either a high-fat or normal-chow diet. This may be due to the ability of exercise to increase adiponectin secretion from muscle through PPARy activation (Amin et al., 2010) and increased AdipoR1 expression (Tsuchida et al., 2004; Zeng et al., 2007) thereby bypassing dysfunctional adiponectin secretion from adipose tissue.

Current modeling of adiponectin signaling indicates a direct linkage between AdipoR1 activation, Ca^{2+} influx, and AMPK phosphorylation however data from C2C12 cells with blocked SOCE and TRPC1$^{-/-}$ EDL suggests a different mechanism. In TRPC1$^{-/-}$ EDL, AdipoRon initiated Ca^{2+} influx was unchanged, however a reduction in AMPK phosphorylation was observed along with an inconclusive PGC1α mRNA change. This may indicate an indirect

reduction in stimulation or increased inhibition of AMPK due to TRPC1 loss that needs to be further researched. This, however, is likely not the cause of the significant reduction in PGC1α, FASN, and ACC observed in TRPC1$^{-/-}$ muscle and instead is the result of reduced serum adiponectin concentrations.

In closing, this dissertation efficiently describes the role of TRPC1 in modulating critical Ca^{2+} mediated processes within adipose tissue which in turn effects whole body metabolic homeostasis.

REFERENCES

Abdelgadir, M., Karlsson, A.F., Berglund, L., and Berne, C. (2013). Low serum adiponectin concentrations are associated with insulin sensitivity independent of obesity in Sudanese subjects with type 2 diabetes mellitus. Diabetol Metab Syndr *5*, 15.

Achari, A.E., and Jain, S.K. (2017). Adiponectin, a Therapeutic Target for Obesity, Diabetes, and Endothelial Dysfunction. Int J Mol Sci *18*.

Ahuja, M., Schwartz, D.M., Tandon, M., Son, A., Zeng, M., Swaim, W., Eckhaus, M., Hoffman, V., Cui, Y., Xiao, B., et al. (2017). Orai1-Mediated Antimicrobial Secretion from Pancreatic Acini Shapes the Gut Microbiome and Regulates Gut Innate Immunity. Cell Metab *25*, 635-646.

Alkhouri, N., Gornicka, A., Berk, M.P., Thapaliya, S., Dixon, L.J., Kashyap, S., Schauer, P.R., and Feldstein, A.E. (2010). Adipocyte apoptosis, a link between obesity, insulin resistance, and hepatic steatosis. J Biol Chem *285*, 3428-3438.

Alonso-Carbajo, L., Kecskes, M., Jacobs, G., Pironet, A., Syam, N., Talavera, K., and Vennekens, R. (2017). Muscling in on TRP channels in vascular smooth muscle cells and cardiomyocytes. Cell Calcium *66*, 48-61.

Ambudkar, I.S., de Souza, L.B., and Ong, H.L. (2017). TRPC1, Orai1, and STIM1 in SOCE: Friends in tight spaces. Cell Calcium *63*, 33-39.

Amin, R.H., Mathews, S.T., Camp, H.S., Ding, L., and Leff, T. (2010). Selective activation of PPARgamma in skeletal muscle induces endogenous production of adiponectin and protects mice from diet-induced insulin resistance. Am J Physiol Endocrinol Metab *298*, E28-37.

Amirkalali, B., Sharifi, F., Fakhrzadeh, H., Mirarefein, M., Ghaderpanahi, M., Badamchizadeh, Z., and Larijani, B. (2010). Low serum leptin serves as a biomarker of malnutrition in elderly patients. Nutr Res *30*, 314-319.

Arita, Y., Kihara, S., Ouchi, N., Takahashi, M., Maeda, K., Miyagawa, J., Hotta, K., Shimomura, I., Nakamura, T., Miyaoka, K., et al. (1999). Paradoxical decrease of an adipose-specific protein, adiponectin, in obesity. Biochem Biophys Res Commun *257*, 79-83.

Armstrong, C.M., Bezanilla, F.M., and Horowicz, P. (1972). Twitches in the presence of ethylene glycol bis(-aminoethyl ether)-N,N'-tetracetic acid. Biochim Biophys Acta *267*, 605-608.

Arruda, A.P., and Hotamisligil, G.S. (2015). Calcium Homeostasis and Organelle Function in the Pathogenesis of Obesity and Diabetes. Cell Metab *22*, 381-397.

Baboota, R.K., Singh, D.P., Sarma, S.M., Kaur, J., Sandhir, R., Boparai, R.K., Kondepudi, K.K., and Bishnoi, M. (2014). Capsaicin induces "brite" phenotype in differentiating 3T3-L1 preadipocytes. PLoS One *9*, e103093.

Baerga, R., Zhang, Y., Chen, P.H., Goldman, S., and Jin, S. (2009). Targeted deletion of autophagy-related 5 (atg5) impairs adipogenesis in a cellular model and in mice. Autophagy *5*, 1118-1130.

Baglioni, S., Cantini, G., Poli, G., Francalanci, M., Squecco, R., Di Franco, A., Borgogni, E., Frontera, S., Nesi, G., Liotta, F., et al. (2012). Functional differences in visceral and subcutaneous fat pads originate from differences in the adipose stem cell. PLoS One *7*, e36569.

Bair, A.M., Thippegowda, P.B., Freichel, M., Cheng, N., Ye, R.D., Vogel, S.M., Yu, Y., Flockerzi, V., Malik, A.B., and Tiruppathi, C. (2009). Ca2+ entry via TRPC channels is necessary for thrombin-induced NF-kappaB activation in endothelial cells through AMP-activated protein kinase and protein kinase Cdelta. J Biol Chem *284*, 563-574.

Banga, A., Bodles, A.M., Rasouli, N., Ranganathan, G., Kern, P.A., and Owens, R.J. (2008). Calcium is involved in formation of high molecular weight adiponectin. Metab Syndr Relat Disord *6*, 103-111.

Barclay, J.W., Morgan, A., and Burgoyne, R.D. (2005). Calcium-dependent regulation of exocytosis. Cell Calcium *38*, 343-353.

Barnea, M., Shamay, A., Stark, A.H., and Madar, Z. (2006). A high-fat diet has a tissue-specific effect on adiponectin and related enzyme expression. Obesity (Silver Spring) *14*, 2145-2153.

Beaven, S.W., Matveyenko, A., Wroblewski, K., Chao, L., Wilpitz, D., Hsu, T.W., Lentz, J., Drew, B., Hevener, A.L., and Tontonoz, P. (2013). Reciprocal regulation of hepatic and adipose lipogenesis by liver X receptors in obesity and insulin resistance. Cell Metab *18*, 106-117.

Berg, A.H., Combs, T.P., Du, X., Brownlee, M., and Scherer, P.E. (2001). The adipocyte-secreted protein Acrp30 enhances hepatic insulin action. Nat Med *7*, 947-953.

Berridge, M.J. (1993). Inositol trisphosphate and calcium signalling. Nature *361*, 315-325.

Berridge, M.J., Bootman, M.D., and Roderick, H.L. (2003). Calcium signalling: dynamics, homeostasis and remodelling. Nat Rev Mol Cell Biol *4*, 517-529.

Berridge, M.J., Lipp, P., and Bootman, M.D. (2000). The versatility and universality of calcium signalling. Nat Rev Mol Cell Biol *1*, 11-21.

Birnbaumer, L. (2009). The TRPC class of ion channels: a critical review of their roles in slow, sustained increases in intracellular Ca(2+) concentrations. Annu Rev Pharmacol Toxicol *49*, 395-426.

Bishnoi, M., Kondepudi, K.K., Gupta, A., Karmase, A., and Boparai, R.K. (2013). Expression of multiple Transient Receptor Potential channel genes in murine 3T3-L1 cell lines and adipose tissue. Pharmacol Rep *65*, 751-755.

Bjursell, M., Ahnmark, A., Bohlooly-Y, M., William-Olsson, L., Rhedin, M., Peng, X.R., Ploj, K., Gerdin, A.K., Arnerup, G., Elmgren, A., et al. (2007). Opposing effects of adiponectin receptors 1 and 2 on energy metabolism. Diabetes *56*, 583-593.

Blüher, M. (2009). Adipose tissue dysfunction in obesity. Exp Clin Endocrinol Diabetes *117*, 241-250.

Bogan, J.S., and Lodish, H.F. (1999). Two compartments for insulin-stimulated exocytosis in 3T3-L1 adipocytes defined by endogenous ACRP30 and GLUT4. J Cell Biol *146*, 609-620.

Bollimuntha, S., Ebadi, M., and Singh, B.B. (2006). TRPC1 protects human SH-SY5Y cells against salsolinol-induced cytotoxicity by inhibiting apoptosis. Brain Res *1099*, 141-149.

Brini, M., and Carafoli, E. (2011). The plasma membrane Ca^{2+} ATPase and the plasma membrane sodium calcium exchanger cooperate in the regulation of cell calcium. Cold Spring Harb Perspect Biol *3*.

Brose, S.A., Marquardt, A.L., and Golovko, M.Y. (2014). Fatty acid biosynthesis from glutamate and glutamine is specifically induced in neuronal cells under hypoxia. J. Neurochem. *129*, 400-412.

Budihardjo, I., Oliver, H., Lutter, M., Luo, X., and Wang, X. (1999). Biochemical pathways of caspase activation during apoptosis. Annu Rev Cell Dev Biol *15*, 269-290.

Bullen, J.W., Bluher, S., Kelesidis, T., and Mantzoros, C.S. (2007). Regulation of adiponectin and its receptors in response to development of diet-induced obesity in mice. Am J Physiol Endocrinol Metab *292*, E1079-1086.

Burgoyne, R.D., and Clague, M.J. (2003). Calcium and calmodulin in membrane fusion. Biochim Biophys Acta *1641*, 137-143.

Cao, X., Choi, S., Maléth, J.J., Park, S., Ahuja, M., and Muallem, S. (2015). The ER/PM microdomain, $PI(4,5)P_2$ and the regulation of STIM1-Orai1 channel function. Cell Calcium *58*, 342-348.

Chan, C.S., Gertler, T.S., and Surmeier, D.J. (2009). Calcium homeostasis, selective vulnerability and Parkinson's disease. Trends Neurosci *32*, 249-256.

Chaolu, H., Asakawa, A., Ushikai, M., Li, Y.X., Cheng, K.C., Li, J.B., Zoshiki, T., Terashi, M., Tanaka, C., Atsuchi, K., et al. (2011). Effect of exercise and high-fat diet on plasma adiponectin and nesfatin levels in mice. Exp Ther Med *2*, 369-373.

Chaudhari, S., and Ma, R. (2016). Store-operated calcium entry and diabetic complications. Exp Biol Med (Maywood) *241*, 343-352.

Cheng, K.K., Lam, K.S., Wang, Y., Huang, Y., Carling, D., Wu, D., Wong, C., and Xu, A. (2007). Adiponectin-induced endothelial nitric oxide synthase activation and nitric oxide production are mediated by APPL1 in endothelial cells. Diabetes *56*, 1387-1394.

Cheng, K.T., Liu, X., Ong, H.L., and Ambudkar, I.S. (2008). Functional requirement for Orai1 in store-operated TRPC1-STIM1 channels. J Biol Chem *283*, 12935-12940.

Cheng, K.T., Ong, H.L., Liu, X., and Ambudkar, I.S. (2013). Contribution and regulation of TRPC channels in store-operated Ca2+ entry. Curr Top Membr *71*, 149-179.

Cho, C.H., Woo, J.S., Perez, C.F., and Lee, E.H. (2017). A focus on extracellular Ca. Exp Mol Med *49*, e378.

Choe, S.S., Huh, J.Y., Hwang, I.J., Kim, J.I., and Kim, J.B. (2016). Adipose Tissue Remodeling: Its Role in Energy Metabolism and Metabolic Disorders. Front Endocrinol (Lausanne) *7*, 30.

Civitarese, A.E., Ukropcova, B., Carling, S., Hulver, M., DeFronzo, R.A., Mandarino, L., Ravussin, E., and Smith, S.R. (2006). Role of adiponectin in human skeletal muscle bioenergetics. Cell Metab *4*, 75-87.

Clapham, D.E. (2007). Calcium signaling. Cell *131*, 1047-1058.

Claycombe, K.J., Uthus, E.O., Roemmich, J.N., Johnson, L.K., and Johnson, W.T. (2013). Prenatal low-protein and postnatal high-fat diets induce rapid adipose tissue growth by inducing Igf2 expression in Sprague Dawley rat offspring. J Nutr *143*, 1533-1539.

Claycombe, K.J., Vomhof-DeKrey, E.E., Garcia, R., Johnson, W.T., Uthus, E., and Roemmich, J.N. (2016). Decreased beige adipocyte number and mitochondrial respiration coincide with increased histone methyl transferase (G9a) and reduced FGF21 gene expression in Sprague-Dawley rats fed prenatal low protein and postnatal high-fat diets. J Nutr Biochem *31*, 113-121.

Claycombe, K.J., Vomhof-DeKrey, E.E., Roemmich, J.N., Rhen, T., and Ghribi, O. (2015). Maternal low-protein diet causes body weight loss in male, neonate Sprague-Dawley rats involving UCP-1-mediated thermogenesis. J Nutr Biochem *26*, 729-735.

Cong, L., Chen, K., Li, J., Gao, P., Li, Q., Mi, S., Wu, X., and Zhao, A.Z. (2007). Regulation of adiponectin and leptin secretion and expression by insulin through a PI3K-PDE3B dependent mechanism in rat primary adipocytes. Biochem J *403*, 519-525.

Cosens, D.J., and Manning, A. (1969). Abnormal electroretinogram from a Drosophila mutant. Nature *224*, 285-287.

Craig, B.W., Hammons, G.T., Garthwaite, S.M., Jarett, L., and Holloszy, J.O. (1981). Adaptation of fat cells to exercise: response of glucose uptake and oxidation to insulin. J Appl Physiol Respir Environ Exerc Physiol *51*, 1500-1506.

Cárdenas, C., Miller, R.A., Smith, I., Bui, T., Molgó, J., Müller, M., Vais, H., Cheung, K.H., Yang, J., Parker, I., et al. (2010). Essential regulation of cell bioenergetics by constitutive InsP3 receptor Ca2+ transfer to mitochondria. Cell *142*, 270-283.

Dadson, K., Liu, Y., and Sweeney, G. (2011). Adiponectin action: a combination of endocrine and autocrine/paracrine effects. Front Endocrinol (Lausanne) *2*, 62.

Davis, F.M., Peters, A.A., Grice, D.M., Cabot, P.J., Parat, M.O., Roberts-Thomson, S.J., and Monteith, G.R. (2012). Non-stimulated, agonist-stimulated and store-operated Ca2+ influx in MDA-MB-468 breast cancer cells and the effect of EGF-induced EMT on calcium entry. PLoS One *7*, e36923.

Decuypere, J.P., Bultynck, G., and Parys, J.B. (2011). A dual role for Ca(2+) in autophagy regulation. Cell Calcium *50*, 242-250.

Dentin, R., Benhamed, F., Hainault, I., Fauveau, V., Foufelle, F., Dyck, J.R., Girard, J., and Postic, C. (2006). Liver-specific inhibition of ChREBP improves hepatic steatosis and insulin resistance in ob/ob mice. Diabetes *55*, 2159-2170.

Di Giovanni, J., Iborra, C., Maulet, Y., Lévêque, C., El Far, O., and Seagar, M. (2010). Calcium-dependent regulation of SNARE-mediated membrane fusion by calmodulin. J Biol Chem *285*, 23665-23675.

Dietrich, A., Fahlbusch, M., and Gudermann, T. (2014). Classical Transient Receptor Potential 1 (TRPC1): Channel or Channel Regulator? Cells *3*, 939-962.

Dirksen, R.T. (2009). Checking your SOCCs and feet: the molecular mechanisms of Ca2+ entry in skeletal muscle. J Physiol *587*, 3139-3147.

East, D.A., and Campanella, M. (2013). Ca2+ in quality control: an unresolved riddle critical to autophagy and mitophagy. Autophagy *9*, 1710-1719.

Ebrahimi-Mamaeghani, M., Mohammadi, S., Arefhosseini, S.R., Fallah, P., and Bazi, Z. (2015). Adiponectin as a potential biomarker of vascular disease. Vasc Health Risk Manag *11*, 55-70.

El Hachmane, M.F., Ermund, A., Brännmark, C., and Olofsson, C.S. (2018). Extracellular ATP activates store-operated Ca. Biochem J *475*, 691-704.

Fabbrini, E., Sullivan, S., and Klein, S. (2010). Obesity and nonalcoholic fatty liver disease: biochemical, metabolic, and clinical implications. Hepatology *51*, 679-689.

Fantuzzi, G. (2013). Adiponectin in inflammatory and immune-mediated diseases. Cytokine *64*, 1-10.

Farmer, S.R. (2006). Transcriptional control of adipocyte formation. Cell Metab *4*, 263-273.

Fasshauer, D., Sutton, R.B., Brunger, A.T., and Jahn, R. (1998). Conserved structural features of the synaptic fusion complex: SNARE proteins reclassified as Q- and R-SNAREs. Proc Natl Acad Sci U S A *95*, 15781-15786.

Filadi, R., Theurey, P., and Pizzo, P. (2017). The endoplasmic reticulum-mitochondria coupling in health and disease: Molecules, functions and significance. Cell Calcium *62*, 1-15.

Fiorio Pla, A., Maric, D., Brazer, S.C., Giacobini, P., Liu, X., Chang, Y.H., Ambudkar, I.S., and Barker, J.L. (2005). Canonical transient receptor potential 1 plays a role in basic fibroblast growth factor (bFGF)/FGF receptor-1-induced Ca2+ entry and embryonic rat neural stem cell proliferation. J Neurosci *25*, 2687-2701.

Foster, M.T., Shi, H., Softic, S., Kohli, R., Seeley, R.J., and Woods, S.C. (2011). Transplantation of non-visceral fat to the visceral cavity improves glucose tolerance in mice: investigation of hepatic lipids and insulin sensitivity. Diabetologia *54*, 2890-2899.

Fruebis, J., Tsao, T.S., Javorschi, S., Ebbets-Reed, D., Erickson, M.R., Yen, F.T., Bihain, B.E., and Lodish, H.F. (2001). Proteolytic cleavage product of 30-kDa adipocyte complement-related protein increases fatty acid oxidation in muscle and causes weight loss in mice. Proc Natl Acad Sci U S A *98*, 2005-2010.

Garin-Shkolnik, T., Rudich, A., Hotamisligil, G.S., and Rubinstein, M. (2014). FABP4 attenuates PPARγ and adipogenesis and is inversely correlated with PPARγ in adipose tissues. Diabetes *63*, 900-911.

Giordano, A., Murano, I., Mondini, E., Perugini, J., Smorlesi, A., Severi, I., Barazzoni, R., Scherer, P.E., and Cinti, S. (2013). Obese adipocytes show ultrastructural features of stressed cells and die of pyroptosis. J Lipid Res *54*, 2423-2436.

Gollisch, K.S., Brandauer, J., Jessen, N., Toyoda, T., Nayer, A., Hirshman, M.F., and Goodyear, L.J. (2009). Effects of exercise training on subcutaneous and visceral adipose tissue in normal- and high-fat diet-fed rats. Am J Physiol Endocrinol Metab *297*, E495-504.

Graham, S.J., Black, M.J., Soboloff, J., Gill, D.L., Dziadek, M.A., and Johnstone, L.S. (2009). Stim1, an endoplasmic reticulum Ca2+ sensor, negatively regulates 3T3-L1 pre-adipocyte differentiation. Differentiation *77*, 239-247.

Guerini, D., Coletto, L., and Carafoli, E. (2005). Exporting calcium from cells. Cell Calcium *38*, 281-289.

Gwozdz, T., Dutko-Gwozdz, J., Schafer, C., and Bolotina, V.M. (2012). Overexpression of Orai1 and STIM1 proteins alters regulation of store-operated Ca2+ entry by endogenous mediators. J Biol Chem *287*, 22865-22872.

Haider, N., Dusseault, J., Rudich, A., and Larose, L. (2017). Nck2, an unexpected regulator of adipogenesis. Adipocyte *6*, 154-160.

Hardie, R.C., and Minke, B. (1992). The trp gene is essential for a light-activated Ca2+ channel in Drosophila photoreceptors. Neuron *8*, 643-651.

He, W., Barak, Y., Hevener, A., Olson, P., Liao, D., Le, J., Nelson, M., Ong, E., Olefsky, J.M., and Evans, R.M. (2003). Adipose-specific peroxisome proliferator-activated receptor gamma knockout causes insulin resistance in fat and liver but not in muscle. Proc Natl Acad Sci U S A *100*, 15712-15717.

Heiker, J.T., Kosel, D., and Beck-Sickinger, A.G. (2010). Molecular mechanisms of signal transduction via adiponectin and adiponectin receptors. Biol Chem *391*, 1005-1018.

Hofer, A.M., and Brown, E.M. (2003). Extracellular calcium sensing and signalling. Nat Rev Mol Cell Biol *4*, 530-538.

Hoffstedt, J., Arvidsson, E., Sjölin, E., Wåhlén, K., and Arner, P. (2004). Adipose tissue adiponectin production and adiponectin serum concentration in human obesity and insulin resistance. J Clin Endocrinol Metab *89*, 1391-1396.

Holloszy, J.O. (1967). Biochemical adaptations in muscle. Effects of exercise on mitochondrial oxygen uptake and respiratory enzyme activity in skeletal muscle. J Biol Chem *242*, 2278-2282.

Holzer, R.G., Park, E.J., Li, N., Tran, H., Chen, M., Choi, C., Solinas, G., and Karin, M. (2011). Saturated fatty acids induce c-Src clustering within membrane subdomains, leading to JNK activation. Cell *147*, 173-184.

Hotamisligil, G.S., Johnson, R.S., Distel, R.J., Ellis, R., Papaioannou, V.E., and Spiegelman, B.M. (1996). Uncoupling of obesity from insulin resistance through a targeted mutation in aP2, the adipocyte fatty acid binding protein. Science *274*, 1377-1379.

Hoth, M., and Penner, R. (1992). Depletion of intracellular calcium stores activates a calcium current in mast cells. Nature *355*, 353-356.

Hu, G., Oboukhova, E.A., Kumar, S., Sturek, M., and Obukhov, A.G. (2009). Canonical transient receptor potential channels expression is elevated in a porcine model of metabolic syndrome. Mol Endocrinol *23*, 689-699.

Hug, C., Wang, J., Ahmad, N.S., Bogan, J.S., Tsao, T.S., and Lodish, H.F. (2004). T-cadherin is a receptor for hexameric and high-molecular-weight forms of Acrp30/adiponectin. Proc Natl Acad Sci U S A *101*, 10308-10313.

Høyer-Hansen, M., Bastholm, L., Szyniarowski, P., Campanella, M., Szabadkai, G., Farkas, T., Bianchi, K., Fehrenbacher, N., Elling, F., Rizzuto, R., et al. (2007). Control of macroautophagy by calcium, calmodulin-dependent kinase kinase-beta, and Bcl-2. Mol Cell *25*, 193-205.

Ibrahim, M.M. (2010). Subcutaneous and visceral adipose tissue: structural and functional differences. Obes Rev *11*, 11-18.

Isakson, P., Hammarstedt, A., Gustafson, B., and Smith, U. (2009). Impaired preadipocyte differentiation in human abdominal obesity: role of Wnt, tumor necrosis factor-alpha, and inflammation. Diabetes *58*, 1550-1557.

Iwabu, M., Yamauchi, T., Okada-Iwabu, M., Sato, K., Nakagawa, T., Funata, M., Yamaguchi, M., Namiki, S., Nakayama, R., Tabata, M., et al. (2010). Adiponectin and AdipoR1 regulate PGC-1alpha and mitochondria by Ca(2+) and AMPK/SIRT1. Nature *464*, 1313-1319.

Jardin, I., Lopez, J.J., Salido, G.M., and Rosado, J.A. (2008). Orai1 mediates the interaction between STIM1 and hTRPC1 and regulates the mode of activation of hTRPC1-forming Ca2+ channels. J Biol Chem *283*, 25296-25304.

Jensen, B., Farach-Carson, M.C., Kenaley, E., and Akanbi, K.A. (2004). High extracellular calcium attenuates adipogenesis in 3T3-L1 preadipocytes. Exp Cell Res *301*, 280-292.

Jeyakumar, S.M., Lopamudra, P., Padmini, S., Balakrishna, N., Giridharan, N.V., and Vajreswari, A. (2009). Fatty acid desaturation index correlates with body mass and adiposity indices of obesity in Wistar NIN obese mutant rat strains WNIN/Ob and WNIN/GR-Ob. Nutr Metab (Lond) *6*, 27.

Jousset, H., Frieden, M., and Demaurex, N. (2007). STIM1 knockdown reveals that store-operated Ca2+ channels located close to sarco/endoplasmic Ca2+ ATPases (SERCA) pumps silently refill the endoplasmic reticulum. J Biol Chem *282*, 11456-11464.

Jäger, S., Handschin, C., St-Pierre, J., and Spiegelman, B.M. (2007). AMP-activated protein kinase (AMPK) action in skeletal muscle via direct phosphorylation of PGC-1alpha. Proc Natl Acad Sci U S A *104*, 12017-12022.

Kadiri, S., Auclair, M., Capeau, J., and Antoine, B. (2017). Depot-Specific Response of Adipose Tissue to Diet-Induced Inflammation: The Retinoid-Related Orphan Receptor α (RORα) Involved? Obesity (Silver Spring) *25*, 1948-1955.

Kadowaki, T., Yamauchi, T., Kubota, N., Hara, K., Ueki, K., and Tobe, K. (2006). Adiponectin and adiponectin receptors in insulin resistance, diabetes, and the metabolic syndrome. J Clin Invest *116*, 1784-1792.

Kalupahana, N.S., Claycombe, K., Newman, S.J., Stewart, T., Siriwardhana, N., Matthan, N., Lichtenstein, A.H., and Moustaid-Moussa, N. (2010). Eicosapentaenoic acid prevents and reverses insulin resistance in high-fat diet-induced obese mice via modulation of adipose tissue inflammation. J Nutr *140*, 1915-1922.

Kato, M., Ospelt, C., Gay, R.E., Gay, S., and Klein, K. (2014). Dual role of autophagy in stress-induced cell death in rheumatoid arthritis synovial fibroblasts. Arthritis Rheumatol *66*, 40-48.

Keshvari, S., Henstridge, D.C., Ng, C., Febbraio, M.A., and Whitehead, J.P. (2017). Muscle-specific overexpression of AdipoR1 or AdipoR2 gives rise to common and discrete local effects whilst AdipoR2 promotes additional systemic effects. Sci Rep *7*, 41792.

Keshvari, S., and Whitehead, J.P. (2015). Characterisation of the adiponectin receptors: Differential cell-surface expression and temporal signalling profiles of AdipoR1 and AdipoR2 are regulated by the non-conserved N-terminal trunks. Mol Cell Endocrinol *409*, 121-129.

Kim, M.S., Zeng, W., Yuan, J.P., Shin, D.M., Worley, P.F., and Muallem, S. (2009). Native Store-operated Ca2+ Influx Requires the Channel Function of Orai1 and TRPC1. J Biol Chem *284*, 9733-9741.

Kim, S.M., Lun, M., Wang, M., Senyo, S.E., Guillermier, C., Patwari, P., and Steinhauser, M.L. (2014). Loss of white adipose hyperplastic potential is associated with enhanced susceptibility to insulin resistance. Cell Metab *20*, 1049-1058.

Klöting, N., and Blüher, M. (2014). Adipocyte dysfunction, inflammation and metabolic syndrome. Rev Endocr Metab Disord *15*, 277-287.

Komai, A.M., Brännmark, C., Musovic, S., and Olofsson, C.S. (2014). PKA-independent cAMP stimulation of white adipocyte exocytosis and adipokine secretion: modulations by Ca2+ and ATP. J Physiol *592*, 5169-5186.

Kondratskyi, A., Yassine, M., Kondratska, K., Skryma, R., Slomianny, C., and Prevarskaya, N. (2013). Calcium-permeable ion channels in control of autophagy and cancer. Front Physiol *4*, 272.

Kou, H., Deng, J., Gao, D., Song, A., Han, Z., Wei, J., Jin, X., Ma, R., and Zheng, Q. (2018). Relationship among adiponectin, insulin resistance and atherosclerosis in non-diabetic hypertensive patients and healthy adults. Clin Exp Hypertens, 1-8.

Kovacova, Z., Tencerova, M., Roussel, B., Wedellova, Z., Rossmeislova, L., Langin, D., Polak, J., and Stich, V. (2012). The impact of obesity on secretion of adiponectin multimeric isoforms differs in visceral and subcutaneous adipose tissue. Int J Obes (Lond) *36*, 1360-1365.

Kovsan, J., Blüher, M., Tarnovscki, T., Klöting, N., Kirshtein, B., Madar, L., Shai, I., Golan, R., Harman-Boehm, I., Schön, M.R., et al. (2011). Altered autophagy in human adipose tissues in obesity. J Clin Endocrinol Metab *96*, E268-277.

Kriketos, A.D., Gan, S.K., Poynten, A.M., Furler, S.M., Chisholm, D.J., and Campbell, L.V. (2004). Exercise increases adiponectin levels and insulin sensitivity in humans. Diabetes Care *27*, 629-630.

Krout, D., Schaar, A., Sun, Y., Sukumaran, P., Roemmich, J.N., Singh, B.B., and Claycombe-Larson, K.J. (2017). The TRPC1 Ca. J Biol Chem *292*, 20799-20807.

Kuda, O., Brezinova, M., Rombaldova, M., Slavikova, B., Posta, M., Beier, P., Janovska, P., Veleba, J., Kopecky, J., Kudova, E., et al. (2016). Docosahexaenoic Acid-Derived Fatty Acid Esters of Hydroxy Fatty Acids (FAHFAs) With Anti-inflammatory Properties. Diabetes *65*, 2580-2590.

La Rovere, R.M., Roest, G., Bultynck, G., and Parys, J.B. (2016). Intracellular Ca(2+) signaling and Ca(2+) microdomains in the control of cell survival, apoptosis and autophagy. Cell Calcium *60*, 74-87.

Lara-Castro, C., Luo, N., Wallace, P., Klein, R.L., and Garvey, W.T. (2006). Adiponectin multimeric complexes and the metabolic syndrome trait cluster. Diabetes *55*, 249-259.

Lee, S., Park, Y., Dellsperger, K.C., and Zhang, C. (2011). Exercise training improves endothelial function via adiponectin-dependent and independent pathways in type 2 diabetic mice. Am J Physiol Heart Circ Physiol *301*, H306-314.

Lehr, S., Hartwig, S., and Sell, H. (2012). Adipokines: a treasure trove for the discovery of biomarkers for metabolic disorders. Proteomics Clin Appl *6*, 91-101.

Levy, J.R., Gyarmati, J., Lesko, J.M., Adler, R.A., and Stevens, W. (2000). Dual regulation of leptin secretion: intracellular energy and calcium dependence of regulated pathway. Am J Physiol Endocrinol Metab *278*, E892-901.

Lindqvist, L.M., Heinlein, M., Huang, D.C., and Vaux, D.L. (2014). Prosurvival Bcl-2 family members affect autophagy only indirectly, by inhibiting Bax and Bak. Proc Natl Acad Sci U S A *111*, 8512-8517.

Liu, M., and Liu, F. (2009). Transcriptional and post-translational regulation of adiponectin. Biochem J *425*, 41-52.

Liu, X., Cheng, K.T., Bandyopadhyay, B.C., Pani, B., Dietrich, A., Paria, B.C., Swaim, W.D., Beech, D., Yildrim, E., Singh, B.B., et al. (2007). Attenuation of store-operated Ca2+ current impairs salivary gland fluid secretion in TRPC1(-/-) mice. Proc Natl Acad Sci U S A *104*, 17542-17547.

Liu, X., Groschner, K., and Ambudkar, I.S. (2004). Distinct Ca(2+)-permeable cation currents are activated by internal Ca(2+)-store depletion in RBL-2H3 cells and human salivary gland cells, HSG and HSY. J Membr Biol *200*, 93-104.

Liu, X., Singh, B.B., and Ambudkar, I.S. (2003). TRPC1 is required for functional store-operated Ca2+ channels. Role of acidic amino acid residues in the S5-S6 region. J Biol Chem *278*, 11337-11343.

Liu, X., Wang, W., Singh, B.B., Lockwich, T., Jadlowiec, J., O'Connell, B., Wellner, R., Zhu, M.X., and Ambudkar, I.S. (2000). Trp1, a candidate protein for the store-operated Ca(2+) influx mechanism in salivary gland cells. J Biol Chem *275*, 3403-3411.

Lopreiato, R., Giacomello, M., and Carafoli, E. (2014). The plasma membrane calcium pump: new ways to look at an old enzyme. J Biol Chem *289*, 10261-10268.

Lorenzo, C., Hanley, A.J., Rewers, M.J., and Haffner, S.M. (2014). Calcium and phosphate concentrations and future development of type 2 diabetes: the Insulin Resistance Atherosclerosis Study. Diabetologia *57*, 1366-1374.

Louis, M., Zanou, N., Van Schoor, M., and Gailly, P. (2008). TRPC1 regulates skeletal myoblast migration and differentiation. J Cell Sci *121*, 3951-3959.

Lundgren, M., Svensson, M., Lindmark, S., Renström, F., Ruge, T., and Eriksson, J.W. (2007). Fat cell enlargement is an independent marker of insulin resistance and 'hyperleptinaemia'. Diabetologia *50*, 625-633.

Lustig, Y., Barhod, E., Ashwal-Fluss, R., Gordin, R., Shomron, N., Baruch-Umansky, K., Hemi, R., Karasik, A., and Kanety, H. (2014). RNA-binding protein PTB and microRNA-221 coregulate AdipoR1 translation and adiponectin signaling. Diabetes *63*, 433-445.

Lönn, M., Mehlig, K., Bengtsson, C., and Lissner, L. (2010). Adipocyte size predicts incidence of type 2 diabetes in women. FASEB J *24*, 326-331.

MacDougald, O.A., and Burant, C.F. (2007). The rapidly expanding family of adipokines. Cell Metab *6*, 159-161.

Manjarrés, I.M., Alonso, M.T., and García-Sancho, J. (2011). Calcium entry-calcium refilling (CECR) coupling between store-operated Ca(2+) entry and sarco/endoplasmic reticulum Ca(2+)-ATPase. Cell Calcium *49*, 153-161.

Mao, X., Kikani, C.K., Riojas, R.A., Langlais, P., Wang, L., Ramos, F.J., Fang, Q., Christ-Roberts, C.Y., Hong, J.Y., Kim, R.Y., et al. (2006). APPL1 binds to adiponectin receptors and mediates adiponectin signalling and function. Nat Cell Biol *8*, 516-523.

Matsuzawa, Y. (2010). Establishment of a concept of visceral fat syndrome and discovery of adiponectin. Proc Jpn Acad Ser B Phys Biol Sci *86*, 131-141.

Maury, E., and Brichard, S.M. (2010). Adipokine dysregulation, adipose tissue inflammation and metabolic syndrome. Mol Cell Endocrinol *314*, 1-16.

Maus, M., Cuk, M., Patel, B., Lian, J., Ouimet, M., Kaufmann, U., Yang, J., Horvath, R., Hornig-Do, H.T., Chrzanowska-Lightowlers, Z.M., et al. (2017). Store-Operated Ca(2+) Entry Controls Induction of Lipolysis and the Transcriptional Reprogramming to Lipid Metabolism. Cell Metab *25*, 698-712.

Montell, C. (1999). Visual transduction in Drosophila. Annu Rev Cell Dev Biol *15*, 231-268.

Montell, C. (2005). The TRP superfamily of cation channels. Sci STKE *2005*, re3.

Montell, C., and Rubin, G.M. (1989). Molecular characterization of the Drosophila trp locus: a putative integral membrane protein required for phototransduction. Neuron *2*, 1313-1323.

Mooradian, A.D., Chehade, J., and Thurman, J.E. (2002). The role of thiazolidinediones in the treatment of patients with type 2 diabetes mellitus. Treat Endocrinol *1*, 13-20.

Nakipova, O.V., Averin, A.S., Evdokimovskii, E.V., Pimenov, O.Y., Kosarski, L., Ignat'ev, D., Anufriev, A., Kokoz, Y.M., Reyes, S., Terzic, A., et al. (2017). Store-operated Ca2+ entry supports contractile function in hearts of hibernators. PLoS One *12*, e0177469.

Neal, J.W., and Clipstone, N.A. (2002). Calcineurin mediates the calcium-dependent inhibition of adipocyte differentiation in 3T3-L1 cells. J Biol Chem *277*, 49776-49781.

Nilius, B. (2007). TRP channels in disease. Biochim Biophys Acta *1772*, 805-812.

O'Rourke, R.W., Metcalf, M.D., White, A.E., Madala, A., Winters, B.R., Maizlin, I.I., Jobe, B.A., Roberts, C.T., Slifka, M.K., and Marks, D.L. (2009). Depot-specific differences in inflammatory mediators and a role for NK cells and IFN-gamma in inflammation in human adipose tissue. Int J Obes (Lond) *33*, 978-990.

Okada-Iwabu, M., Yamauchi, T., Iwabu, M., Honma, T., Hamagami, K., Matsuda, K., Yamaguchi, M., Tanabe, H., Kimura-Someya, T., Shirouzu, M., et al. (2013). A small-molecule AdipoR agonist for type 2 diabetes and short life in obesity. Nature *503*, 493-499.

Ong, H.L., and Ambudkar, I.S. (2011). The dynamic complexity of the TRPC1 channelosome. Channels (Austin) *5*, 424-431.

Ong, H.L., and Ambudkar, I.S. (2015). Molecular determinants of TRPC1 regulation within ER-PM junctions. Cell Calcium *58*, 376-386.

Ong, H.L., and Ambudkar, I.S. (2017). STIM-TRP Pathways and Microdomain Organization: Contribution of TRPC1 in Store-Operated Ca. Adv Exp Med Biol *993*, 159-188.

Ouchi, N., Kihara, S., Funahashi, T., Matsuzawa, Y., and Walsh, K. (2003). Obesity, adiponectin and vascular inflammatory disease. Curr Opin Lipidol *14*, 561-566.

Ouchi, N., Parker, J.L., Lugus, J.J., and Walsh, K. (2011). Adipokines in inflammation and metabolic disease. Nat Rev Immunol *11*, 85-97.

Ouguerram, K., Maugeais, C., Gardette, J., Magot, T., and Krempf, M. (2006). Effect of n-3 fatty acids on metabolism of apoB100-containing lipoprotein in type 2 diabetic subjects. Br J Nutr *96*, 100-106.

Pan, Z., Bhat, M.B., Nieminen, A.L., and Ma, J. (2001). Synergistic movements of Ca(2+) and Bax in cells undergoing apoptosis. J Biol Chem *276*, 32257-32263.

Pani, B., Cornatzer, E., Cornatzer, W., Shin, D.M., Pittelkow, M.R., Hovnanian, A., Ambudkar, I.S., and Singh, B.B. (2006). Up-regulation of transient receptor potential canonical 1 (TRPC1) following sarco(endo)plasmic reticulum Ca2+ ATPase 2 gene silencing promotes cell survival: a potential role for TRPC1 in Darier's disease. Mol Biol Cell *17*, 4446-4458.

Pani, B., Ong, H.L., Liu, X., Rauser, K., Ambudkar, I.S., and Singh, B.B. (2008). Lipid rafts determine clustering of STIM1 in endoplasmic reticulum-plasma membrane junctions and regulation of store-operated Ca2+ entry (SOCE). J Biol Chem *283*, 17333-17340.

Pap, A., Cuaranta-Monroy, I., Peloquin, M., and Nagy, L. (2016). Is the Mouse a Good Model of Human PPARγ-Related Metabolic Diseases? Int J Mol Sci *17*.

Parekh, A.B., Fleig, A., and Penner, R. (1997). The store-operated calcium current I(CRAC): nonlinear activation by InsP3 and dissociation from calcium release. Cell *89*, 973-980.

Parekh, A.B., and Putney, J.W. (2005). Store-operated calcium channels. Physiol Rev *85*, 757-810.

Patel, S.A., Hoehn, K.L., Lawrence, R.T., Sawbridge, L., Talbot, N.A., Tomsig, J.L., Turner, N., Cooney, G.J., Whitehead, J.P., Kraegen, E.W., et al. (2012). Overexpression of the adiponectin receptor AdipoR1 in rat skeletal muscle amplifies local insulin sensitivity. Endocrinology *153*, 5231-5246.

Pedersen, S.F., Owsianik, G., and Nilius, B. (2005). TRP channels: an overview. Cell Calcium *38*, 233-252.

Peinelt, C., Vig, M., Koomoa, D.L., Beck, A., Nadler, M.J., Koblan-Huberson, M., Lis, A., Fleig, A., Penner, R., and Kinet, J.P. (2006). Amplification of CRAC current by STIM1 and CRACM1 (Orai1). Nat Cell Biol *8*, 771-773.

Pinnamaneni, S.K., Southgate, R.J., Febbraio, M.A., and Watt, M.J. (2006). Stearoyl CoA desaturase 1 is elevated in obesity but protects against fatty acid-induced skeletal muscle insulin resistance in vitro. Diabetologia *49*, 3027-3037.

Poburko, D., Liao, C.H., Lemos, V.S., Lin, E., Maruyama, Y., Cole, W.C., and van Breemen, C. (2007). Transient receptor potential channel 6-mediated, localized cytosolic [Na+] transients drive Na+/Ca2+ exchanger-mediated Ca2+ entry in purinergically stimulated aorta smooth muscle cells. Circ Res *101*, 1030-1038.

Postic, C., and Girard, J. (2008). Contribution of de novo fatty acid synthesis to hepatic steatosis and insulin resistance: lessons from genetically engineered mice. J Clin Invest *118*, 829-838.

Prakriya, M., and Lewis, R.S. (2015). Store-Operated Calcium Channels. Physiol Rev *95*, 1383-1436.

Pramme-Steinwachs, I., Jastroch, M., and Ussar, S. (2017). Extracellular calcium modulates brown adipocyte differentiation and identity. Sci Rep *7*, 8888.

Putney, J.W. (1986). A model for receptor-regulated calcium entry. Cell Calcium *7*, 1-12.

Putney, J.W. (1990). Capacitative calcium entry revisited. Cell Calcium *11*, 611-624.

Putney, J.W., Steinckwich-Besançon, N., Numaga-Tomita, T., Davis, F.M., Desai, P.N., D'Agostin, D.M., Wu, S., and Bird, G.S. (2017). The functions of store-operated calcium channels. Biochim Biophys Acta *1864*, 900-906.

Qiu, J., Fang, Y., Rønnekleiv, O.K., and Kelly, M.J. (2010). Leptin excites proopiomelanocortin neurons via activation of TRPC channels. J Neurosci *30*, 1560-1565.

Rao, J.N., Platoshyn, O., Golovina, V.A., Liu, L., Zou, T., Marasa, B.S., Turner, D.J., Yuan, J.X., and Wang, J.Y. (2006). TRPC1 functions as a store-operated Ca2+ channel in intestinal epithelial cells and regulates early mucosal restitution after wounding. Am J Physiol Gastrointest Liver Physiol *290*, G782-792.

Rasouli, N., and Kern, P.A. (2008). Adipocytokines and the metabolic complications of obesity. J Clin Endocrinol Metab *93*, S64-73.

Reddy, A., Caler, E.V., and Andrews, N.W. (2001). Plasma membrane repair is mediated by Ca(2+)-regulated exocytosis of lysosomes. Cell *106*, 157-169.

Redondo, P.C., Harper, A.G., Salido, G.M., Pariente, J.A., Sage, S.O., and Rosado, J.A. (2004). A role for SNAP-25 but not VAMPs in store-mediated Ca2+ entry in human platelets. J Physiol *558*, 99-109.

Ren, X.H., Yao, Y.S., He, L.P., Jin, Y.L., Chang, W.W., Li, J., Chen, Y., Song, X.L., Tang, H., Ding, L.L., et al. (2013). Overweight and obesity associated with increased total serum calcium level: comparison of cross-sectional data in the health screening for teaching faculty. Biol Trace Elem Res *156*, 74-78.

Rosen, E.D., Sarraf, P., Troy, A.E., Bradwin, G., Moore, K., Milstone, D.S., Spiegelman, B.M., and Mortensen, R.M. (1999). PPAR gamma is required for the differentiation of adipose tissue in vivo and in vitro. Mol Cell *4*, 611-617.

Rosen, E.D., and Spiegelman, B.M. (2006). Adipocytes as regulators of energy balance and glucose homeostasis. Nature *444*, 847-853.

Rosen, E.D., and Spiegelman, B.M. (2014). What we talk about when we talk about fat. Cell *156*, 20-44.

Royle, S.J., and Murrell-Lagnado, R.D. (2003). Constitutive cycling: a general mechanism to regulate cell surface proteins. Bioessays *25*, 39-46.

Ruiz-Ojeda, F.J., Rupérez, A.I., Gomez-Llorente, C., Gil, A., and Aguilera, C.M. (2016). Cell Models and Their Application for Studying Adipogenic Differentiation in Relation to Obesity: A Review. Int J Mol Sci *17*.

Sabourin, J., Le Gal, L., Saurwein, L., Haefliger, J.A., Raddatz, E., and Allagnat, F. (2015). Store-operated Ca2+ Entry Mediated by Orai1 and TRPC1 Participates to Insulin Secretion in Rat β-Cells. J Biol Chem *290*, 30530-30539.

Saltevo, J., Niskanen, L., Kautiainen, H., Teittinen, J., Oksa, H., Korpi-Hyövälti, E., Sundvall, J., Männistö, S., Peltonen, M., Mäntyselkä, P., et al. (2011). Serum calcium level is associated with metabolic syndrome in the general population: FIN-D2D study. Eur J Endocrinol *165*, 429-434.

Saltiel, A.R., and Olefsky, J.M. (1996). Thiazolidinediones in the treatment of insulin resistance and type II diabetes. Diabetes *45*, 1661-1669.

Saunders, R.D., and Horrocks, L.A. (1984). Simultaneous extraction and preparation for high-performance liquid chromatography of prostaglandins and phospholipids. Anal Biochem *143*, 71-75.

Savage, D.B., Choi, C.S., Samuel, V.T., Liu, Z.X., Zhang, D., Wang, A., Zhang, X.M., Cline, G.W., Yu, X.X., Geisler, J.G., et al. (2006). Reversal of diet-induced hepatic steatosis and hepatic insulin resistance by antisense oligonucleotide inhibitors of acetyl-CoA carboxylases 1 and 2. J Clin Invest *116*, 817-824.

Scalzo, R.L., Peltonen, G.L., Binns, S.E., Shankaran, M., Giordano, G.R., Hartley, D.A., Klochak, A.L., Lonac, M.C., Paris, H.L., Szallar, S.E., et al. (2014). Greater

muscle protein synthesis and mitochondrial biogenesis in males compared with females during sprint interval training. FASEB J *28*, 2705-2714.

Scherer, P.E., Williams, S., Fogliano, M., Baldini, G., and Lodish, H.F. (1995). A novel serum protein similar to C1q, produced exclusively in adipocytes. J Biol Chem *270*, 26746-26749.

Seale, P., Conroe, H.M., Estall, J., Kajimura, S., Frontini, A., Ishibashi, J., Cohen, P., Cinti, S., and Spiegelman, B.M. (2011). Prdm16 determines the thermogenic program of subcutaneous white adipose tissue in mice. J Clin Invest *121*, 96-105.

Selvaraj, S., Sun, Y., Watt, J.A., Wang, S., Lei, S., Birnbaumer, L., and Singh, B.B. (2012). Neurotoxin-induced ER stress in mouse dopaminergic neurons involves downregulation of TRPC1 and inhibition of AKT/mTOR signaling. J Clin Invest *122*, 1354-1367.

Selvaraj, S., Watt, J.A., and Singh, B.B. (2009). TRPC1 inhibits apoptotic cell degeneration induced by dopaminergic neurotoxin MPTP/MPP(+). Cell Calcium *46*, 209-218.

Shi, H., Halvorsen, Y.D., Ellis, P.N., Wilkison, W.O., and Zemel, M.B. (2000). Role of intracellular calcium in human adipocyte differentiation. Physiol Genomics *3*, 75-82.

Shi, J., Ju, M., Abramowitz, J., Large, W.A., Birnbaumer, L., and Albert, A.P. (2012). TRPC1 proteins confer PKC and phosphoinositol activation on native heteromeric TRPC1/C5 channels in vascular smooth muscle: comparative study of wild-type and TRPC1-/- mice. FASEB J *26*, 409-419.

Shum, M., Pinard, S., Guimond, M.O., Labbé, S.M., Roberge, C., Baillargeon, J.P., Langlois, M.F., Alterman, M., Wallinder, C., Hallberg, A., et al. (2013). Angiotensin II type 2 receptor promotes adipocyte differentiation and restores adipocyte size in high-fat/high-fructose diet-induced insulin resistance in rats. Am J Physiol Endocrinol Metab *304*, E197-210.

Siersbaek, R., Nielsen, R., and Mandrup, S. (2010). PPARgamma in adipocyte differentiation and metabolism--novel insights from genome-wide studies. FEBS Lett *584*, 3242-3249.

Singh, B.B., Lockwich, T.P., Bandyopadhyay, B.C., Liu, X., Bollimuntha, S., Brazer, S.C., Combs, C., Das, S., Leenders, A.G., Sheng, Z.H., et al. (2004).

VAMP2-dependent exocytosis regulates plasma membrane insertion of TRPC3 channels and contributes to agonist-stimulated Ca2+ influx. Mol Cell *15*, 635-646.

Singh, R., Xiang, Y., Wang, Y., Baikati, K., Cuervo, A.M., Luu, Y.K., Tang, Y., Pessin, J.E., Schwartz, G.J., and Czaja, M.J. (2009). Autophagy regulates adipose mass and differentiation in mice. J Clin Invest *119*, 3329-3339.

Skurk, T., Alberti-Huber, C., Herder, C., and Hauner, H. (2007). Relationship between adipocyte size and adipokine expression and secretion. J Clin Endocrinol Metab *92*, 1023-1033.

Soboloff, J., Spassova, M., Hewavitharana, T., He, L.P., Luncsford, P., Xu, W., Venkatachalam, K., van Rossum, D., Patterson, R.L., and Gill, D.L. (2007). TRPC channels: integrators of multiple cellular signals. Handb Exp Pharmacol, 575-591.

Sorisky, A., Magun, R., and Gagnon, A.M. (2000). Adipose cell apoptosis: death in the energy depot. Int J Obes Relat Metab Disord *24 Suppl 4*, S3-7.

Sorva, A., and Tilvis, R.S. (1990). Low serum ionized to total calcium ratio: association with geriatric diabetes mellitus and with other cardiovascular risk factors? Gerontology *36*, 212-216.

Stanford, K.I., Middelbeek, R.J., Townsend, K.L., Lee, M.Y., Takahashi, H., So, K., Hitchcox, K.M., Markan, K.R., Hellbach, K., Hirshman, M.F., et al. (2015). A novel role for subcutaneous adipose tissue in exercise-induced improvements in glucose homeostasis. Diabetes *64*, 2002-2014.

Stern, J.H., Rutkowski, J.M., and Scherer, P.E. (2016). Adiponectin, Leptin, and Fatty Acids in the Maintenance of Metabolic Homeostasis through Adipose Tissue Crosstalk. Cell Metab *23*, 770-784.

Stiber, J., Hawkins, A., Zhang, Z.S., Wang, S., Burch, J., Graham, V., Ward, C.C., Seth, M., Finch, E., Malouf, N., et al. (2008). STIM1 signalling controls store-operated calcium entry required for development and contractile function in skeletal muscle. Nat Cell Biol *10*, 688-697.

Strehler, E.E., and Treiman, M. (2004). Calcium pumps of plasma membrane and cell interior. Curr Mol Med *4*, 323-335.

Strübing, C., Krapivinsky, G., Krapivinsky, L., and Clapham, D.E. (2001). TRPC1 and TRPC5 form a novel cation channel in mammalian brain. Neuron *29*, 645-655.

Su, J., Zhou, L., Kong, X., Yang, X., Xiang, X., Zhang, Y., Li, X., and Sun, L. (2013). Endoplasmic reticulum is at the crossroads of autophagy, inflammation, and apoptosis signaling pathways and participates in the pathogenesis of diabetes mellitus. J Diabetes Res *2013*, 193461.

Sukumar, P., Sedo, A., Li, J., Wilson, L.A., O'Regan, D., Lippiat, J.D., Porter, K.E., Kearney, M.T., Ainscough, J.F., and Beech, D.J. (2012). Constitutively active TRPC channels of adipocytes confer a mechanism for sensing dietary fatty acids and regulating adiponectin. Circ Res *111*, 191-200.

Sukumaran, P., Schaar, A., Sun, Y., and Singh, B.B. (2016). Functional role of TRP channels in modulating ER stress and Autophagy. Cell Calcium *60*, 123-132.

Sukumaran, P., Sun, Y., Vyas, M., and Singh, B.B. (2015). TRPC1-mediated Ca^{2+} entry is essential for the regulation of hypoxia and nutrient depletion-dependent autophagy. Cell Death Dis *6*, e1674.

Sun, X., and Zemel, M.B. (2007). Calcium and 1,25-dihydroxyvitamin D3 regulation of adipokine expression. Obesity (Silver Spring) *15*, 340-348.

Söllner, T., Whiteheart, S.W., Brunner, M., Erdjument-Bromage, H., Geromanos, S., Tempst, P., and Rothman, J.E. (1993). SNAP receptors implicated in vesicle targeting and fusion. Nature *362*, 318-324.

Südhof, T.C., and Rothman, J.E. (2009). Membrane fusion: grappling with SNARE and SM proteins. Science *323*, 474-477.

Tchoukalova, Y., Koutsari, C., and Jensen, M. (2007). Committed subcutaneous preadipocytes are reduced in human obesity. Diabetologia *50*, 151-157.

Thörne, A., Lönnqvist, F., Apelman, J., Hellers, G., and Arner, P. (2002). A pilot study of long-term effects of a novel obesity treatment: omentectomy in connection with adjustable gastric banding. Int J Obes Relat Metab Disord *26*, 193-199.

Torre-Villalvazo, I., Bunt, A.E., Alemán, G., Marquez-Mota, C.C., Diaz-Villaseñor, A., Noriega, L.G., Estrada, I., Figueroa-Juárez, E., Tovar-Palacio, C., Rodriguez-López, L.A., et al. (2018). Adiponectin synthesis and secretion by subcutaneous adipose tissue is impaired during obesity by endoplasmic reticulum stress. J Cell Biochem.

Trimble, W.S., Cowan, D.M., and Scheller, R.H. (1988). VAMP-1: a synaptic vesicle-associated integral membrane protein. Proc Natl Acad Sci U S A *85*, 4538-4542.

Tsatsanis, C., Zacharioudaki, V., Androulidaki, A., Dermitzaki, E., Charalampopoulos, I., Minas, V., Gravanis, A., and Margioris, A.N. (2005). Adiponectin induces TNF-alpha and IL-6 in macrophages and promotes tolerance to itself and other pro-inflammatory stimuli. Biochem Biophys Res Commun *335*, 1254-1263.

Tsuchida, A., Yamauchi, T., Ito, Y., Hada, Y., Maki, T., Takekawa, S., Kamon, J., Kobayashi, M., Suzuki, R., Hara, K., et al. (2004). Insulin/Foxo1 pathway regulates expression levels of adiponectin receptors and adiponectin sensitivity. J Biol Chem *279*, 30817-30822.

Tung, Y.C., Hsieh, P.H., Pan, M.H., and Ho, C.T. (2017). Cellular models for the evaluation of the antiobesity effect of selected phytochemicals from food and herbs. J Food Drug Anal *25*, 100-110.

Turer, A.T., and Scherer, P.E. (2012). Adiponectin: mechanistic insights and clinical implications. Diabetologia *55*, 2319-2326.

Vaca, L., Sinkins, W.G., Hu, Y., Kunze, D.L., and Schilling, W.P. (1994). Activation of recombinant trp by thapsigargin in Sf9 insect cells. Am J Physiol *267*, C1501-1505.

Venkatachalam, K., and Montell, C. (2007). TRP channels. Annu Rev Biochem *76*, 387-417.

Viganò, A., Zuccotti, G.V., Cerini, C., Stucchi, S., Puzzovio, M., Giacomet, V., and Mora, S. (2011). Lipodystrophy, insulin resistance, and adiponectin concentration in HIV-infected children and adolescents. Curr HIV Res *9*, 321-326.

Villarreal-Molina, M.T., and Antuna-Puente, B. (2012). Adiponectin: anti-inflammatory and cardioprotective effects. Biochimie *94*, 2143-2149.

Wang, J., Li, J., Dasgupta, S., Zhang, L., Golovko, M., Golovko, S., and Fang, J. (2014). Alterations in Membrane Phospholipid Fatty Acids of Gram-Positive Piezotolerant Bacterium Sporosarcina sp. DSK25 in Response to Growth Pressure. Lipids *49*, 347-356.

Wang, S., and Peng, D. (2012). Regulation of adipocyte autophagy--the potential anti-obesity mechanism of high density lipoprotein and ApolipoproteinA-I. Lipids Health Dis *11*, 131.

Wang, X., You, T., Murphy, K., Lyles, M.F., and Nicklas, B.J. (2015). Addition of Exercise Increases Plasma Adiponectin and Release from Adipose Tissue. Med Sci Sports Exerc *47*, 2450-2455.

Wang, Y., Zhou, M., Lam, K.S., and Xu, A. (2009). Protective roles of adiponectin in obesity-related fatty liver diseases: mechanisms and therapeutic implications. Arq Bras Endocrinol Metabol *53*, 201-212.

Wei, M.C., Zong, W.X., Cheng, E.H., Lindsten, T., Panoutsakopoulou, V., Ross, A.J., Roth, K.A., MacGregor, G.R., Thompson, C.B., and Korsmeyer, S.J. (2001). Proapoptotic BAX and BAK: a requisite gateway to mitochondrial dysfunction and death. Science *292*, 727-730.

Weimbs, T., Low, S.H., Chapin, S.J., Mostov, K.E., Bucher, P., and Hofmann, K. (1997). A conserved domain is present in different families of vesicular fusion proteins: a new superfamily. Proc Natl Acad Sci U S A *94*, 3046-3051.

Wes, P.D., Chevesich, J., Jeromin, A., Rosenberg, C., Stetten, G., and Montell, C. (1995). TRPC1, a human homolog of a Drosophila store-operated channel. Proc Natl Acad Sci U S A *92*, 9652-9656.

Weyer, C., Foley, J.E., Bogardus, C., Tataranni, P.A., and Pratley, R.E. (2000). Enlarged subcutaneous abdominal adipocyte size, but not obesity itself, predicts type II diabetes independent of insulin resistance. Diabetologia *43*, 1498-1506.

Williams, A.S., Kasahara, D.I., Verbout, N.G., Fedulov, A.V., Zhu, M., Si, H., Wurmbrand, A.P., Hug, C., Ranscht, B., and Shore, S.A. (2012). Role of the adiponectin binding protein, T-cadherin (Cdh13), in allergic airways responses in mice. PLoS One *7*, e41088.

Witczak, C.A., Wamhoff, B.R., and Sturek, M. (2006). Exercise training prevents Ca2+ dysregulation in coronary smooth muscle from diabetic dyslipidemic yucatan swine. J Appl Physiol (1985) *101*, 752-762.

Woodard, G.E., and Rosado, J.A. (2005). G-protein coupled receptors and calcium signaling in development. Curr Top Dev Biol *65*, 189-210.

Wu, L.J., Sweet, T.B., and Clapham, D.E. (2010). International Union of Basic and Clinical Pharmacology. LXXVI. Current progress in the mammalian TRP ion channel family. Pharmacol Rev *62*, 381-404.

Wu, Z., Rosen, E.D., Brun, R., Hauser, S., Adelmant, G., Troy, A.E., McKeon, C., Darlington, G.J., and Spiegelman, B.M. (1999). Cross-regulation of C/EBP alpha and PPAR gamma controls the transcriptional pathway of adipogenesis and insulin sensitivity. Mol Cell *3*, 151-158.

Xie, L., O'Reilly, C.P., Chapes, S.K., and Mora, S. (2008). Adiponectin and leptin are secreted through distinct trafficking pathways in adipocytes. Biochim Biophys Acta *1782*, 99-108.

Xu, X.Z., Li, H.S., Guggino, W.B., and Montell, C. (1997). Coassembly of TRP and TRPL produces a distinct store-operated conductance. Cell *89*, 1155-1164.

Yamada, H., Yoshida, M., Ito, K., Dezaki, K., Yada, T., Ishikawa, S.E., and Kakei, M. (2016). Potentiation of Glucose-stimulated Insulin Secretion by the GPR40-PLC-TRPC Pathway in Pancreatic β-Cells. Sci Rep *6*, 25912.

Yamada, T., Oka, Y., and Katagiri, H. (2008). Inter-organ metabolic communication involved in energy homeostasis: potential therapeutic targets for obesity and metabolic syndrome. Pharmacol Ther *117*, 188-198.

Yamauchi, T., and Kadowaki, T. (2013). Adiponectin receptor as a key player in healthy longevity and obesity-related diseases. Cell Metab *17*, 185-196.

Yamauchi, T., Kamon, J., Ito, Y., Tsuchida, A., Yokomizo, T., Kita, S., Sugiyama, T., Miyagishi, M., Hara, K., Tsunoda, M., et al. (2003). Cloning of adiponectin receptors that mediate antidiabetic metabolic effects. Nature *423*, 762-769.

Yamauchi, T., Kamon, J., Minokoshi, Y., Ito, Y., Waki, H., Uchida, S., Yamashita, S., Noda, M., Kita, S., Ueki, K., et al. (2002). Adiponectin stimulates glucose utilization and fatty-acid oxidation by activating AMP-activated protein kinase. Nat Med *8*, 1288-1295.

Yamauchi, T., Nio, Y., Maki, T., Kobayashi, M., Takazawa, T., Iwabu, M., Okada-Iwabu, M., Kawamoto, S., Kubota, N., Kubota, T., et al. (2007). Targeted disruption of AdipoR1 and AdipoR2 causes abrogation of adiponectin binding and metabolic actions. Nat Med *13*, 332-339.

Yang, J., Eliasson, B., Smith, U., Cushman, S.W., and Sherman, A.S. (2012). The size of large adipose cells is a predictor of insulin resistance in first-degree relatives of type 2 diabetic patients. Obesity (Silver Spring) *20*, 932-938.

Yang, W.S., Jeng, C.Y., Wu, T.J., Tanaka, S., Funahashi, T., Matsuzawa, Y., Wang, J.P., Chen, C.L., Tai, T.Y., and Chuang, L.M. (2002). Synthetic peroxisome proliferator-activated receptor-gamma agonist, rosiglitazone, increases plasma levels of adiponectin in type 2 diabetic patients. Diabetes Care *25*, 376-380.

Ye, F., Than, A., Zhao, Y., Goh, K.H., and Chen, P. (2010). Vesicular storage, vesicle trafficking, and secretion of leptin and resistin: the similarities, differences, and interplays. J Endocrinol *206*, 27-36.

Ye, L., Kleiner, S., Wu, J., Sah, R., Gupta, R.K., Banks, A.S., Cohen, P., Khandekar, M.J., Boström, P., Mepani, R.J., et al. (2012). TRPV4 is a regulator of adipose oxidative metabolism, inflammation, and energy homeostasis. Cell *151*, 96-110.

Yee, J.K., Mao, C.S., Ross, M.G., Lee, W.N., Desai, M., Toda, A., Kjos, S.L., Hicks, R.A., and Patterson, M.E. (2014). High oleic/stearic fatty-acid desaturation index in cord plasma from infants of mothers with gestational diabetes. J Perinatol *34*, 357-363.

Yki-Järvinen, H. (2005). Fat in the liver and insulin resistance. Ann Med *37*, 347-356.

Yuan, J.P., Kim, M.S., Zeng, W., Shin, D.M., Huang, G., Worley, P.F., and Muallem, S. (2009). TRPC channels as STIM1-regulated SOCs. Channels (Austin) *3*, 221-225.

Yuan, J.P., Zeng, W., Huang, G.N., Worley, P.F., and Muallem, S. (2007). STIM1 heteromultimerizes TRPC channels to determine their function as store-operated channels. Nat Cell Biol *9*, 636-645.

Zanou, N., Schakman, O., Louis, P., Ruegg, U.T., Dietrich, A., Birnbaumer, L., and Gailly, P. (2012). Trpc1 ion channel modulates phosphatidylinositol 3-kinase/Akt pathway during myoblast differentiation and muscle regeneration. J Biol Chem *287*, 14524-14534.

Zanou, N., Shapovalov, G., Louis, M., Tajeddine, N., Gallo, C., Van Schoor, M., Anguish, I., Cao, M.L., Schakman, O., Dietrich, A., et al. (2010). Role of TRPC1 channel in skeletal muscle function. Am J Physiol Cell Physiol *298*, C149-162.

Zeng, Q., Isobe, K., Fu, L., Ohkoshi, N., Ohmori, H., Takekoshi, K., and Kawakami, Y. (2007). Effects of exercise on adiponectin and adiponectin receptor levels in rats. Life Sci *80*, 454-459.

Zhang, X., Rebane, A.A., Ma, L., Li, F., Jiao, J., Qu, H., Pincet, F., Rothman, J.E., and Zhang, Y. (2016). Stability, folding dynamics, and long-range conformational transition of the synaptic t-SNARE complex. Proc Natl Acad Sci U S A *113*, E8031-E8040.

Zhang, Y., and Calderwood, S.K. (2011). Autophagy, protein aggregation and hyperthermia: a mini-review. Int J Hyperthermia *27*, 409-414.

Zhang, Y., Goldman, S., Baerga, R., Zhao, Y., Komatsu, M., and Jin, S. (2009). Adipose-specific deletion of autophagy-related gene 7 (atg7) in mice reveals a role in adipogenesis. Proc Natl Acad Sci U S A *106*, 19860-19865.

Zhou, H.R., Kim, E.K., Kim, H., and Claycombe, K.J. (2007). Obesity-associated mouse adipose stem cell secretion of monocyte chemotactic protein-1. Am J Physiol Endocrinol Metab *293*, E1153-1158.